THE ROLE OF AKAP350 SPLICE VARIANTS IN CELLULAR STRESS RESPONSE

By

Twila Annette Mason

Dissertation

Submitted to the Faculty of the

Graduate School of Vanderbilt University

in partial fulfillment of the requirements

for the degree of

DOCTOR OF PHILOSOPHY

in

Cell and Developmental Biology

December, 2013

Nashville, TN

Approved:

Susan Wente, Ph.D. (Chair)

James R. Goldenring, M.D., Ph.D.

James E. Crowe, Jr., M.D.

Anne Kenworthy, Ph.D.

Todd Graham, Ph.D.

To my amazing husband, Dustin.

ACKNOWLEDGEMENTS

This work was made possible by funding from National Institutes of Health grants RO1DK43405 (to James R. Goldenring) and NS042205 (to Chin Chiang). Financial support was also provided by a gift from Ziopharma (to James R. Goldenring) and funding from the Childhood Brain Tumor Foundation (to Chin Chiang). Graduate training support was provided by the Cellular, Biochemical, and Molecular Sciences Training Program (to Twila A. Mason and James R. Goldenring). Confocal fluorescence microscopy and TEM imaging were performed through the use of the VUMC Cell Imaging Shared Resource supported by National Institute of Health (NIH) Grants CA68485, DK20593, DK58404 and HD15052.

I am grateful to the many people who have contributed to my graduate school experience. First, thank you to everyone in the Goldenring lab for scientific and moral support. Thank you for discussing the intricacies, pitfalls, and safety nets involved in experimental design while I made my way through some difficult scientific patches. Also, I appreciate those who offered reminders of life outside the lab when I needed a break or distraction (with such topics as pets, family, gardening, and books). I have to thank Emily Poulin for volunteering to the majority of my thesis. Dr. Ki Taek Nam offered endless patience and wisdom when it came to the development and characterization of my AKAP9 mouse lines. All of my knowledge of mouse work came from Dr. Nam and Dr. Victoria Weis. Special thanks must go to Dr. Elena Kolobova for her ongoing help in navigating through the highs and lows of graduate studies. She

taught me too many things to list, provided guidance on many topics (scientific and otherwise), and is a friend as well as mentor.

To my Dissertation Committee members, thank you for your advice throughout my ever-changing project. I thank Dr. Susan Wente for being my committee chair and helping guide my progression. I would especially like to thank Dr. James Goldenring, my mentor, for helping me grow as a scientist and a critical thinker. He showed me that no matter where your career or life takes you, you should always follow you passion and retain passion for what you are doing.

Last but certainly not least, I am grateful to all of my family and friends that have supported me along this journey. The most important person in this endeavor has been my wonderful, supportive husband, Dustin. It is difficult to put into words how instrumental he was in my success, but suffice it to say I could not have done this without his support. He made me laugh when I was under stress and wanted to cry, smile when I was disappointed, and hopeful when I was desperate. I was able to accomplish so much more knowing he was there to support me and catch me if I fell. I must also thank my cats, Tiger and Snowflake, for constantly reminding me that there is a life outside of lab and more important things in life than experimental results. Petting a cat can make any problem go away and turn any frown into a smile. They even showed their support for my scientific endeavors by donating many, many cat whiskers for use in electron microscopy.

TABLE OF CONTENTS

Page

LIST OF TABLES

LIST OF FIGURES

CHAPTER I

INTRODUCTION

Organisms experience several types of stress.

Stress occurs when homeostasis is threatened, causing physiological and pathological changes (Jaggi *et al*., 2011). Organisms can experience acute or chronic stress from internal or external sources (Figure 1). Acute stress is short-lived and typically experienced once, such as a sudden, quick immersion in cold water or a single dose of ingested poison (Bhatia et al., 2011). Chronic stress is long-lived, reoccurring several times subsequently or persisting, such as prolonged exposure to an environmental toxin or extreme temperatures (Bhatia et al., 2011). Internal stressors are those that come

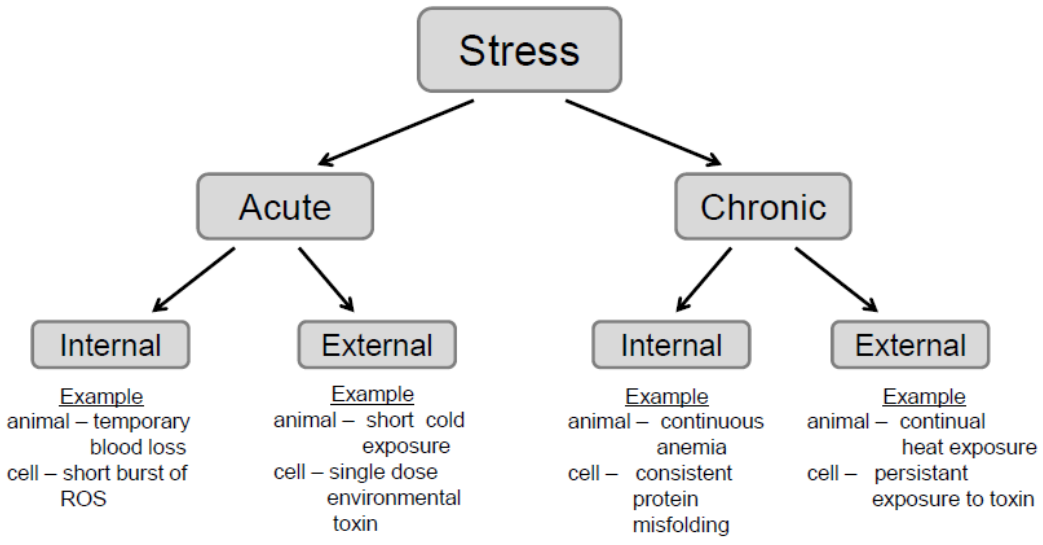

Figure 1. Types of stress and stressors. Stress can either be acute (short-lived) or chronic (long-lived, continuous). Both acute and chronic stress can be induced by internal or external stressors.

from within the organism, such as toxic metabolic byproducts. External stressors are those from the environment, such as heat or physical trauma.

The physiological and pathological changes within an organism upon stress occur in an attempt to maintain or restore homeostasis and enhance the probability of survival (Jaggi *et al*., 2011). These changes are collectively known as the stress response. All organisms experience various stressors at the whole animal and cellular levels. Stressors at the animal level include lack of food, predation, poison, infection, and extreme temperatures. The whole animal stress responses, "fight-or-flight" for acute stressors and "general adaptation syndrome" for chronic stressors, are typically controlled by hormonal changes within the animal (Charmandari, 2005).

Stress also occurs at the cellular level, and all cells experience various stressors as part of their normal physiology. Cellular stress typically involves the damage or defect of one or more types of macromolecules within the cell, such as DNA or proteins (Kültz, 2005). For this reason, molecular chaperones such as heat shock proteins (Hsps) are key components in several stress response mechanisms. Another common type of cellular stress is the generation of reactive oxygen species (ROS) or other oxidative damage (Pastori, 2002). Common stressors include heat shock, oxidative conditions, viral infection, hypoxia, mitochondrial stress, unfolded proteins, DNA-damaging agents, pharmaceuticals, and irradiation (Kolobova *et al*., 2009; Kedersha and Anderson, 2007).

Cells have several mechanisms for stress response.

Cells must be able to respond to stressors and have developed several mechanisms to do so. The response to stress is tailored depending on the type and level of stress

(Fulda *et al*., 2010). Cells have stress responses that can directly counteract stress-induced damage (Kültz, 2005). Other mechanisms can temporarily increase cell tolerance for stress-induced damage. All stress responses aim for protection of the basic cellular functions and components such as DNA repair and stability, cell cycle control, and protein quality control (Kültz, 2005).

Some mechanisms of stress response aid in cell survival and recovery, while other mechanisms induce cell death (Fulda *et al*., 2010). Response mechanisms to enhance cell survival are employed to maintain and repair otherwise healthy cells (Kültz, 2005; Fulda *et al*., 2010). Mechanisms to induce cell death are necessary to remove unhealthy cells that are beyond recovery (Kültz, 2005; Fulda *et al*., 2010). Cells initially employ response mechanisms to aid in cell recovery, but if the stressor persists or the damage is too great, cells then activate death signaling pathways (Fulda *et al*., 2010).

When cells undergo cell death as a stress response, there are several different pathways: apoptosis (Kerr *et al*., 1972), autophagic cell death (Clark, 1957), and necrosis (Gulliver, 1838). Apoptosis, or programmed cell death, is a common stress response that involves nuclei rounding and fragmentation, cell shrinkage and blebbing, and phagocytosis of cell fragments (Kerr *et al*., 1972; Elmore, 2007). Apoptosis is a highly conserved process throughout evolution and a common target for therapeutics. This process of cell death plays critical roles in embryonic development and aging in addition to stress response (Elmore, 2007). There are two major apoptotic pathways in mammals (Kültz, 2005; Elmore, 2007). The intrinsic apoptotic pathway involves the release of cytochrome c and other factors from mitochondria (Elmore, 2007). This is described in more detail below. The extrinsic apoptotic pathway is induced by specific ligands

binding to cell surface receptors, activating a signaling cascade (Elmore, 2007). Both pathways involve the activation of caspase proteins, a family of cysteine proteases, and this largely accounts for the morphological changes seen (Samali *et al*., 1999). Distinct caspases are activated during intrinsic versus extrinsic signaling (Kanamaru *et al*., 2012). Apoptosis has now also become known as caspase-dependent programmed cell death (Samali *et al*., 1999).

Autophagic cell death is another programmed cell death pathway, and it involves the process of autophagy, or self eating (He and Klionsky, 2009). During autophagy, long-lived proteins and organelles in the cytoplasm are sequestered in vesicles and degraded. The double-membraned vesicle that results is termed an autophagosome (He and Klionsky, 2009). It remains controversial whether the process of autophagy is toxic or protective for cells. One role of autophagy is to rid the cell of unhealthy mitochondria through a specific process called mitophagy (Ashrafi and Schwarz, 2013). There is evidence of cross-talk between apoptosis and autophagic cell death (Shimizu *et al*., 2004; Yu *et al*., 2004; Ullman *et al*., 2008)

Necrosis is traditionally considered non-programmed cell death, instead associated with loss of ionic balance control that leads to swelling and membrane rupture, resulting in cellular lysis (Festjens *et al*., 2006). Recently, evidence has mounted suggesting the process of necrosis is regulated by signaling pathways, termed necroptosis (Vandenabeele *et al*., 2010). Evidence also suggests the mechanisms that promote necrosis can function to inhibit apoptosis (Festjens *et al*., 2006). Necrosis induces an immune response due to the release of cellular contents (Festjens *et al*., 2006).

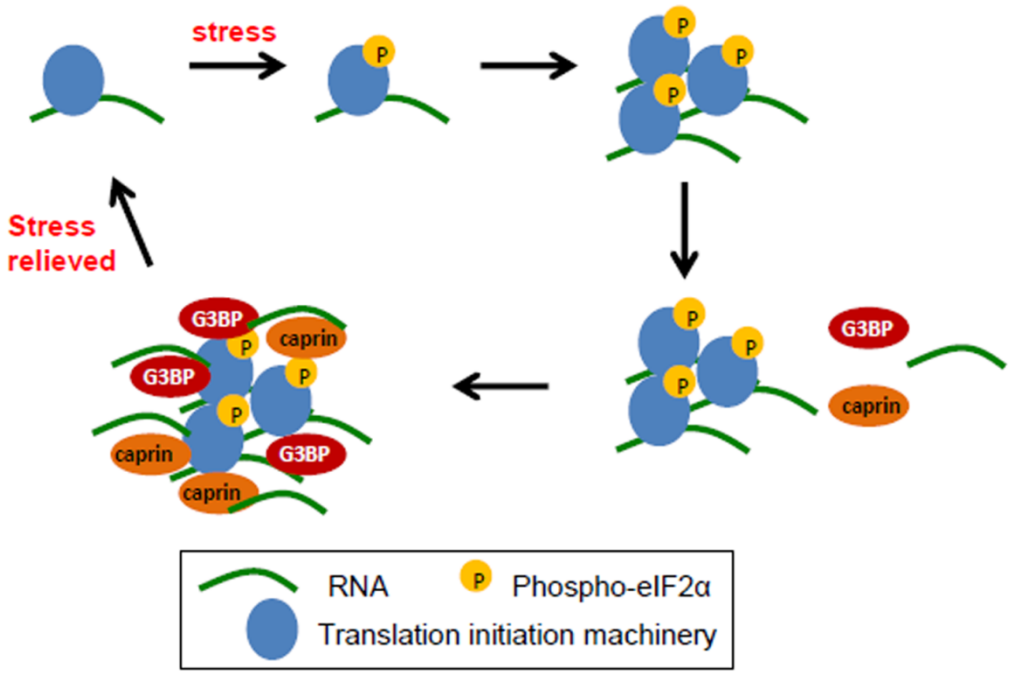

Figure 2. Stress granule formation and dispersal. Upon stress, translation initiation factor eIF2α is phosphorylated, stalling the initiation complexes. This leads to coalescence of stalled initiation complexes. Through an unknown mechanism, other mRNAs and proteins are recruited and sequestered in the stress granule. When the stress is relieved, stress granule components disperse into the cytoplasm through an unknown mechanism.

Stress granule formation is one type of stress response.

One type of stress response is the formation of stress granules (Nover *et al*., 1989). The formation of stress granules is induced by many types of stress, including heat shock, UV irradiation, and oxidative conditions (Anderson and Kedersha, 2006). Other stressors, such as DNA-damaging agents, do not induce stress granule formation (Kedersha and Anderson, 2007). Typically, the assembly of stress granules is triggered by stress-induced phosphorylation of translation initiation factor eIF2α (Figure 2)

(Kedersha and Anderson, 2007). This phosphorylation event prevents the recycling of GDP-bound eIF2α to GTP-bound eIF2α, which leads to a stalling of the translation initiation complex (Srivastava *et al*., 1998). These stalled initiation complexes then coalesce to form stress granules, the exact mechanism of which remains unknown (Figure 2). Stress granules are generally composed of stalled initiation complexes, other mRNA translation machinery, mRNAs, proteins involved in mRNA regulation and metabolism, and other signaling proteins that have no known link to RNA (Kedersha and Anderson, 2007).

Stress granules serve to spatially and temporally sequester mRNAs and proteins during stress (Figure 2) (Kedersha and Anderson, 2007). Proteins and mRNAs that are needed during stress response, such as heat shock proteins (Hsps), are not sequestered. Stress granules also act as triage centers, sorting mRNAs for sequestration or decay during times of cellular stress (Anderson and Kedersha, 2006). For this reason, the composition of stress granules can be highly dynamic. Stress granule components have diverse localizations and functions when cells are not experiencing stress. Some stress granule proteins are known to interact with mRNAs and possibly recruit additional mRNAs to stress granules. One of these proteins is G3BP (Ras-GAP SH3 domain binding protein), which is a major component of stress granules (Tourrière *et al*., 2003). Caprin-1 (cytoplasmic activation/proliferation-associated protein-1) is also a mRNA-associated stress granule protein (Solomon *et al*., 2007). G3BP, Caprin-1, or other critical stress granule components can self-aggregate and trigger stress granule formation when overexpressed, independently of eIF2α phosphorylation (Kedersha *et al*., 1999). Once stress is no longer present, stress granules disperse, and the sequestered mRNAs

can be immediately translated. However, if the stress signal does not allow for stress granule dispersal, cells undergo apoptosis, or programmed cell death (Kedersha and Anderson, 2007).

Mitochondria are highly involved in cellular stress response.

Mitochondria were first identified over a century ago (Henle, 1841) and are vital organelles to the cell. Mitochondria have various crucial functions within cells, including metabolism, ATP-generation, redox biochemistry, and calcium homeostasis (Horbinski and Chu, 2005). Mitochondria also play a role in calcium signaling, in concert with and independently of the ER (Dorn and Scorrano, 2010; Gunter *et al*., 2000). Because of their many roles, mitochondria are critical locations for signal integration.

Mitochondria are also crucial organelles in regulation of stress response and decisions between cell survival and death. As mentioned, cell death is one response to stress. Mitochondria are responsible for releasing several pro-apoptotic factors, and mitochondria are acted upon by many other apoptosis-regulating proteins (Kanamaru *et al*., 2012). Every pathway to apoptosis converges upon the mitochondria, the site of activation and release of caspases, cysteinyl aspartate proteases. When cytochrome C is released from mitochondria into the cytoplasm, it triggers a signaling cascade that ultimately leads to apoptosis (Samali *et al*., 1999). Recently, studies show mitochondria also play several roles in necroptosis, and the disruption of mitochondrial membranes is key to the execution of necroptosis (Vandenabeele *et al*., 2010). Mitochondria also play roles in whether a cell undergoes autophagy, or "self eating".

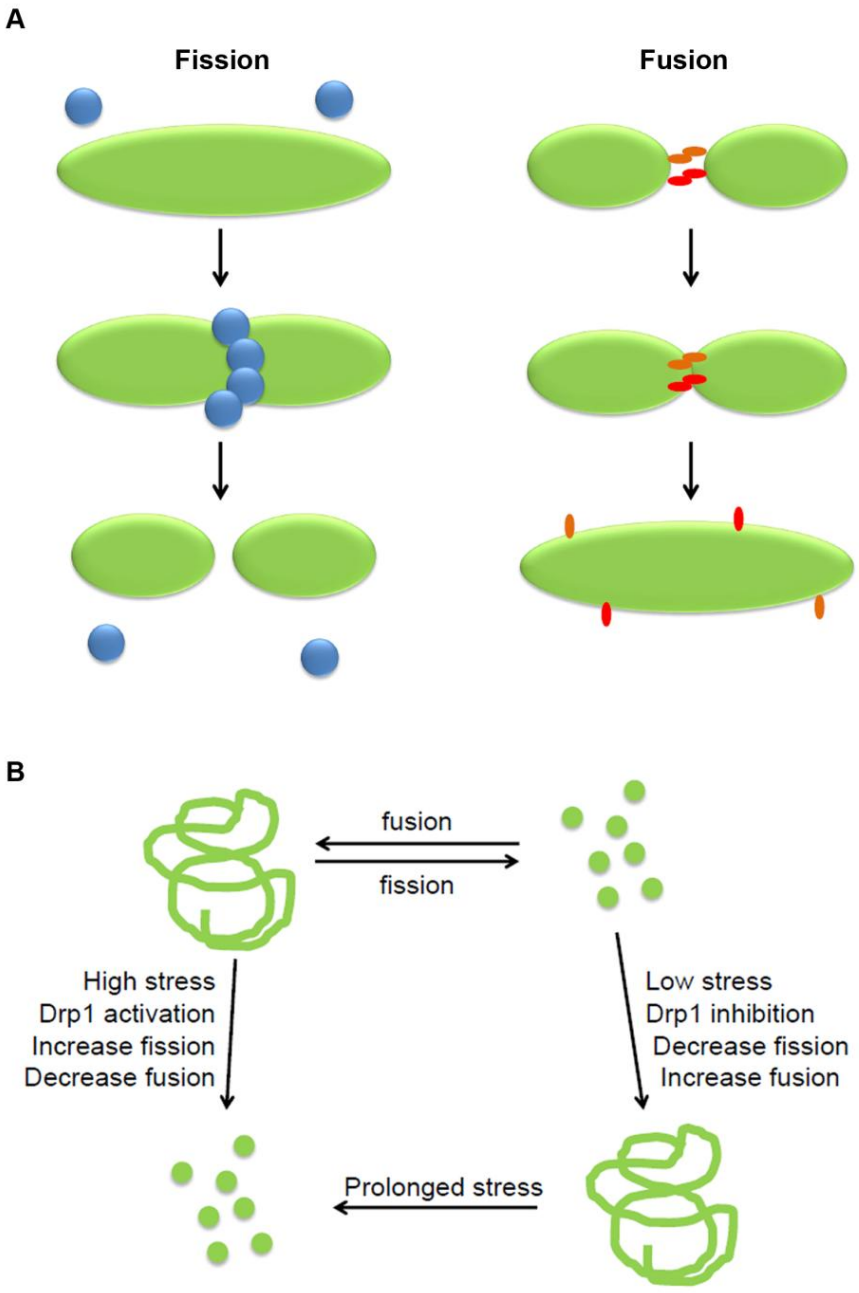

Figure 3. Mitochondria are highly dynamic organelles. A) Mitochondria (green) undergo fission and fusion. During fission, active Drp1 (blue) is recruited to mitochondria outer membranes where it oligomerizes and promotes fission. During fusion, mitofusins 1 and 2 (red and orange, respectively) interact on mitochondria outer membranes to bring mitochondria in close proximity to one another. Mitofusins facilitate outer membrane fusion, while Opa1 facilitates inner membrane fusion. **B)** Mitochondria normally maintain a balance between fission and fusion. Several factors can cause mitochondria fragmentation, such as increased fission. Mitochondria hyperfusion and elongation can also be caused by several factors, including an increased rate of fusion.

Mitochondria themselves undergo mitophagy, a form of autophagy specifically associated with mitochondria (Ashrafi and Schwarz, 2013). Mitochondria experience various stresses due to the production of stressors, such as reactive oxygen species (ROS), during metabolic processes (Kanamaru *et al*., 2012). Due to this constant exposure to stressors, mitochondria have continuous quality control mechanisms. Dysfunction of mitochondria can result in a loss of membrane potential or overproduction of ROS, and other metabolic products, which then become cytotoxic (Nunnari and Suomalainen, 2012). Mitophagy is one method to remove damaged mitochondria from the cell (Kissová et al., 2004; Lemasters, 2005). Loss of membrane potential is one trigger for mitophagy, recruiting the E3 ubiquitin ligase, Parkin, to the mitochondrial outer membrane to degrade specific outer membrane proteins (Ashrafi and Schwarz, 2013).

Mitochondria are highly dynamic, constantly undergoing fission and fusion and maintaining a balance between these two processes (Figure 3) (Chen and Chan, 2009). Fusion serves as a quality control mechanism because it allows mixing of mitochondrial contents (Kanamaru *et al*., 2012). If one mitochondrion has a mutation in a specific mtDNA gene, mitochondrial fusion allows for the chance to acquire a version that is not mutated. Various events, such as cellular stress, can induce a shift in the balance between fission and fusion (Figure 3) (Chan 2012). When the balance is shifted towards increased fusion or decreased fission, mitochondria become elongated and hyperfused (Figure 3) (Chen and Chan, 2009). This is protective against apoptosis, partially due to limiting the release of pro-apoptotic factors from the mitochondria (Nunnari and Suomalainen, 2012). Hyperfused mitochondria are also protected from mitophagy. When the balance is

shifted towards decreased fusion or increased fission, the mitochondria become fragmented (Figure 3) (Chen and Chan, 2009). This is pro-apoptotic, in part due to an increase in mitochondrial outer-membrane permeabilization (Nunnari and Suomalainen, 2012). Fragmented mitochondria are smaller and more readily removed via mitophagy (Kanamaru *et al*., 2012).

Inadequate stress response leads to disease development or progression.

Inadequate or inappropriate stress response influences disease in several ways. Cells can respond to a stressor too strongly, not strongly enough, or inappropriately. First, the stressor could be too prolonged or strong, but not to the point of inducing cell death, and it could hinder the cell's ability to completely recover to normal status (Fulda *et al*., 2010). This would allow unhealthy cells to survive and possibly develop into a diseased state. For example, a mutated gene or long-lived protein could remain within a cell causing it to become transformed and acquire tumor-initiating characteristics. Second, while in a diseased state, cells may have either a strengthened or weakened stress response, both of which could have detrimental effects (Fulda *et al*., 2010). For instance, cancer cells with a strengthened stress response could be more resistant to treatment. In contrast, diseased neurons with a weakened stress response could die upon even a weak stress episode. The importance of proper stress response is apparent in the high degree of conservation of basic stress response pathways throughout evolution (Fulda *et al*., 2010).

The ability or inability of a cell to respond to stress is highly associated with several disease states. There is a growing body of literature that suggests progression of neurodegenerative diseases involves altered cellular stress response (Wolozin, 2012;

Roussel et al., 2013; Lagouge and Larsson, 2013). Chronic stress has been linked to the development of depression and the progression of neurodegenerative and other diseases (Jaggi *et al*., 2011). The loss of proper stress response in neurons has been implicated as a common factor across all neurodegenerative diseases (Fulda *et al*., 2010).

Parkinson's disease is the second most common neurodegenerative disease, and is characterized by the degeneration of dopaminergic neurons in the substantia nigra pars compacta. Commonly mutated proteins in some cases of Parkinson's disease are associated with mitochondrial function and resistance to oxidative stress, a common feature of Parkinson's disease (Dodson and Guo, 2007). Other mutated proteins include those involved in degradation of misfolded or damaged proteins (Dodson and Guo, 2007). Parkinson's disease has been associated with activation of several stress response pathways, including heat shock response and unfolded protein response (Banerjee *et al*., 2009). Similarly, proper stress response is also important for related neurodegenerative diseases such as Alzheimer's and Huntington's (Gorman, 2008).

Proper stress response is also vital to the maintenance of myocardial function, and improper stress response can lead to cardiovascular disease and myocardial infarction (Cook *et al*., 1999; von Harsdorf *et al*., 1999). Cardiovascular disease is a group of disorders, and in many cases cardiomyocyte death occurs via necrosis and apoptosis. During ischemia/reperfusion-induced injury, ROS are produced and cause oxidative damage to cardiomyocytes (von Harsdorf *et al*., 1999). If mitochondrial function can be maintained, oxidative stress-induced cardiomyocyte death is prevented (Neuss *et al*., 2001). Therefore, cardiomyocytes must maintain a robust response mechanism to oxidative stress.

Stress response is also a critical factor in the development, progression, and treatment of cancer (Lowe and Lin, 2000; Hanahan and Weinberg, 2000; Lowe *et al*., 2004). Tumor formation occurs when the balance between cell proliferation and cell death is disrupted within a tissue. If cells respond inappropriately to stress, unhealthy cells can avoid cell death. This can result in cells with genetic instability, which then accumulate mutations that lead to cancerous growth (Lowe *et al*., 2004). Resistance to cell death and enhanced stress response also contributes to the development of treatment-resistant cancers. Chemotherapy, irradiation, and immunotherapy are meant to stress cancer cells to the point of triggering cell death (Makin and Dive, 2001; Johnstone et al., 2002; Fulda and Debatin, 2004). Cancer cells that are resistant to the stress of therapeutic treatments hinder remission of the disease.

Stress response is a complex, highly regulated process.

Because stress response can literally determine the difference between life and death, cellular stress response is a highly regulated process. Both intrinsic and extrinsic apoptotic pathways are highly regulated by pro- and anti-apoptotic signals and cascades (Kültz, 2005). A critical anti-apoptotic pathway is the PI-3-K (phosphatidyl inositol 3 kinase)/AKT (V-Akt murine thymoma viral oncogene homolog) pathway (Kültz, 2005). The p53 pathway is critical for many pro-apoptotic signals as it transactivates many proteins in pro-apoptotic cascades (Kültz, 2005). Autophagy is also a highly regulated process and a family of autophagy-related proteins regulates each aspect of the autophagic process (Kanamaru *et al*., 2012). The most upstream regulators of autophagy are the Unc51-like kinases 1 and 2 (ULK1/2), which are recruited to autophagosome

formation sites upon starvation (Kanamaru *et al*., 2012). The elongation and closure of the autophagosome is partially regulated by the LC3-phosphatidylethanolamine conjugate. Selective autophagy events, such as mitophagy, also have unique regulators. Mitophagy-specific regulators include PINK (PTEN-induced putative kinase 1) and Parkin (E3 ubiquitin ligase) (Kanamaru *et al*., 2012).

As described above, mitochondrial dynamics, specifically the balance between fission and fusion, is vital to the role of mitochondria in stress response (Youle and van der Bliek, 2012). Both mitochondrial dynamics and stress response are highly regulated processes, and protein kinase A (PKA) has emerged as an important regulator of mitochondrial dynamics (Rambold and Lippincott-Schwartz, 2011). Both mitochondrial fission and fusion proteins have been identified as substrates for PKA phosphorylation. The mitochondria fission protein, Drp1 (dynamin-related protein 1), is inactivated by PKA phosphorylation. This results in a decreased rate of fission, which leads to increased mitochondria elongation, a process that promotes cell survival (Figure 3) (Chang and Blackstone, 2007). During starvation, the elongated mitochondria resulting from Drp1 inhibition do not undergo mitophagy, and help stressed cells maintain ATP levels (Gomes *et al*., 2011). During hypoxia, the phosphorylation of Drp1 is suppressed, which leads to mitochondrial fragmentation and induction of cell death (Kim *et al*., 2011). Mfn2, a mitochondrial fusion protein, is also phosphorylated by PKA, and this promotes cell survival (Chen *et al*., 2004). PKA signaling at the mitochondria regulates mitochondrial dynamics and stress response, as well as many other cellular processes. The complete details of signal integration at mitochondria remain unclear.

AKAPs provide signal integration.

One way to integrate these signaling pathways is through scaffolding proteins in close proximity. A-Kinase Anchoring Proteins (AKAPs) are a large, diverse family of functionally similar scaffolding proteins that associate with a variety of signaling proteins (Tröger *et al*., 2012). AKAPs were discovered as PKA (Protein kinase A) anchors that provide localized cAMP (cyclic AMP)/PKA signaling (Sarkar *et al*., 1984; Lohmann *et al*., 1984). Cyclic AMP is a second messenger molecule (Krebs and Fischer, 1956; Rall *et al*., 1957; Sutherland and Rall, 1958; Wosilait and Sutherland, 1957) that activates PKA by causing dissociation of the catalytic subunits from the regulatory subunits (Beavo and Brunton, 2002). The PKA holoenzyme is a tetrameric complex that consists of two catalytic (C_{α}, C_{β}, or C_{γ}) and two regulatory ($R_{I\alpha}$, $R_{I\beta}$, $R_{II\alpha}$, or $R_{II\beta}$) subunits. AKAPs associate with PKA via binding the regulatory subunits (Scott, 1997). Most AKAPs bind the $R_{II\alpha/\beta}$ regulatory subunits of PKA, but there are some AKAPs that bind $R_{I\alpha/\beta}$ subunits or both $R_{I\alpha/\beta}$ and $R_{II\alpha/\beta}$ (known as dual-specificity AKAPs) (Tröger *et al*., 2012). Dual-specificity AKAPs include AKAP1, AKAP2, AKAP3, AKAP4, $AKAP7_{\beta}$, AKAP10, AKAP11, BIG2, Ezrin, PAP7, SFRS17A, and cTnT (Table 1). Though these dual-specificity AKAPs have the ability to bind both $R_{I\alpha/\beta}$ and $R_{II\alpha/\beta}$ subunits, the affinities can vary drastically (Jarnaess *et al*., 2008). SKIP is an AKAP that specifically binds only $R_{I\alpha/\beta}$ subunits (Means *et al*., 2011).

Though AKAPs were identified as PKA anchors, it has since been shown they play many other roles as well (Theurkauf and Vallee, 1982; Lohmann *et al*., 1984; Skroblin *et al*, 2010; Greenwald and Saucerman, 2011). AKAPs function as anchors for targeting proteins to specific sub-cellular locations, and the localization and composition of AKAP

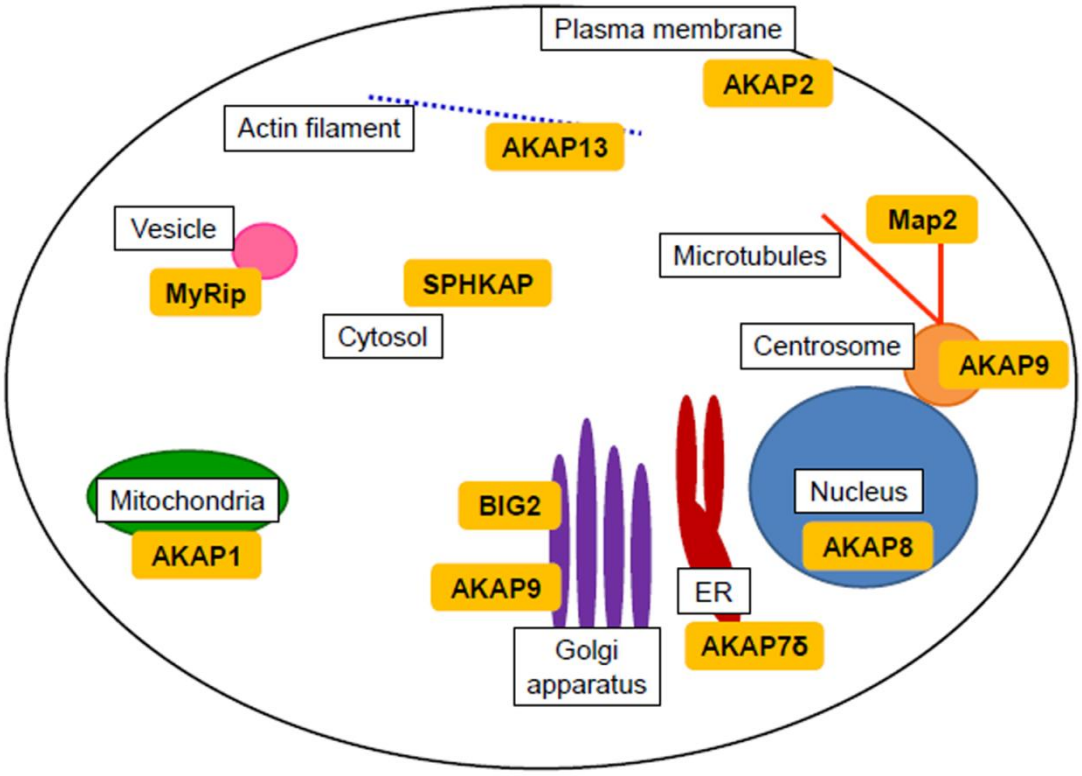

Figure 4. AKAPs scaffold PKA and other proteins to various subcellular locations. Some examples are shown here. For details, see text and Table 1.

complexes is dynamic (Figure 4). Several AKAPs, including AKAP1, AKAP7, AKAP9, AKAP10, BIG2, MTG8, and MTG16b, can localize to more than more subcellular location with this localization dependent on a variety of factors (Figure 4 and Table 1). AKAPs associate with both signaling enzymes and their substrates to bring the components of signaling cascades in close proximity (Michel and Scott, 2002). An AKAP can interact with components of various signaling pathways/cascades simultaneously (Greenwald and Saucerman, 2011). This allows AKAPs to provide spatiotemporal regulation of cAMP/PKA signaling, as well as serve as signal integration centers (Tröger *et al*., 2012).

Table 1. Summary of current AKAP protein knowledge. For each protein the following information is given: 1) all names for the protein; 2) the most well-documented subcellular localizations; 3) the most well-documented cellular processes the protein is implicated in playing a role; 4) diseases in which the protein has been shown to have a direct role, and 5) references for the data in the table.

Protein name(s)	Localization(s)	Cellular process(es)	Disease association(s)	References
AKAP1, D-AKAP1, AKAP121, AKAP149, AKAP140, AKAP84, S-AKAP84	Mitochondria, endoplasmic reticulum, nuclear envelope	Nuclear envelope maintenance; reverse transcription; mitochondrial function	Female infertility; hypoxia	Lin *et al*., 1995; Trendelenburg *et al*., 1996; Steen *et al*., 2003; Newhall *et al*., 2006; Lemay *et al*., 2008; Rogne *et al*., 2009; Kim *et al*., 2011
AKAP2, AKAP-KL	Apical surface, plasma membrane	Actin cytoskeleton; cell polarity; aquaporin-0 stabilization	Cataracts	Dong *et al*., 1998; Gold *et al*., 2012
AKAP3, AKAP110, FSP95, Fibrousheathin-1	Sperm flagella fibrous sheath	Sperm motility	Male infertility; ovarian cancer	Vijayaraghavan *et al*., 1999; Turner *et al*., 2001; Hasegawa *et al*., 2004
AKAP4, AKAP82, FSC1	Sperm flagella fibrous sheath	Sperm motility	Male infertility; cervical cancer	Turner *et al*., 1998; Turner *et al*., 2001; Saini *et al*., 2013
AKAP5, AKAP79, AKAP150, AKAP75	Plasma membrane; primary cilia	Neuronal ion transport; pepsinogen secretion	Altered synaptic transmission; Timothy syndrome; polycystic kidney disease	Sarkar *et al*., 1984; Xie and Raufman, 2001; Cheng *et al*., 2011; Choi *et al*., 2011; Gold, 2012
AKAP6, mAKAP, AKAP100	Nuclear envelope, sarcoplasmic reticulum	Cardiomyocyte contractility	Cardiac hypertrophy	McCartney *et al*., 1995; Yang *et al*., 1998; Fink *et al*., 2001; Bauman *et al*., 2007
AKAP7, AKAP18/15α/β	Plasma membrane	Ion transport		Fraser *et al*., 1998; Gray *et al*., 1998; Trotter *et al*., 1999

Table 1. (continued)

AKAP7, AKAP18/15γ	Cytosol, nucleus	Ion transport		Trotter *et al*., 1999
AKAP7, AKAP18/15δ	Endoplasmic reticulum, cytosol, vesicles	Ion transport	Heart failure	Henn *et al*., 2004; Lygren *et al*., 2007; Lygren and Taskén, 2008
AKAP8, AKAP95	Nucleus, condensed chromatin	Transcription regulation; chromatin condensation		Eide *et al*., 1998; Collas *et al*., 1999; Akileswaran *et al*., 2001
AKAP9, Yotiao	Plasma membrane	Cardiac repolarization; ion transport; NMDA receptor regulation	Long QT Syndrome; cardiac arrhythmias	Lin *et al*., 1998; Chen *et al*., 2007; Piggott *et al*., 2008
AKAP9, AKAP350, AKAP450, CG-NAP, hyperion	Centrosome, Golgi apparatus, stress granules	Cell cycle; microtubule dynamics; canaliculi development; stress granule formation		Schmidt *et al*., 1999; Larocca *et al*., 2006; Kolobova *et al*., 2009; Mattaloni *et al*., 2012
AKAP10, D-AKAP2	Mitochondria, vesicles	Receptor recycling	Breast cancer; cardiac diseases	Huang *et al*., 1997a; Wang *et al*., 2001; Tingley *et al*., 2007; Wirtenberger *et al*., 2007; Eggers *et al*., 2009
AKAP11, AKAP220	Vesicles, centrosome, peroxisomes	Cell cycle; cell migration	Oral carcinogenesis	Lester *et al*., 1996; Reinton *et al*., 2000; Garnis *et al*., 2005; Logue *et al*., 2011
AKAP12, Gravin, AKAP250, SSeCKS	Cytosol, actin cytoskeleton	Cell migration; cytoskeletal structure	Prostate hyperplasia; acute myeloid leukemia; colorectal carcinoma	Gordon *et al*., 1992; Akakura *et al*., 2008; Liu *et al*., 2011; Akakura and Gelman, 2012; Mostafa *et al*., 2013

Table 1. (continued)

AKAP13, AKAP-Lbc, Ht31, Rt31, Brx-1	Cytosol, actin cytoskeleton	Guanine nucleotide exchange; cytoskeletal dynamics	Breast cancer; cardiac diseases	Toksoz and Williams, 1994; Sterpetti *et al*., 1999; Wirtenberger *et al*., 2007; Smith and Scott, 2013
AKAP14, AKAP28, TAKAP80	Cilia	Cilia beat frequency		Kultgen *et al*., 2002
MAP2	Microtubules	Cytoskeleton stabilization; microtubule bundling	Prion diseases	Dhamodharan and Wadsworth, 1995; Zhang and Dong, 2012
Ezrin, AKAP78, Villin-2	Actin cytoskeleton	Tubulogenesis	Polycystic kidney disease	Orellana *et al*., 2003
Rab32	Mitochondria, mitochondria associated membranes (MAM), vesicles	Mitochondria dynamics; enzyme trafficking	Gastric and endometrial adenocarcinomas	Alto *et al*., 2002; Shibata *et al*., 2006; Wasmeier *et al*., 2006; Bui *et al*., 2010
GSKIP, C14ORF129, HSPC210	cytosol	Wnt signaling		Chou *et al*., 2006; Hundsrucker *et al*., 2010
BIG2, ARFGEF2, ARFGEP2	Golgi apparatus, cytosol	Vesical trafficking	autosomal recessive periventricular heterotopia	Tanaka *et al*., 1989; Shinotsuka *et al*., 2002; Li *et al*., 2003; Bui *et al*., 2009
SPHKAP, SKIP	Cytosol, mitochondria	Apoptosis		Lacaná *et al*., 2002; Means *et al*., 2011
MyRIP, SlaC2-c	Secretory vesicles, actin cytoskeleton	Vesicle trafficking	Griscelli syndrome	El-Amraoui *et al*., 2002; Fukuda and Kuroda, 2002; Goehring et al., 2007; Van Gele et al., 2009
Pericentrin, kendrin	Centrosome	Microtubule organization; cell division	Microcephalic osteodysplastic primordial dwarfism type II; schizophrenia	Doxsey *et al*., 1994; Diviani *et al*., 2000; Rauch *et al*., 2008; Numata *et al*., 2010

Table 1. (continued)

Neurobeachin	Golgi apparatus, postsynaptic plasma membrane	Neuronal membrane trafficking	Autism; synaptic function	Gilbert *et al*., 1999; Wang *et al*., 2000; Castermans *et al*., 2003
WAVE-1, Scar	Actin cytoskeleton	Actin organization; cytoskeleton		Miki *et al*., 1998
MTG8, RUNX1T1	Nucleus, Golgi apparatus	Transcription regulation	Acute myeloid leukemia	Miyoshi *et al*., 1993; Fukuyama *et al*., 2001; Rochford *et al*., 2004
Myosin VIIA	Actin cytoskeleton	Cellular trafficking	Usher syndrome type 1B	Weil *et al*., 1995
MTG16b, CBFA2T3, ZMYND4	Golgi apparatus, plasma membrane	T cell activation	Leukemia	Calabi and Cilli, 1998; Schillace *et al*., 2002; Asirvatham *et al*., 2004; Fiedler *et al*., 2010
Synemin, desmuslin	Z-discs, intermediate filaments	Cell junctions	Glioblastoma	Granger and Lazarides, 1980; Russell *et al*., 2006; Lund *et al*., 2012; Pitre *et al*., 2012
PAP7	mitochondria	Cholesterol transport; steroid transport		Li *et al*., 2001; Hauet *et al*., 2002
Myospryn	Z-discs, perinuclear	Muscle contraction	Muscular dystrohpy	Benson *et al*., 2004; Kouloumenta *et al*., 2007; Reynolds *et al*., 2008
SFRS17A, XE7	nucleus	Splicing		Ellison *et al*., 1992; Jarnaess *et al*., 2009
Merlin, schwannomin, neurofibromin-2	Actin cytoskeleton, adherens juntions	Cell proliferation; motility	Neurofibromatosis type 2; Schwannomas	Rouleau *et al*., 1993; Sainz *et al*., 1994; Lutchman M, Rouleau, 1995; Pećina-Šlaus, 2013

Table 1. (continued)

Moesin	Cytosol, plasma membrane-cytoskeleton interface	Cytoskeleton ; migration	Glioma	Lankes and Furthmayr, 1991; Emery and Ramel, 2013; Zhu *et al*., 2013
AKAP85, RSPH3	Golgi apparatus, motile cilia	Motility		Jivan *et al*., 2009
RSK1	Cytosol, nucleus	Cell survival; proliferation		Richards *et al*., 1999; Romeo *et al*., 2012
cTnT, cardiac troponin T	Sarcomere	Contractility	Cardiomyopathy	Long and Ordahl, 1988; Tardiff, 2005; Sumandea *et al*., 2011
Cypher, ZASP	Sarcomere	Cytoskeleton	Myofibrillar myopathy; cardiomyopathy	Faulkner *et al*., 1999; Arimura *et al*., 2004; Kraya *et al*., 2013; Lin *et al*., 2013
smAKAP	Plasma membrane			Burgers *et al*., 2012
Myomegalin	Golgi apparatus, centrosome	Cytoskeleton, contractility		Verde *et al*., 2001; Uys *et al*., 2011; Roubin *et al*., 2013

AKAPs comprise a very diverse family of proteins, and over 50 AKAPs have been identified to date in humans (Table 1) with many orthologues found in other species (Wong and Scott, 2004; Tröger *et al*., 2012). At least one AKAP is found in every tissue in the body (Welch *et al*., 2010). The importance of AKAP function is evident in the lethality and severe phenotypes of many AKAP knockout mice (Carnegie *et al*., 2009; Skroblin *et al*., 2010). Lethality is observed in knockout mice for AKAP6, AKAP10, AKAP13, WAVE-1, Ezrin, and Neurobeachin (Skroblin *et al*., 2010). Knockout of AKAP1 and AKAP4 results in infertility in female and male mice, respectively. Severe phenotypes are seen in many knockout mice, including prostate hyperplasia (AKAP12), neurological deficits (MAP2 and AKAP13), and primordial dwarfism (Pericentrin)

(Skroblin et al., 2010). In many cases, diseases associated with AKAP proteins result from an alteration in specific AKAP complexes rather than a global cAMP/PKA signaling change (Tröger *et al*., 2012). Many AKAPs have loose associations with many diseases, but for simplicity only those diseases with a clear connection to an AKAP are included in Table 1. Select AKAPs from Table 1 are discussed below.

AKAP1

AKAP1 (also known as D-AKAP1, AKAP121, AKAP149, AKAP140, AKAP84, and S-AKAP84) was first identified in mammalian spermatozoa, and localizes to the outer mitochondrial membrane (Lin *et al*., 1995) (Figure 4 and Table 1). An amino terminal mitochondrial targeting sequence targets AKAP1 to mitochondria (Huang *et al*., 1997b). Disputing the belief that only PKA type II is scaffolded, AKAP1 was identified as the first dual-specificity AKAP associating with both R_I and R_{II} subunits (Huang *et al*., 1997b; Ma and Taylor, 2008). It was later discovered that AKAP1 also has dual localization to both the ER and mitochondria, achieved by alternatively splicing the amino terminus (Huang *et al*., 1999) and via a bi-functional element that is required for targeting to both organelles (Ma and Taylor, 2002). Localization of AKAP1 to the nuclear envelope has also been observed, though the targeting domain is not identified (Steen *et al*., 2000).

Due to the various subcellular localizations, AKAP1 also has several functions within the cell. AKAP1 at the nuclear envelope scaffolds PKA, protein phosphatase 1 (PP1), and lamins and functions to stabilize the nuclear lamina (Steen *et al*., 2000). Nuclear envelope-targeted AKAP1 serves to maintain the integrity of the nuclear

envelope (Steen *et al*., 2003). AKAP1 also contains an RNA-binding KH domain (Trendelenburg *et al*., 1996) and has been shown to play a role in translation regulation (Ranganathan et al., 2002). AKAP1 also anchors proteins and RNAs at the mitochondrial outer membrane (Ginsberg *et al*., 2003), and this RNA-tethering is important for maintaining the mitochondrial network (Rogne *et al*., 2009). Mitochondrial-targeted AKAP1 regulates cytochrome c release from the mitochondria, with overexpression of AKAP1 protecting cells from apoptosis (Affaitati et al., 2003). Mitochondrial oxidative metabolism is also partially regulated by AKAP1-scaffolded proteins (Livigni *et al*., 2006). When AKAP1 is displaced from the mitochondria it induces mitochondrial dysfunction, resulting in an increase in ROS, and therefore, induced oxidative stress in cardiomyocytes, smooth muscle cells, and hypertrophic mouse hearts *in vivo* (Perrino *et al*., 2010). AKAP1 also plays a protective role in stress response in cardiomyocytes (Rogne *et al*., 2009; Perrino *et al*., 2010). During cellular hypoxia, the proteolytic degredation of AKAP1 is up-regulated to alter the cAMP/PKA signaling at the mitochondria (Carlucci *et al*., 2008b). Loss of AKAP1 expression leads to cardiomyocyte hypertrophy while increased expression protects cells against hypertrophy (Abrenica et al., 2009). Interestingly, AKAP1 has also been linked to oocyte maturation and female infertility, though it remains unclear which subcellular pool functions in these processes (Newhall *et al*., 2006). The full functionality of AKAP1 is an ongoing investigation that will likely yield more correlations to human disease.

Rab32

As the name suggests, Rab32 was originally identified as a Rab GTPase involved in cellular trafficking (Bao *et al*., 2002) (Table 1). Melanocytes, platelets, and mast cells express the highest levels of Rab32 (Cohen-Solal *et al*., 2003), most likely due to the critical role of Rab32 in the formation of granules, such as dense granules in platelets (Ambrosio *et al*., 2012) and pigmentation granules in melanocytes (Cohen-Solal *et al*., 2003). Rab32 is important for post-Golgi trafficking and the vesicular trafficking required for pigmentation (Wasmeier *et al*., 2006). The trafficking facilitated by Rab32 is also critical to the lysosomal degredation of proteins (Bultema *et al*., 2012). Down-regulation of Rab32 occurs in colon cancers (Mori *et al*., 2004) and gastric and endometrial adenocarcinomas (Shibata *et al*., 2006), but the cause or effect of this has not been further investigated. Some evidence suggests Rab32 plays a role in tumor progression, invasion, and metastasis (Hofsli *et al*., 2008).

It was quickly discovered that Rab32 also functions as an AKAP by scaffolding PKA with R_{II} subunits (Alto *et al*., 2002). Rab32 localizes to mitochondria, where it plays a role in mitochondrial dynamics regulation. More specifically, Rab32 localizes to mitochondria-associated membranes (MAMs), the junctions between mitochondria and the endoplasmic reticulum (ER) (Bui *et al*., 2010). There it serves to regulate MAM properties and ER-mitochondria crosstalk. To regulate mitochondrial dynamics, Rab32 interacts with Drp1, a mitochondrial fission protein (Bui *et al*., 2010). Rab32 also has roles in the regulation of ER calcium release and the induction of apoptosis. High expression levels of Rab32 delay apoptosis, while low expression levels of Rab32

accelerate apoptosis (Bui *et al*., 2010). Further investigations are needed to fully understand the complex functions of Rab32 within the cell as well as in human disease.

Pericentrin

Pericentrin (also known as kendrin) was first identified as a protein found in the pericentriolar material and at acentriolar microtubule-organization centers (Doxsey *et al*., 2004; Flory *et al*., 2000) (Table 1). Antibodies against pericentrin can disrupt cell division, which suggests a role for pericentrin in microtubule organization. It is theorized that pericentrin and gamma-tubulin associate with one another and form a reticular lattice at the centrosome that is distinct from the gamma-tubulin ring complex (Dictenberg *et al*., 1998). This lattice changes as a cell progresses through the cell cycle. Pericentrin also interacts with dynein intermediate light chain, and this interaction is necessary for proper microtubule organization (Purohit *et al*., 1999). Pericentrin is a cargo protein for dynein, and this interaction traffics pericentrin to the centrosomes (Young *et al*., 2000). It was later discovered that pericentrin is also an AKAP (Diviani *et al*., 2000). The pericentrin and AKAP centrosomal-targeting (PACT) domain was then identified (Gillingham and Munro, 2000).

The crucial role of centrosomes in cell cycle regulation and microtubule organization is evidenced by the many diseases associated with centrosomal defects. For example, disruption of proper centrosomal function and localization is common in tumor cells, which gives rise to genetic instability (Boveri, 1929; Pihan *et al*., 1998). Because pericentrin is a critical component of centrosomes, pericentrin is also associated with various human diseases. Many tumors have increased pericentrin expression or defects

in pericentrin localization or organization (Pihan *et al*., 1998). Mutations in the pericentrin gene have been directly linked to Majewski/microcephalic osteodysplastic primordial dwarfism type II (MOPDII), in which all patients have loss-of-function pericentrin mutations (Rauch et al., 2008). Patients with MOPDII have an extremely shortened stature of roughly twenty inches and have a much smaller brain for their body size (microcephaly). The pericentrin mutations result in disorganized mitotic spindles and missegregation of chromosomes (Rauch *et al*., 2008). Because the pericentrin gene is located on chromosome 21, researchers have begun investigating whether pericentrin plays a role in Down's Syndrome (Salemi *et al*., 2013). Furthermore, single nucleotide polymorphisms (SNPs) within the pericentrin gene have been linked with schizophrenia (Numata *et al*., 2010). There are also reports of pericentrin mutations or SNPs being associated with other neurological problems such as major depressive disorder (Numata *et al*., 2009). It is likely number of diseases associate with pericetrin mutations will continue to increase.

AKAP9 gene products

I am specifically interested in proteins encoded by the AKAP9 gene. The multiply spliced gene contains 50 exons and is located on chromosome 7q21-22 (Schmidt *et al*., 1999; Witczak *et al*., 1999). There are several splice variants, including yotiao, AKAP350A, AKAP350B, and AKAP350C (Figure 5). AKAP350A and yotiao are the most well-studied splice variants (Table 1). We have previously identified AKAP350B and AKAP350C isoforms as potential splice variants, but their functions have not been studied further (Shanks *et al*., 2002a) (Figure 6).

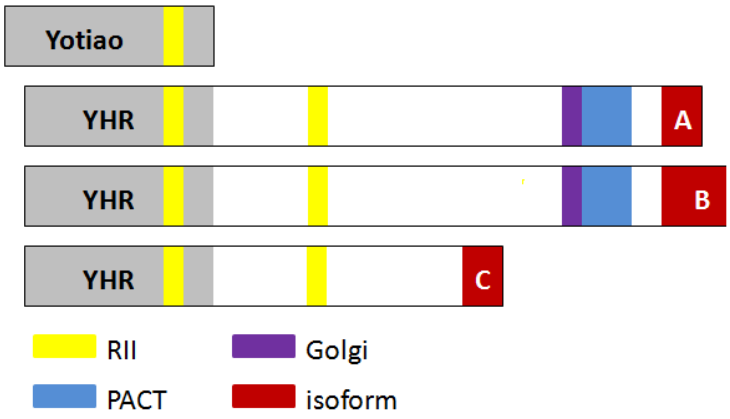

Figure 5. AKAP350 isoforms. Each isoform is determined by the carboxyl-terminus of the protein. Yotiao only contains one R_{II} domain (binding site of PKA regulatory subunit type II). Other domains include YHR (Yotiao homology region), Golgi (Golgi-targeting domain), and PACT (pericentrin and AKAP350 centrosomal-targeting domain).

Yotiao (AKAP9)

Yotiao is the shortest splice variant and was the first AKAP9 gene product discovered (Lin *et al*., 1998) (Figure 5 and Table 1). It is highly expressed in the brain and skeletal muscle, especially at neuromuscular junctions. Yotiao associates with the NMDA (N-methyl-D-aspartate) receptor in neurons, and may assist in the cytoskeletal attachment of the receptor (Lin et al., 1998) (Figure 6). The anchoring of protein phosphatase 1 (PP1) and PKA by yotiao facilitates the regulation of the NMDA receptor (Feliciello *et al*., 1999; Westphal *et al*., 1999). The NMDA receptor is also regulated by Traf2 and NcK interacting kinase (TNiK), which is scaffolded near the receptor via yotiao (Coba *et al*., 2012). Proper yotiao-anchoring of PP1 and other proteins is essential to dopamine-induced calcium flux (Tang and Bezprozvanny, 2004). In the brain, yotiao

also binds to and regulates various adenylyl cyclase isoforms, anchoring isoforms 1, 2, 3, and 9 with an inhibitory effect on isoforms 2 and 3 (Piggott *et al*., 2008).

Yotiao is also highly expressed in the heart and other muscle tissues (Lin *et al*., 1998). Yotiao interacts with KCNQ1 via the leucine zipper region in the carboxyl terminus of yotiao (Marx *et al*., 2002). Yotiao anchors PKA, PP1, and InsP3R1 (inositol 1,4,5 trisphosphate receptor type 1) in close proximity to KCNQ1 to regulate the ion flow through the potassium channel (Marx *et al*., 2002; Tu *et al*., 2004; Chen *et al*., 2007; Piggott *et al*., 2008). A mutation in yotiao disrupting the anchoring of KCNQ1 by Yotiao

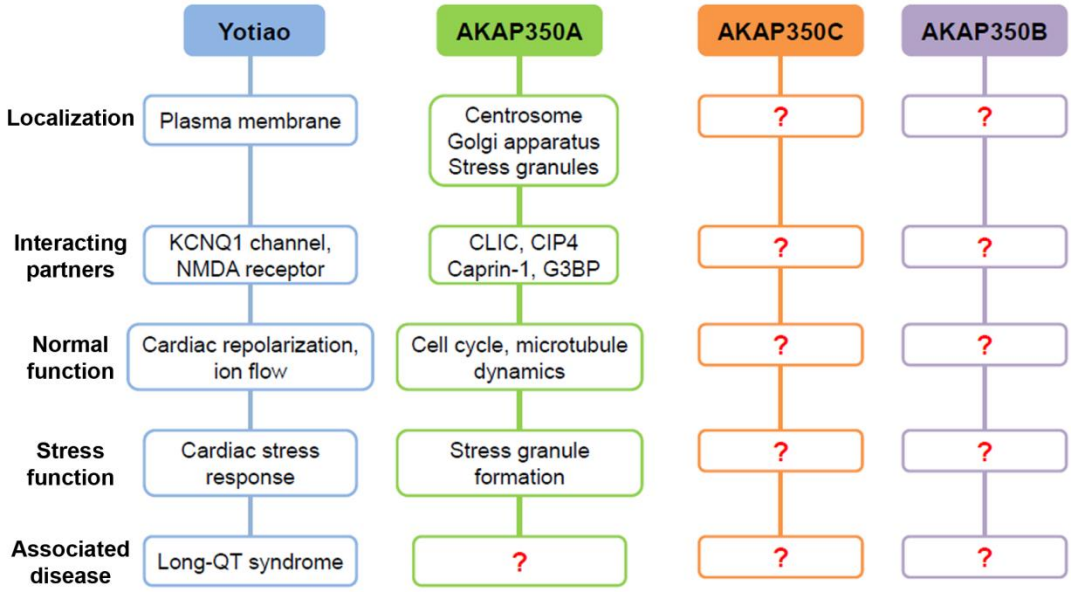

Figure 6. Summary of current knowledge for AKAP9 gene products. AKAP9 gene products include yotiao, AKAP350A, AKAP350B, and AKAP350C. For each, this diagram lists the major sub-cellular localization, select interacting partners, the normal function during non-stress conditions, the function during stress, and diseases directly associated with mutations and/or dysregulation of the protein. For more information, see the text.

leads to long QT syndrome, a potentially fatal heart arrhythmia (Chen *et al*., 2007) (Figure 6). Yotiao also scaffolds PKA, PP1 (Chen *et al*., 2005), and adenylyl cyclase 9 (Li *et al*., 2012) to control the phosphorylation state of the I(Ks) (slowly activating potassium current) channel. The phosphorylation state of I(Ks) channel is a critical regulator of cardiac cell response to stimulation by the sympathetic nervous system. The yotiao-mediated regulation of I(Ks) channel function is regulated by the PKA-mediated phosphorylation of serine-43 in yotiao (Chen *et al*., 2005). These studies suggest yotiao not only acts to scaffold proteins in close proximity to the I(Ks) channel, but also has an active role in regulating channel function (Chen and Kass, 2006). The yotiao-anchored complex of PKA and InsP3R1 also works in concert with the EGFR (epidermal growth factor receptor) to regulate calcium flux by sensitizing cells to epidermal growth factor (EGF) (Hur *et al*., 2005). Due to its regulation of ion flow, yotiao is critical for repolarization of cardiomyocytes, and its dysregulation can lead to chronic heart failure (Tröger *et al*., 2012). Therefore, yotiao is an important regulator in normal cardiac function as well as cardiac stress response (Figure 6).

AKAP350A (AKAP9)

AKAP350A (also known as AKAP450/AKAP9/CG-NAP) was identified shortly after yotiao (Schmidt *et al*., 1999; Witczak *et al*., 1999; Takahashi *et al*., 1999) (Table 1). AKAP350A localizes to the centrosome via the pericentrin and AKAP centrosomal targeting (PACT) domain (Gillingham and Munro, 2000) (Figure 5 and Figure 6). In polarized MDCK (Madin-Darby canine kidney) cells the localization was asymmetrically on one pole of the centrosome (Schmidt *et al*., 1999; Witczak *et al*., 1999). Localization

of AKAP350A to the Golgi apparatus was also observed (Takahashi *et al*., 1999), and a Golgi-targeting domain was identified (Shanks *et al*., 2002a) (Figure 5 and Figure 6). There are currently two PKA R_{II}-binding sites identified in the AKAP350A protein.

Several interacting partners for AKAP350A have been identified though the functions of some interactions have not been elucidated. Transforming acidic coiled-coil-containing protein 4 (TACC4) interacts with and is possibly sequestered by AKAP350A at the centrosome (Steadman *et al*., 2002). AKAP350A interacts with CLIC4 (chloride intracellular channel 4) at the centrosome (Berryman and Goldenring, 2003) and CLIC5B at the Golgi (Shanks *et al*., 2002b) (Figure 6). The function of the CLIC proteins remains ambiguous, and the significance of these interactions has not yet been discovered. The association of AKAP350A with protein kinase C delta (PKC_{δ}) is modulated by the PKA phosphorylation of serine-370 in PCK_{δ}, but the exact function of this interaction is not well known (Giamas *et al*., 2007). AKAP350A also associates with protein kinase N (PKN) (Takahashi *et al*., 1999), protein phosphotase 2A (PP2A) (Takahashi *et al*., 1999), protein kinase C epsilon (PKCε) (Takahashi *et al*., 2000), casein kinase 1 delta/epsilon ($CK1_{\delta/\varepsilon}$) (Sillibourne *et al*., 2002), pituitary tumor transforming gene 1 (PTTG1)/securin (Moreno-Mateos *et al*., 2011), CDK5RAP2 (Wang *et al*., 2010), and Miki (Ozaki *et al*., 2012). The exact functions of these interactions have not yet been elucidated and require further investigation.

AKAP350A is involved in several cellular processes including the cell cycle (Schmidt *et al*., 1999) and microtubule dynamics (Larocca *et al*., 2006). The presence of AKAP350A is required for proper centrosomal function and maintenance, and when AKAP350A is dissociated from centrosomes, centriole duplication and progression of the

cell cycle is significantly impaired (Keryer *et al*. 2003a). Some research suggests Cep72 may be responsible for recruiting AKAP350A to the centrosome (Oshimori *et al*., 2009). AKAP350A recruits cyclin E/cdk2 to the centrosome to regulate centrosome amplification (Nishimura *et al*., 2005). The interaction between AKAP350A and calmodulin likely regulates the structure and composition of the centrosomal matrix (Moisoi *et al*., 2002; Takahashi *et al*., 2002). AKAP350A also anchors PDE4D3 (phosphodiesterase 4D3) at the centrosome, and this interaction is involved in regulation of cAMP signaling at the centrosome and cell cycle progression (Taskén *et al*., 2001; McCahill *et al*., 2005; Terrin *et al*., 2012). In conjunction with pericentrin, AKAP350A anchors the gamma-tubulin ring complex at the centrosome and helps create the microtubule nucleation center (Takahashi *et al*., 2002). Cyclin G2 is potentially scaffolded with PP2A by AKAP350A to regulate microtubule stability and cell cycle progression (Arachchige *et al*., 2006). The small GTPase, Ran, (Keryer *et al*., 2003b) and CM1 (CM-myomegalin) (Roubin *et al*., 2013) are anchored at the centrosome by AKAP350A, and these interactions function in microtubule organization.

AKAP350A is also important for microtubule organization at the Golgi apparatus, as well as maintenance of the integrity and structure of the Golgi (Larocca *et al*., 2006; Rivero *et al*., 2009). These effects are partly through the interaction of AKAP350A with CIP4 (Cdc42 interacting protein 4) (Larocca *et al*., 2004) (Figure 6). AKAP350A localizes to the Golgi in a microtubule-dependent manner through interactions with the dynein-dynactin complex, specifically via the p150(Glued) subunit (Kim *et al*., 2007). Once there, AKAP350A is anchored to the Golgi via interaction with gm130, a cis-Golgi protein (Rivero *et al*., 2009). Overexpression of gm130 increases the amount of Golgi-

localized AKAP350A, and this increases the size of the Golgi (Roy *et al*., 2012). AKAP350A is required for proper structure, positioning, and function of the pericentrosomal Golgi ribbon, which is critical for directional migration and ciliogenesis this structure (Hurtado *et al*., 2011).

Some cell-specific functions of AKAP350A have also been identified. First, AKAP350A normally localizes at the centrosome and Golgi apparatus in T-cells, but upon activation of T-cell migration, AKAP350A is redistributed along microtubules in trailing cell extensions (El Din El Homasany *et al*., 2005). There, AKAP350A localizes with tubulin, PKC, and LFA-1 integrin, an activator of T-cell migration, to partially regulate T-cell migration. AKAP350A also serves to organize and regulate the activation of receptor proteins at the immune synapse during T-cell activation (Robles-Valero *et al*., 2010). Second, in cerebellar granule cells, AKAP350 scaffolds PKA and phosphotases in proximity to InsP3R1 to regulate calcium flux (Collado-Hilly and Coquil, 2009). Third, in epithelial cells, AKAP350A regulates the formation of new adhesions by regulated the activity of Epac-1 (exchange protein directly activated by cAMP-1) (Sehrawat *et al*., 2011). Finally, AKAP350A is critical for the formation of canaliculi in hepatocytes (Mattaloni *et al*., 2012). Knock-down of AKAP350A in hepatocytes disrupts the organization of filamentous-actin and inhibits the formation of canaliculi. These data show AKAP350A has both ubiquitous and cell-specific functions during normal conditions.

AKAP350A is also involved in cellular stress response, specifically RNA stress granule formation (Kolobova *et al*., 2009) (Figure 6). There is a cytosolic pool of AKAP350A that relocates to stress granules upon cellular stress. Under normal and

stressed conditions, AKAP350A associates with other stress granule proteins such as Caprin-1 (cytoplasmic activation/proliferation-associated protein-1) and CCAR1 (cell cycle and apoptosis regulatory protein 1) (Kolobova *et al*., 2009) (Figure 6). AKAP350A also associates with mRNAs in the absence and presence of stress, suggesting AKAP350A also functions to bring mRNAs into stress granules for sequestration (Kolobova *et al*., 2009). Upon stress, there is also a loss of AKAP350A from the Golgi and fragmentation of the Golgi. A decrease in the expression of AKAP350A leads to smaller, incomplete stress granules, suggesting AKAP350A is necessary for complete stress granule formation (Kolobova *et al*., 2009; Mason *et al*., 2011). AKAP350A appears to serve many functions within cells, during stressed and non-stressed conditions.

AKAP9 and disease

The AKAP9 gene is associated with many diseases. The only direct functional connection of an AKAP9 protein to disease is yotiao mutations in patients with long QT syndrome (Chen *et al*., 2007) (Figure 6 and Table 1). However, there are several indirect associations of AKAP9 gene products with various diseases that require further investigation. An AKAP9-BRAF fusion has oncogenic effects by activating the MAPK (MAP kinase) pathway in radiation-associated thyroid papillary carcinoma (Ciampi *et al*., 2005; Fusco *et al*., 2005). This fusion occurs via a paracentric inversion of the chromosome 7 long arm leading to a fusion of exons 1-8 of AKAP9 and exons 9-18 of BRAF. This fusion causes constitutive BRAF serine/threonine kinase activity because it removes the amino-terminal autoinhibitory portion of BRAF (Ciampi *et al*., 2005). The role, if any, of the AKAP9 portion of this fusion protein in the development and

progression of thyroid cancer remains unclear. Single nucleotide polymorphisms (SNPs) occurring in the AKAP9 gene have been associated with an increased risk of lung (Rudd *et al*., 2006; Truong *et al*., 2010) and breast (Frank *et al*., 2008a; Milne *et al*., 2011) cancers, as well as metastatic melanoma (Kabbarah *et al*., 2010). An increased risk of alcohol dependence has been associated with SNPs occurring in the AKAP9 gene in European Americans (Kendler *et al*., 2011). Most recently, AKAP9 SNPs have been linked to an increased risk for schizophrenia (Costas *et al*., 2013). The validity and mechanism of these associations remain unclear. AKAP9 SNPs have also been linked to colorectal cancer (Webb *et al*., 2006), though other studies refute those findings (Frank *et al*., 2008b). There is also a role for AKAP9 proteins in the formation of lung fibrosis that requires further investigation (Okunishi *et al*., 2011). Knockout mouse studies have also shown that AKAP9 is essential for spermatogenesis and the maturation of sertoli cells (Schimenti *et al*., 2013). Further investigations are needed to identify more roles for AKAP9 proteins in disease, as well as to clarify the associations already discovered.

Rationale and Aims

As demonstrated in Figure 6, many aspects of the AKAP9 gene products remain to be investigated. Of the AKAP350 splice variants, AKAP350A is the most studied. However, the literature on AKAP350A is eclectic and implies many different interacting proteins and many different roles within the cell. Further data is needed to begin connecting the pieces of literature together. Given the many potential roles of AKAP350A within the cell, a greater understanding of AKAP350A would provide a greater understanding of master-regulatory proteins and the interconnectedness of various

signaling pathways. The role of AKAP350A in stress response is a relatively new area of research, and the exact mechanisms and roles require further definition. This knowledge would provide a better view of proteins with dual functions during stressed and non-stressed conditions, as well as the molecular switch that occurs to activate stress responses. Also, AKAP350A has yet to be directly linked to a disease though a connection likely exists (Figure 6).

Two very obvious gaps in AKAP9 knowledge are the AKAP350B and AKAP350C splice variants, of which nothing is known (Figure 6). To begin, the complete sequence of each splice variant remains unidentified, as does the sub-cellular localization. Once these are known, work can begin on elucidating the roles of both splice variants. Investigating these splice variants will allow us learn the similarities and differences among the AKAP9 splice variants. Both yotiao and AKAP350A have distinct roles during non-stress and stress conditions (Figure 6). I hypothesize that all AKAP9 splice variants have dual roles within cells, with distinct roles during non-stress and stressed conditions.

To test this hypothesis, I developed several aims. First, I further investigated the mechanism of involvement for AKAP350A in stress granule formation, maintenance, and dispersal. Second, I elucidated the roles of AKAP350C during non-stressed and stressed conditions. Third, I developed a mouse to knock out or conditionally knock out all known AKAP9 gene products. This mouse will be a tool to investigate the roles of AKAP9 splice variants in whole-organism development and disease.

This body of work further investigates the roles of AKAP9 splice variants in stress response. Chapter II further investigates the mechanisms of stress granule

formation, maintenance, and dispersal, including the localization of AKAP350A during these processes. This work also details the use of Darinaparsin-treatment as a tool to further study the role of AKAP350A in stress granule processes. In Chapter III, we complete cloning of AKAP350C and characterize its targeting and association with mitochondria. AKAP350C plays a role in regulation of mitochondrial dynamics, and this adaptive system is important in regulating the mitochondrial response to stress. Indeed, AKAP350C also serves as a regulator of stress-induced apoptosis. The importance of the AKAP9 gene products in cellular stress response is evident, and it is important to learn as much as possible about these proteins and their roles within those responses. Chapter IV details two stories of phosphorylation data gathered throughout our investigations. Caprin-1 is phosphorylated within the AKAP350A complex in response to ultraviolet light irradiation. Also, a third, novel PKA-binding site within the AKAP350 splice variants was discovered. As it is integral to study the function of a protein within an organism as a whole, Chapter V details the development and partial characterization of AKAP9-null and AKAP9$^{F/F}$ mice. These mice are tools for studying the roles of AKAP9 proteins in organism development and disease. In conclusion, AKAP9 splice variants play dual roles in cells during non-stress and stressed conditions, and are required for proper stress response.

CHAPTER II

DARINAPARSIN IS A MULTIVALENT CHEMOTHERAPEUTIC WHICH INDUCES INCOMPLETE STRESS RESPONSE WITH DISRUPTION OF MICROTUBULES AND SHH SIGNALING

Appears as: Mason TA, Kolobova E, Liu J, Roland JT, Chiang C, and Goldenring JR. (2011) Darinaparsin is a multivalent chemotherapeutic which induces incomplete stress response with disruption of microtubules and Shh signaling. *PLoS One*, **6**, e27699

Introduction

All cells experience various stressors during their physiological processes. Stress is a ubiquitous problem and can trigger a range of responses within cells. Common stressors include heat shock, oxidative conditions, viral infection, hypoxia, mitochondrial stress, DNA-damaging agents, and ultraviolet irradiation (Kolobova *et al*., 2009; Kedersha and Anderson, 2007). Chemotherapeutic drugs and other pharmaceuticals are other common sources of cellular stress.

Arsenicals are one category of chemotherapeutics undergoing continual investigation. Organic and inorganic arsenicals have been used in the treatment of disease for thousands of years (Verstovsek *et al.*, 2006; Tsimberidou *et al*., 2009). However, arsenicals are typically very potent and their toxicity typically limits their use (Tsimberidou *et al*., 2009; Campàs and Castañer, 2009). Currently, arsenic trioxide (ATO, As2O3), an inorganic arsenical, is used for treatment in cases of recurrent acute promyelocytic leukemia (Mann *et al*., 2009). This drug is limited by its toxicity on the liver and cardiovascular system. Because of these toxicity issues, the development of less toxic arsenicals has become an area of great interest.

Darinaparsin (ZIO-101, S-dimethylarsino-glutathione) is an organic arsenical that is currently in Phase II clinical trials as a chemotherapeutic agent (Campàs and Castañer, 2009; Wu *et al*., 2010). While darinaparsin shows clinical promise, the drug's mechanism of action continues to be investigated. A series of in vitro and in vivo studies, coupled with observed differences in toxicity and potency, suggest darinaparsin employs a mechanism of action that is different from that of ATO. Darinaparsin appears more potent than ATO as some ATO-resistant cells are sensitive to the drug. Moreover, other cell types have shown an increased sensitivity to darinaparsin compared to ATO (Campàs and Castañer, 2009; Mann *et al*., 2009; Diaz *et al*., 2008; Matulis *et al*., 2009). Importantly darinaparsin does not demonstrate the same level or type of toxicity as ATO with no apparent toxicity to the liver or cardiovascular system.

Previous studies have shown that both ATO and darinaparsin cause apoptosis and cell cycle arrest at G2/M in tumor cells (Tsimberidou *et al*., 2009; Mann *et al*., 2009). This effect is thought to occur in part through the disruption of mitochondrial functions, which leads to increased production of reactive oxygen species (ROS) (Quintás-Cardama *et al*., 2008). An increase in ROS, if great enough, can trigger a cellular stress response. Recent preclinical studies of darinaparsin have shown anti-angiogenic activity in vitro and in vivo through controlling several signal transduction pathways and that darinaparsin is more potent than ATO under hypoxic conditions (Mann *et al*., 2009; Tian *et al*., 2010).

One critical mechanism in the cellular stress response is the formation of RNA stress granules. Stress granules function to sequester mRNAs and proteins during cellular stress. Importantly, stress granules are not stable structures, but are dynamic with

a constant flux of proteins and mRNAs. Stress granules are generally composed of a variety of preinitiation- and translation-related factors, proteins linked to mRNA metabolism, mRNAs, and RNA-binding proteins, as well as signaling proteins with no known link to mRNA (Kedersha and Anderson, 2007). Typically, proteins and mRNAs necessary for cell survival during stress, such as heat shock proteins, are not sequestered in stress granules. The mRNAs are sequestered in stress granules until the cell is no longer stressed or undergoes apoptosis (Thomas *et al*., 2011). Once stress is no longer present, stress granules disperse, and the sequestered mRNAs can be translated. Other RNA granules also exist in cells without stress, such as processing bodies (P-bodies) (Kolobova *et al*., 2009). The different RNA granules do contain unique components, with stress granules containing components specialized for adaptation to dynamic stressors. Though stress granule formation appears to be a ubiquitous cellular response, the mechanisms regulating formation, maintenance, and dispersal remain largely obscure.

In this study, we examined both the mechanism of action for darinaparsin and the dynamics of stress granules formation, maintenance, and dispersal. We propose that darinaparsin is a potent chemotherapeutic because it initiates a stress response, while also stalling the completion of the stress response by simultaneously depolymerizing microtubules. The depolymerization of microtubules causes the stress granules to form incompletely, preventing the coalescence of stress granule components. When darinaparsin is withdrawn, stress granules progress to final coalescence as microtubules repolymerize and disperse only after complete granule formation. In addition, likely due to microtubule depolymerization, darinaparsin causes a loss of primary cilia and a

reduction in Shh signaling. These findings support the concept that darinaparsin is a multivalent chemotherapeutic affecting several critical processes in neoplastic cells.

Results

Darinaparsin and sodium arsenite induce stress granule formation.

Since darinaparsin is an organic arsenical, we first sought to evaluate whether darinaparsin could elicit RNA stress granules. To determine the effect of darinaparsin on cells, we treated cells with darinaparsin and compared its effects to those of sodium arsenite. Treatment of HeLa cells with 0.05 mM darinaparsin for 30 minutes induced stress granule formation, detected with antibodies against G3BP (Figure 7). A titration of darinaparsin for short incubations showed stress granule formation was induced in a majority of cells at 0.03 mM. Sodium arsenite treatment at 0.5 mM induced stress granule formation, as previously reported (Kolobova *et al*., 2009; Kedersha and Anderson, 2007). Nevertheless, the stress granules induced by darinaparsin appeared smaller and were significantly greater in number when compared to sodium arsenite-induced stress granules, and the granules were more dispersed throughout the cytoplasm (Figure 7E).

As noted above, stress granule formation is a dynamic process. Upon initial stress granule induction, many small granules form throughout the cytoplasm. As stress continues, the smaller granules coalesce near the nucleus to form large, complete stress granules (Kolobova *et al*., 2009). The large, complete stress granules generally have similar compositions, but the smaller granules can vary in composition (Kolobova *et al*., 2009). Because stress granules can vary in composition, we evaluated the stress granules

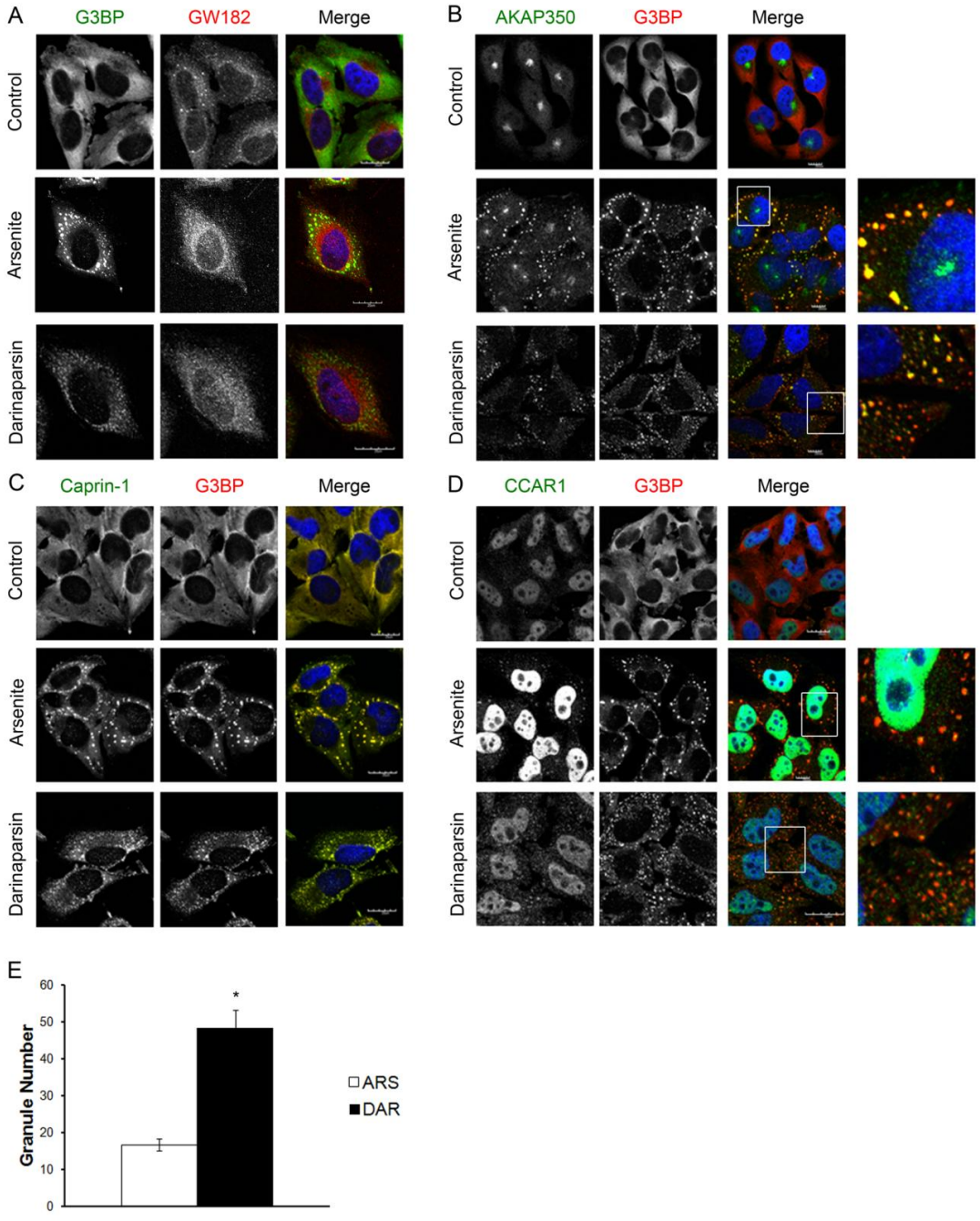

Figure 7. Darinaparsin and sodium arsenite induce RNA stress granules. HeLa cells were treated with 0.5 mM Sodium arsenite or 0.05 mM darinaparsin for 45 minutes at 37°C. Cells were fixed with supplemented 4% PFA. All cells are stained for DNA with Dapi (blue) and **A)** G3BP (green) and GW-182 (red), **B)** AKAP350 (green) and G3BP (red), **C)** Caprin-1 (green) and G3BP (red), **D)** CCAR1 (green) and G3BP (red). **E)** The number of granules in sodium arsenite- and darinaparsin-treated cells was quantified using ImageJ software. Results are mean +/- standard error. *p<0.0001 vs. sodium-arsenite (Scale bars: 20 µM)

induced by darinaparsin in HeLa cells compared with stress granules induced by sodium arsenite, and cells that received no treatment served as a control (Figure 7). We first studied the association of markers of Processing bodies (P bodies) with induced stress granules. P-bodies serve as RNA degradation centers and are present in the absence or presence of cellular stress (Kolobova *et al*., 2009; Anderson and Kedersha, 2006). Stress granules and P-bodies are separate entities, but they do communicate with one another and are dynamically linked (Kedersha *et al*., 2005). To ensure the granules induced by darinaparsin were not P-bodies, we compared staining of a P-body marker, GW182, and a stress granule marker, G3BP (Figure 7A). In untreated cells, GW182-stained P-bodies were small and distributed throughout the cytoplasm, while G3BP was diffuse throughout the cytosol. Sodium arsenite treatment induced large G3BP-staining stress granules that clustered in the perinuclear region. Only a few of the larger stress granules showed dual immunostaining with both G3BP and GW182. Similarly, there was little overlap between the smaller darinaparsin-induced granules and GW182-labelled P-bodies.

We next examined the presence of proteins previously found in stress granules in the granules induced by darinaparsin. AKAP350A, a large scaffolding protein, localizes to stress granules and is important for their complete formation (Kolobova *et al*., 2009). Knockdown of AKAP350A with siRNA results in smaller stress granules upon treatment with sodium arsenite. AKAP350A colocalized with G3BP in stress granules induced by sodium arsenite (Figure 7B). After darinaparsin treatment, some granules contained both AKAP350A and G3BP, while others contained only one of the components. Granules containing only one component were typically smaller and in the periphery of the cytoplasm. AKAP350A interacts with RNA-binding proteins Caprin-1 and CCAR1, both

of which are also present in stress granules (Kolobova *et al*., 2009; Solomon *et al*., 2007; Rishi *et al*., 2003). Caprin-1 colocalized with G3BP in stress granules induced by both sodium arsenite and darinaparsin (Figure 7C). CCAR1 and G3BP colocalized in stress granules induced by sodium arsenite (Figure 7D). However, as with AKAP350A, in darinaparsin-treated cells some stress granules contain both CCAR1 and G3BP, but many smaller granules stained for only one of the components.

Darinaparsin inhibits microtubule polymerization.

In previous studies, we have shown that microtubules are necessary for complete stress granule formation (Kolobova *et al*., 2009). Pre-treatment of cells with nocodazole, which inhibits microtubule polymerization, prior to treatment with sodium arsenite, leads to the formation of stress granules which are smaller and greater in number. The smaller granules suggest incomplete stress granule formation. The similarity between darinaparsin-induced and nocodazole/sodium arsenite-induced stress granules led us to hypothesize that darinaparsin induces incomplete stress granule formation due to microtubule depolymerization. Immunofluorescence in HeLa cells demonstrated that treatment with darinaparsin did induce microtubule depolymerization along with inducing stress granule formation (Figure 8A). In cells treated with darinaparsin, microtubules were almost completely depolymerized, showing mainly cytosolic alpha-tubulin staining. In contrast, sodium arsenite treatment had no demonstrable effect on microtubules.

To verify the effects of darinaparsin on microtubules, we assessed in vitro microtubule polymerization (Figure 8B). Darinaparsin inhibited GTP-stimulated microtubule polymerization in a concentration-dependent manner. Darinaparsin also

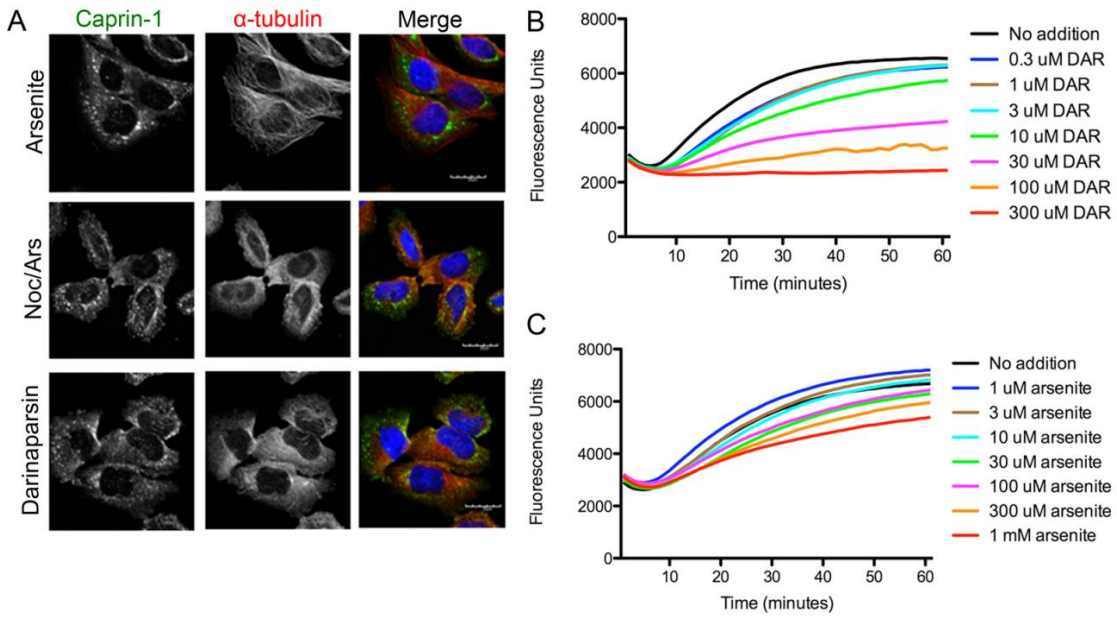

Figure 8. Darinaparsin inhibits microtubule polymerization. A) HeLa cells were treated with 0.5 mM Sodium arsenite or 0.05 mM darinaparsin, or 33 nM Nocodazole/ 0.5 mM Sodium arsenite. Cells are stained for DNA (Dapi, blue), a-tubulin (red), and Caprin-1 (green; stress granule marker). GTP-initiation of microtubule polymerization in the presence of darinaparsin **(B)** and sodium arsenite **(C)** was measured *in vitro*. (Scale bars: 20 µM)

inhibited polymerization of microtubules stimulated by taxol, a microtubule stabilizer, at similar concentrations (data not shown). These results suggest that darinaparsin sequesters free tubulin monomers, similar to the action of nocodazole (Xu *et al*., 2002). In contrast, sodium arsenite had only minimal effect on microtubule polymerization at concentrations up to 1 mM (Figure 8C). Importantly, darinaparsin had no ability in vitro to depolymerize already polymerized microtubules (data not shown).

Stress granules must complete formation before dispersal.

We have previously shown that stress granules initially form as small granules in the cytosol, that then coalesce into the final, complete stress granules in the perinuclear region (Kolobova *et al*., 2009). We now sought to evaluate stress granule dynamics further by investigating their dispersal once stress is relieved. Because darinaparsin,

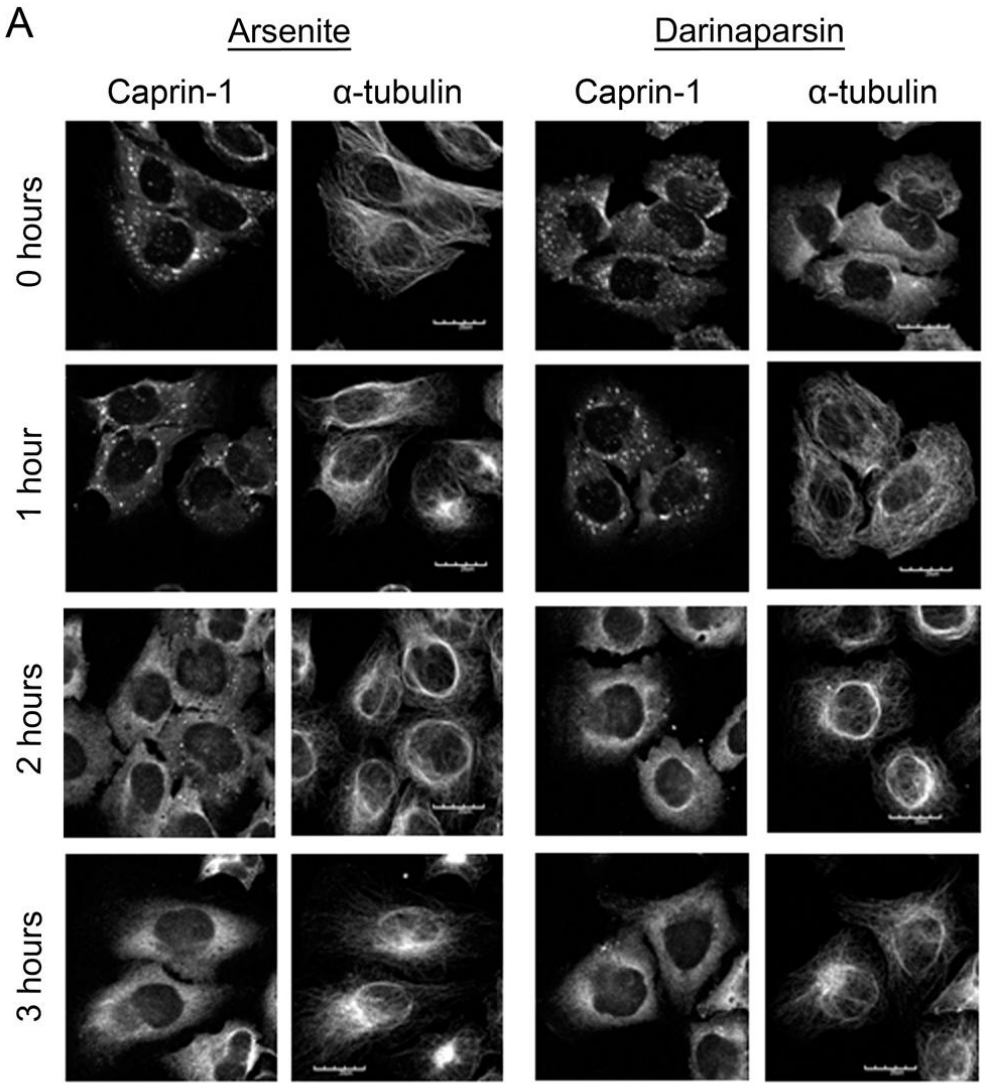
A
Arsenite
Darinaparsin
Caprin-1
α-tubulin
Caprin-1
α-tubulin
0 hours
1 hour
2 hours
3 hours

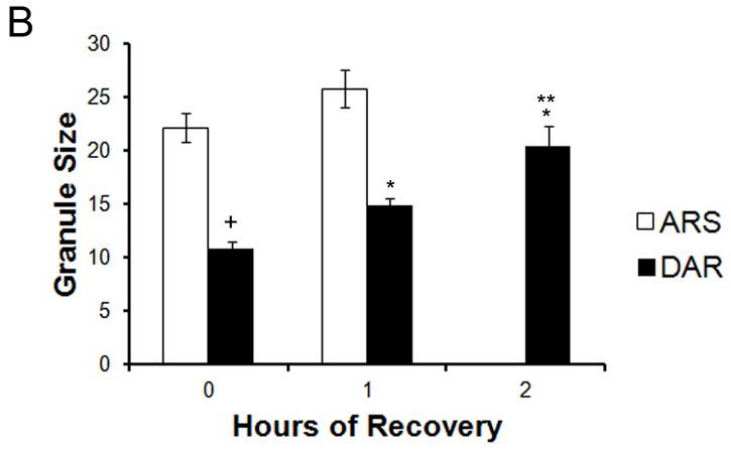
B
Granule Size
30
25
20
15
10
5
0
+
*
**
*
0
1
2
Hours of Recovery
ARS
DAR

Figure 9. Stress granules must complete formation before dispersal. HeLa cells were treated with 0.5 mM Sodium arsenite or 0.05 mM darinaparsin. The 0 hour timepoint was taken at the end of treatment. For recovery, cells were incubated in complete RPMI media. Cells were fixed at timepoints with supplemented 4% PFA and stained for Caprin-1 and α-tubulin **(A)**. **B)** Granule size was quantified for each hour of recovery using ImageJ software. There were no granules at 2 hours of recovery from sodium arsenite. Results are mean +/- standard error. +$p<0.0001$ vs. sodium arsenite-treated. *$p<0.0001$ vs. darinaparsin 0 hours of recovery. **$p<0.0001$ vs. darinaparsin 1 hour of recovery. (Scale bars: 20 μM)

sodium arsenite, and nocodazole/sodium arsenite have differing effects, we monitored the dynamics of stress granule formation and dispersal during each treatment.

We assessed the course of recovery of HeLa cells after treatment with 0.05 mM darinaparsin, 0.5 mM sodium arsenite, or a combination of 33 nM nocodazole and 0.5 mM sodium arsenite. Cells were fixed at the end of treatment for 45 minutes and after periods of recovery without treatment for up to three hours in complete media (Figure 9). At the end of treatment, sodium arsenite-treated cells had large, complete stress granules and intact microtubules, as expected (Figure 9). After recovering without drug for one hour, the sodium arsenite-treated cells showed fewer stress granules, and by two hours of recovery, the stress granules had completely dispersed into the cytoplasm. The microtubules remained unaffected by the sodium arsenite treatment for the duration of the experiment.

In cells treated with darinaparsin, the microtubules were depolymerized and stress granules were significantly smaller than sodium arsenite-induced stress granules at the end of treatment (Figure 9). After one hour of recovery in the absence of drug, the microtubules in cells treated with darinaparsin were repolymerized, and larger stress granules were now observed, especially in the perinuclear region. After three hours of

recovery, darinaparsin treated cells fully recovered with dispersal of stress granules. Similar results were obtained in recovery from the combination of treatment with both nocodazole and sodium arsenite, but recovery occurred more slowly (data not shown). The dynamics of stress granule formation are more clearly seen in continuous live cell imaging. Similar to data shown in Figure 9, live cell imaging demonstrates that following removal of darinaparsin, small G3BP-labeled stress granules first coalesced in the perinuclear region and then dispersed (data not shown). These results suggest that stress granules must complete formation by coalescence along microtubule-dependent tracks before they can disperse into the cytoplasm.

Darinaparsin affects Sonic Hedgehog signaling.

Recent investigations have reported that ATO inhibits hedgehog signaling (Beauchamp *et al*., 2011; Kim *et al*., 2010). We sought to investigate whether darinaparsin also affects hedgehog signaling. Previous studies have shown that ATO does not affect primary cilium formation in mouse embryonic fibroblasts (MEFs) (Beauchamp *et al*., 2011). To test the effects of darinaparsin on primary cilia, NIH 3T3 cells were grown and induced to form primary cilia. The cells were treated with 100 nM Smoothened Agonist (SAG) with or without 600 nM or 1 μM darinaparsin for 24 hours (Ehtesham *et al*., 2007). The concentration of darinaparsin needed for long incubations was titrated, and 600 nM was the optimal concentration to have an effect while not causing cell death. Fixed cells were stained for Arl13b to mark primary cilia. Unlike cells treated with ATO, cells treated with 600 nM darinaparsin had a significant decrease in the number of primary cilia. There was further loss of primary cilia at 1 μM

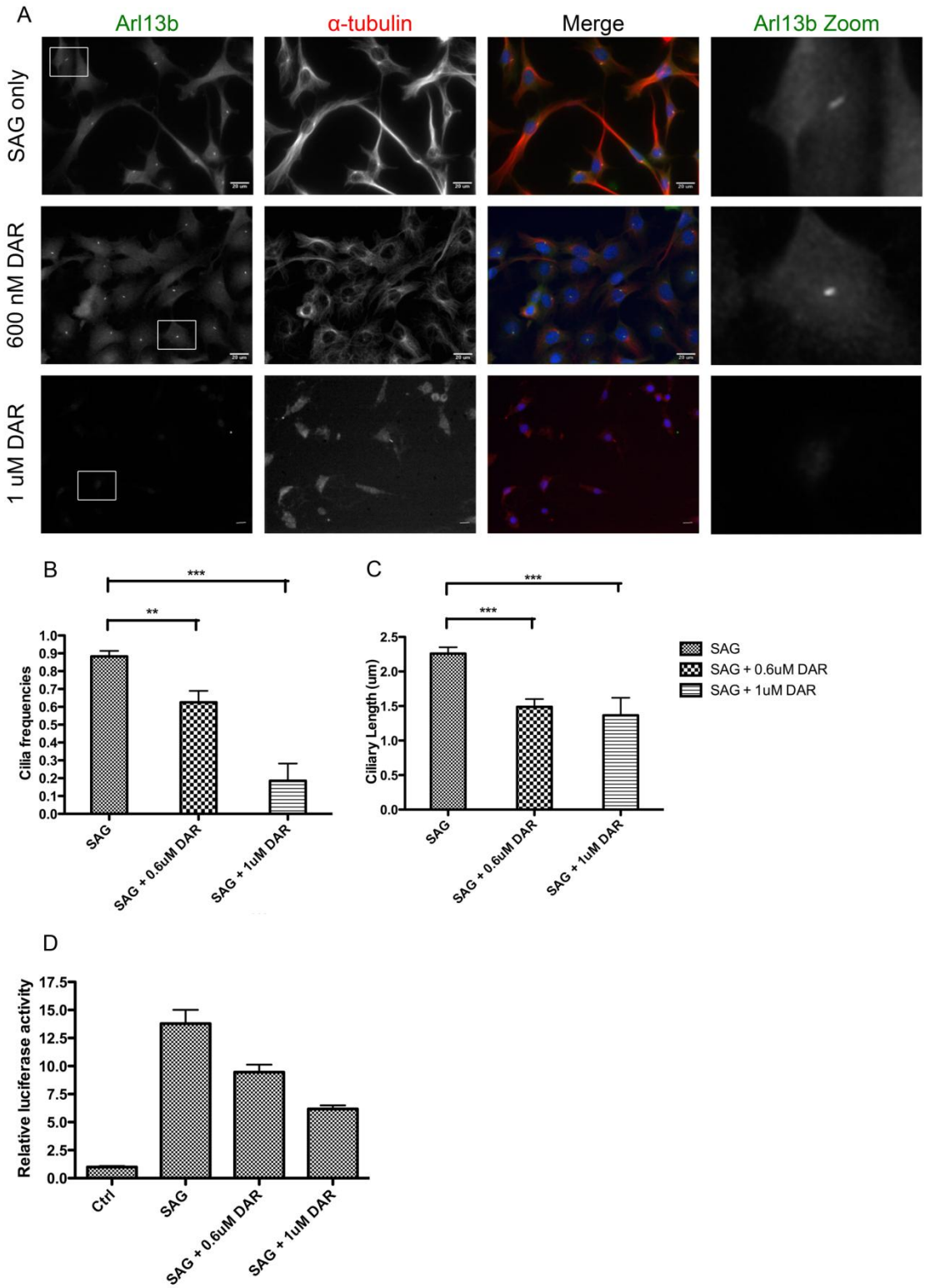
A
Arl13b
α-tubulin
Merge
Arl13b Zoom
SAG only
600 nM DAR
1 uM DAR
B
Cilia frequencies
SAG
SAG + 0.6uM DAR
SAG + 1uM DAR
C
Ciliary Length (um)
SAG
SAG + 0.6uM DAR
SAG + 1uM DAR
D
Relative luciferase activity
Ctrl
SAG
SAG + 0.6uM DAR
SAG + 1uM DAR

Figure 10. Darinaparsin inhibits Sonic Hedgehog signaling and primary cilia formation. NIH 3T3 fibroblasts were treated with 100 nM SAG (Shh agonist) with or without 0.6 μM or 1 μM darinaparsin (ZIO-101). **A)** Cells were fixed with 4% PFA and stained for DNA (Dapi; blue), primary cilia (Arl13b; green), and α-tubulin (red). **B)** The number of primary cilia was determined from 6 samples per genotype (15-30 cells per sample). **C)** The length of primary cilia was determined using Image J software. P values were calculated using unpaired t-test with n–1 degree of freedom (GraphPad). **p<0.005, ***p<0.0001. **D)** Luciferase assays were performed in the absence or presence of darinaparsin. (Scale bars: 20 μM)

darinaparsin, suggesting a concentration-dependent decrease in primary cilia (Figure 10). In darinaparsin-treated cells that did form primary cilia, the primary cilia were shorter in length. Similar to ATO (Beauchamp *et al*., 2011), darinaparsin treatment did not alter the intracellular localization of Gli1 (data not shown). Given the loss of primary cilia observed with darinaparsin treatment, we also evaluated the drug's effect on Shh signaling through an assay of Gli1 activation. Figure 10 demonstrates that darinaparsin elicited a concentration-dependent inhibition of Shh signaling, as seen with ATO (Kim *et al*., 2010). These results indicate that darinaparsin has broad effects on stress granule formation, microtubule dynamics and Shh signaling.

Darinaparsin effects are independent of Mdr1 expression.

Darinaparsin is a multivalent drug that appears to be more potent than similar drugs, such as ATO. Therefore, we tested its efficacy in cells with multiple drug resistance. Multiple drug resistance transporters are often a limiting factor on the practical efficacy of chemotherapeutic agents, especially in recurrent cancers (Chan *et al*., 2006).While ATO is used to treat hematological malignancies, its use is limited in cancers expressing the multiple drug resistance protein, MRP-1 (Diaz *et al*., 2008). MRP1-expressing cells are resistant to ATO treatment, but are sensitive to treatment with

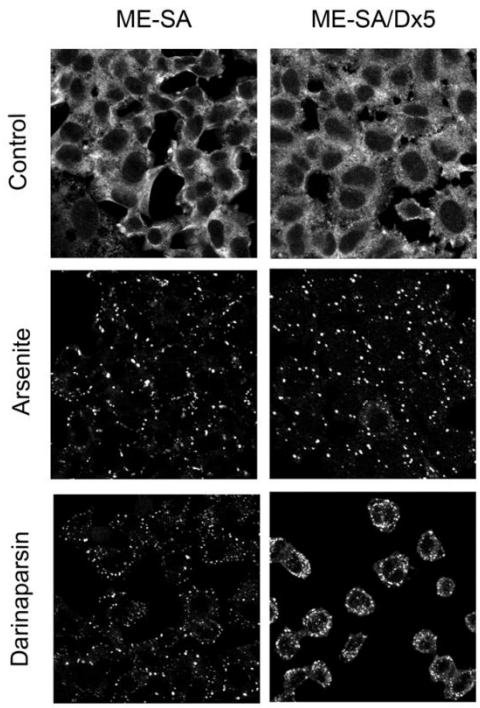

Figure 11. Darinaparsin is effective in Mdr-1-expressing cells. ME-SA and ME-SA/Dx5 cells were untreated or treated with 0.5 mM Sodium arsenite or 0.05 mM darinaparsin for 30 minutes at 37°C. Cells were fixed with supplemented 4% PFA and stained for G3BP.

darinaparsin (Diaz *et al*., 2008). This prompted us to examine another major drug resistance protein, Mdr1, which can rapidly pump drugs out of resistant cancer cells.

Previous investigations have shown that ATO is not a substrate for Mdr1, and thus is effective in Mdr1-expressing cells (Chan *et al*., 2006). We evaluated the effects of darinaparsin on stress granule formation in uterine sarcoma cells lines with or without expression of Mdr1. Figure 11 demonstrates that darinaparsin and sodium arsenite induced stress granules in both ME-SA cells, which do not express Mdr1, and ME-SA/Dx5 cells, which strongly over-express Mdr1. Indeed, the Mdr1-over-expressing cells appeared to be more susceptible to darinaparsin treatment as shown by the rapid rounding up of these cells after treatment. Along with previous studies, these results

demonstrate that darinaparsin effects are not altered by expression of multiple-drug resistance transporters.

Discussion

Arsenic salts are one of the oldest pharmaceutical classes (Verstovsek *et al.*, 2006). Treatment with arsenicals has been utilized for both infectious diseases and cancer. While ATO is approved for treatment of refractory leukemias, its toxicity limits its use (Mann *et al*., 2009). In contrast, darinaparsin, an organic arsenical, shows a wide range of potency against many cancer cells and has low toxicity when administered in humans (Mann *et al*., 2009). While darinaparsin induces apoptosis and G2/M arrest in a number of cell lines, the exact mechanism responsible for the anti-neoplastic effects of the compound seem to vary according to cell types (Mann *et al*., 2009). The present investigation indicates that darinaparsin acts as a multivalent pharmaceutical that induces a stress response, but does not permit its completion due to its influence as a microtubule polymerization inhibitor. Microtubule depolymerization by darinaparsin also causes loss of primary cilia and Shh signaling. The effect on Shh signaling is probably due to the loss of Smoothened presentation on primary cilia. Inhibition of microtubule polymerization by darinaparsin likely accounts for the arrest of cells in G2/M noted in previous studies (Mann *et al*., 2009). The G2/M arrest is characteristic of microtubule depolymerization inhibitors such as nocodazole (Jordan *et al*., 1992). Together these effects make this organic arsenical drug a potent chemotherapeutic with multiple mechanisms that target key regulators of neoplasia.

Formation of RNA stress granules following various cellular stressors is considered a critical adaptive mechanism in cell survival. Stress granules accumulate translational intermediates including critical mRNAs that are important for reestablishment of cell function after the release of stress (Kedersha and Anderson, 2007). Darinaparsin induces stress granule formation and simultaneously inhibits microtubule polymerization. This scenario leads to incomplete formation of stress granules. The inability to form stress granules or incomplete stress granule formation likely leads to apoptosis in affected cells (Thomas *et al*., 2011). Importantly, the unique property of darinaparsin to stimulate incomplete stress granule formation has allowed us to investigate the process of stress granule processing after removal of the blockade. Removal of darinaparsin led to completion of stress granule formation, with coalescence of smaller granules into larger perinuclear granules, coincident with the repolymerization of microtubules. These results are consistent with our previous results that stress granules form initially in the cell periphery and then coalesce after centripetal transport along microtubule tracks (Kolobova *et al*., 2009). Following withdrawal of darinaparsin, stress granules only dissipated after completion of granule formation. These findings indicate that stress granules must complete their full program of formation and coalescence prior to subsequent disassembly.

Recent investigations have noted that arsenic trioxide can inhibit Shh signaling (Beauchamp *et al*., 2011; Kim *et al*., 2010). Similarly, we have observed that darinaparsin also strongly inhibits Shh-induced Gli1 expression. Nevertheless, in contrast with arsenic trioxide, darinaparsin also causes the loss of microtubules and the primary cilium, the site of Smoothened presentation (Beauchamp *et al*., 2011; Kim *et al*.,

2010). Since Shh is considered a major driver in multiple cancers, it appears that darinaparsin has the ability to dismantle key aspects of Shh signaling machinery necessary for the proliferative drive in neoplastic cells.

Darinaparsin appears to be more potent but less toxic than ATO. Previous studies have noted that darinaparsin and ATO both induce an increase in ROS, but darinaparsin produces a greater increase (Tsimberidou *et al*., 2009). Darinaparsin is a potent inhibitor of microtubule polymerization while the effects of ATO on microtubules can vary. Some studies have reported that ATO is a strong microtubule polymerizing agent that synergizes with taxol, while others have shown ATO inhibition of the effects of taxol (Carré *et al*., 2002; Duan *et al*., 2010; Ling *et al*., 2002). Also, darinaparsin is effective in cells with ATO-resistance (Diaz *et al*., 2008; Matulis *et al*., 2009). Part of this latter difference may be due to the ability of some multiple drug resistance transporters, such as MRP1, to transport ATO out of cells (Matulis *et al*., 2009). In contrast, the expression of MRP1 does not alter the effects or potency of darinaparsin (Diaz *et al*., 2008). As noted previously for ATO (Chan *et al*., 2006), effectiveness of darinaparsin is not altered in Mdr1-expressing cells. In clinical trials, darinaparsin appears less toxic than ATO (Mann *et al*., 2009). In general, organic arsenicals, such as darinaparsin, are typically less toxic than inorganic arsenicals, such as ATO (Matulis *et al*., 2009). The lower toxicity of darinaparsin may seem a bit counterintuitive given its broad range of activities, including strong action against microtubule polymerization. Indeed, the differences in practical therapeutic effects of darinaparsin may accrue from a relative therapeutic index of multiple specific target activities impacting neoplastic cells versus non-specific generalized effects of arsenicals affecting mitochondrial functions (Mann *et al*., 2009).

In any case, the range of actions of darinaparsin against multiple drivers of neoplastic cells may make this organic arsenical an effective therapy for multiple resistant solid and hematological malignancies.

Methods

Cell Culture

HeLa cells (American Type Culture Collection, ATCC) were maintained at 37°C in 5% CO2 using complete RPMI media supplemented with 10% fetal bovine serum (FBS). Polyjet was used for transfections according to the manufacturer's protocol (SignaGen). NIH 3T3 fibroblasts were maintained in high-glucose Dulbecco's modified Eagle's (DMEM) medium supplemented with 10% FBS. To induce cilia formation, 3T3 cells were grown on poly-L-lysine coated coverslips and maintained in DMEM medium supplemented with 0.5% calf serum. ME-SA and ME-SA/Dx5 cells (American Type Culture Collection, ATCC) were maintained at 37°C in 5% CO2 using complete McCoy's media supplemented with 10% FBS.

Cell stress and recovery

For stress induction, HeLa cells were incubated at 37°C for 45 minutes (fixed cells) or 30 minutes (live cells) with a final concentration of either 0.5 mM sodium arsenite (Riedel de Haen) or 0.05 mM darinaparsin (gift from Ziopharm). For microtubule depolymerization, cells were first incubated on ice for 30 minutes. Then, cells were treated with 33 nM nocodazole (Calbiochem) for 90 minutes at 37°C. In recovery experiments, cells were washed twice with serum-free media after treatment, and incubated in complete RPMI media at 37°C for duration of recovery. For primary cilia

staining, 3T3 cells were treated with100 nM Smoothened Agonist (SAG) (Ehtesham *et al*., 2007), and with or without darinaparsin 18 hours before staining.

Fluorescence microscopy and analysis

For stress and recovery studies, HeLa cells grown on coverslips were fixed at room temperature for 15 minutes using 4% paraformaldehyde (PFA) supplemented with 0.1% Triton X-100, 80 mM K-PIPES pH 7.2, 1 mM EGTA, 1 mM MgSO4, and 30% glycerol. Cells were permeabilized with 0.25% Triton X-100 and blocked with 5% normal serum for one hour at room temperature. The cells were incubated with primary antibodies for one hour at room temperature: rabbit anti-AKAP350A (1:200), rabbit anti-Caprin-1 (1:1000, gift from John Schrader), mouse anti-α-tubulin (1:5000, Sigma), rabbit anti-CCAR1 (1:1000), goat anti-GW182 (1:100, Santa Cruz), and mouse anti-G3BP (1:800, BD Transduction). This was followed by incubation at room temperature for one hour with species-specific fluorescent secondary antibodies (1:500; Invitrogen or Jackson Immunoresearch). Coverslips were mounted using Prolong Gold with DAPI (Invitrogen). Cells were imaged using a 60x oil immersion lens on Olympus FV-1000 confocal fluorescence microscope (Vanderbilt Cell Imaging Shared Resource). The number and average size of granules in sodium arsenite- and darinaparsin-treated cells were determined using ImageJ software (NIH). At least ten cells were used per calculation. Changes in granule number and size were analyzed using a Student's t-test. Changes in granule size over time in darinaparsin-treated cells were analyzed using a one-way analysis of variance (ANOVA). Live-cell imaging was performed using a 60x oil immersion lens on the DeltaVision Deconvolution microscope (Vanderbilt Epithelial Biology Center Imaging Resource).

For primary cilia staining, 3T3 cells grown on coverslips were fixed for 20 minutes in 4% paraformaldehyde and permeabilized for 15 minutes in PBS with 0.3% Triton-X 100. The cells were incubated in primary antibodies overnight at 4°C: rabbit-anti-Arl13b (1:2000; gift from Tamara Caspary, Emery University) and mouse-anti-α-tubulin (1:5000; Calbiochem). This was followed by incubation at room temperature for one hour with species-specific fluorescent secondary antibodies (1:1000; Invitrogen). DAPI was included in the final washes before the samples were mounted in Fluor Saver (Calbiochem) for microscopy. Images were taken with Opti-Grid Confocal microscope. Cilia frequencies were determined from Arl13b/DAPI- stained cells from 6 samples per treatment (15-30 cells per sample). Ciliary length was measured using NIH ImageJ software. Bases and ends of immunolabeled individual cilia were marked in the confocal z-stack images and outlined, and the calculated length was recorded. P values were calculated using unpaired t-test (GraphPad).

Microtubule polymerization

The effects of darinaparsin on microtubule polymerization were assayed using a fluorescence-based polymerization assay (Cytoskeleton, Inc). Microtubule polymerization was initiated by GTP or GTP/Taxol (1 µM) in the presence of increasing concentrations of either darinaparsin (0.3 µM to 300 µM) or arsenite (1 µM to 1 mM). Polymerization was monitored each minute by fluorescence measurement for a total of one hour in a Biotek Fluorescence plate reader.

Luciferase reporter assay

NIH3T3 cells were plated at 1.0X105 cells/ml (24-well plate) 16 hours before transfection. Cells were co-transfected with 0.3 µg 8XGli1-luciferase reporter construct

and 0.03 µg Renilla-luciferase control construct in each well. At 8 hours after transfection, cells were fed low serum medium (0.5% calf serum + DMEM), and then treated with Shh agonist (10 nM SAG) with or without darinaparsin for an additional 20 hours. Luciferase assays were performed with the Dual-Glo Luciferase System (Promega) according to the manufacturer's instructions. Each assay was performed in triplicate and the results are presented as the relative fold-increase (normalized to Renilla-luciferase activity) over non-SAG-treated cells.

CHAPTER III

AKAP350C TARGETS TO MITOCHONDRIA VIA A NOVEL DOMAIN AND AFFECTS MITOCHONDRIAL MORPHOLOGY

Partially appears as: Mason TA, Goldenring JR, and Kolobova E. (submitted) AKAP350C targets to mitochondria via a novel domain and affects mitochondrial morphology.

Introduction

Mitochondria have crucial roles within cells regulating metabolism, decisions between cell survival and death, redox biochemistry, and calcium homeostasis (Horbinski and Chu, 2005). Mitochondria also play a role in calcium signaling, in concert with and independently of the endoplasmic reticulum (ER) (Dorn and Scorrano, 2010; Gunter *et al*., 2000). Because of their many roles, mitochondria are critical locations for signal integration. Mitochondria also exhibit localized cyclic AMP (cAMP)/Protein Kinase A (PKA) signaling, and cAMP is involved in many aspects of cell function and survival (Carlucci *et al*., 2008a). Decisions between cell survival and cell death, through apoptosis or autophagy, are largely regulated by mitochondria (Fulda *et al*., 2010). Mitochondrial biogenesis and activity can be regulated by changes in cAMP/PKA signaling. PKA-regulated ion channels also exist in the mitochondrial membranes (Nishida *et al*., 2009). Some cAMP/PKA-regulated calcium and potassium channels play roles cardioprotection (Nishida *et al*., 2009).

Mitochondria are highly dynamic, constantly undergoing fission and fusion and maintaining a balance between the two processes (Chen and Chan, 2009). Various

events, such as cellular stress, can induce a shift in the balance between fission and fusion (Chan 2012). When the balance is shifted towards increased fusion or decreased fission, mitochondria become elongated and hyperfused (Chen and Chan, 2009). When the balance is shifted towards decreased fusion or increased fission, the mitochondria become fragmented (Chen and Chan, 2009). This dynamic nature of mitochondria morphology also affects nearly every aspect of mitochondrial function.

The importance of proper mitochondrial dynamics is evident in the various diseases associated with defects in mitochondrial dynamics. Mutations in mitofusin 2 (Mfn2), a mitochondrial outer membrane fusion protein, are known to cause Charcot-Marie-Tooth type 2A (Züchner *et al*., 2004). Autosomal dominant Optic Atrophy is caused by mutations in optic atrophy 1 (Opa1), a mitochondrial inner membrane fusion protein (Eiberg *et al*., 1994). Defects in mitochondrial dynamics have also been associated with Parkinson's, Alzheimer's, and Huntington's diseases (Chen and Chan, 2009; Liesa *et al*., 2009). When mitochondrial dynamics are disrupted, this can lead to oxidative stress which has been found to play a role in the pathology of Parkinson's and Huntington's diseases (Subramaniam and Chesselet, 2013; Jin *et al*., 2013).

Because of the importance of mitochondrial dynamics, the processes of fission and fusion are highly regulated. PKA is an important regulator of mitochondrial dynamics (Rambold and Lippincott-Schwartz, 2011). Drp1 (dynamin-related protein 1), a mitochondria fission protein, is inactivated by PKA phosphorylation, resulting in decreased fission and increased mitochondria elongation, a process that promotes cell survival (Chang and Blackstone, 2007). Mfn2 is also phosphorylated by PKA, and again promotes cell survival (Chen *et al*., 2004). PKA signaling at the mitochondria regulates

mitochondrial dynamics, but it also is involved in other signaling pathways as well. The complete details of signal integration at mitochondria remain unclear.

A-Kinase Anchoring Proteins (AKAPs) were discovered as PKA anchors that establish localized cAMP/PKA signaling through sequestration of PKA, but they play many other roles in protein scaffolding (Theurkauf and Vallee, 1982; Lohmann *et al*., 1984). AKAPs function as anchors for targeting proteins to specific subcellular locations, and the localization and composition of AKAP complexes is dynamic. AKAPs comprise a very diverse family of proteins, with over 50 AKAPs identified to date (Wong and Scott, 2004). The importance of AKAP function is evident in the embryonic lethality of most AKAP knockout mice (Carnegie *et al*., 2009). At least one AKAP is found in every tissue in the body (Welch *et al*., 2010).

Previous studies have identified AKAPs involved with the mitochondria. AKAP149 (also known as D-AKAP1 and AKAP121 in mouse) localizes to both the ER and mitochondria and plays a role in stress response in cardiomyocytes (Ma and Taylor, 2008; Rogne *et al*., 2009; Perrino *et al*., 2010). When AKAP149 is displaced from the mitochondria it induces mitochondrial dysfunction (Perrino *et al*., 2010). This causes an increase in reactive oxygen species, and therefore induced oxidative stress in cardiomyocytes, smooth muscle cells, and hypertrophic mouse hearts *in vivo* (Perrino *et al*., 2010). AKAP149 anchors proteins and RNAs at the mitochondrial outer membrane and plays an important role in cAMP signaling. Overexpression of AKAP149 reduces apoptosis (Affaitati *et al*., 2003). Rab32, also an AKAP, interacts with the ER and mitochondria. Rab32 localizes to mitochondria-associated membranes (MAMs), where it serves to regulate MAM properties and interacts with Drp1 (Bui *et al*., 2010). High

expression levels of Rab32 delay apoptosis, while low expression levels of Rab32 accelerate apoptosis. It is possible other AKAPs localize to mitochondria and serve as regulators of their dynamics and functions.

We have investigated the function of a splice variant of AKAP350, also known as AKAP450, AKAP9, and CG-NAP (Schmidt *et al*., 1999; Witczak *et al*., 1999; Takahashi *et al*., 1999). There are several known splice isoforms of AKAP350: yotiao, AKAP350A, AKAP350B, and AKAP350C. Yotiao, associated with plasma membranes in excitable cells, and AKAP350A, associated with centrosomes and the Golgi apparatus, are the most studied isoforms. We previously identified AKAP350B and AKAP350C isoforms as potential splice variants, but their functions have not been studied further (Shanks *et al*., 2002a).

In this study, we completed cloning of AKAP350C and identified it as a mitochondria-targeted AKAP. AKAP350C lacks the centrosome- and Golgi-targeting domains found in AKAP350A. AKAP350C has a unique mitochondrial targeting sequence in its carboxyl terminus consisting of an amphipathic alpha helix. This alpha helix is necessary and sufficient for mitochondrial localization of AKAP350C. Overexpression of full-length AKAP350C induces a collapse of mitochondria towards the nucleus. AKAP350C interacts with Mff (mitochondria fission factor) and mitofusins 1 and 2, and over-expression of AKAP350C is associated with increased apoptosis. Our results suggest that AKAP350C is responsible for coordination of mitochondrial structural dynamics.

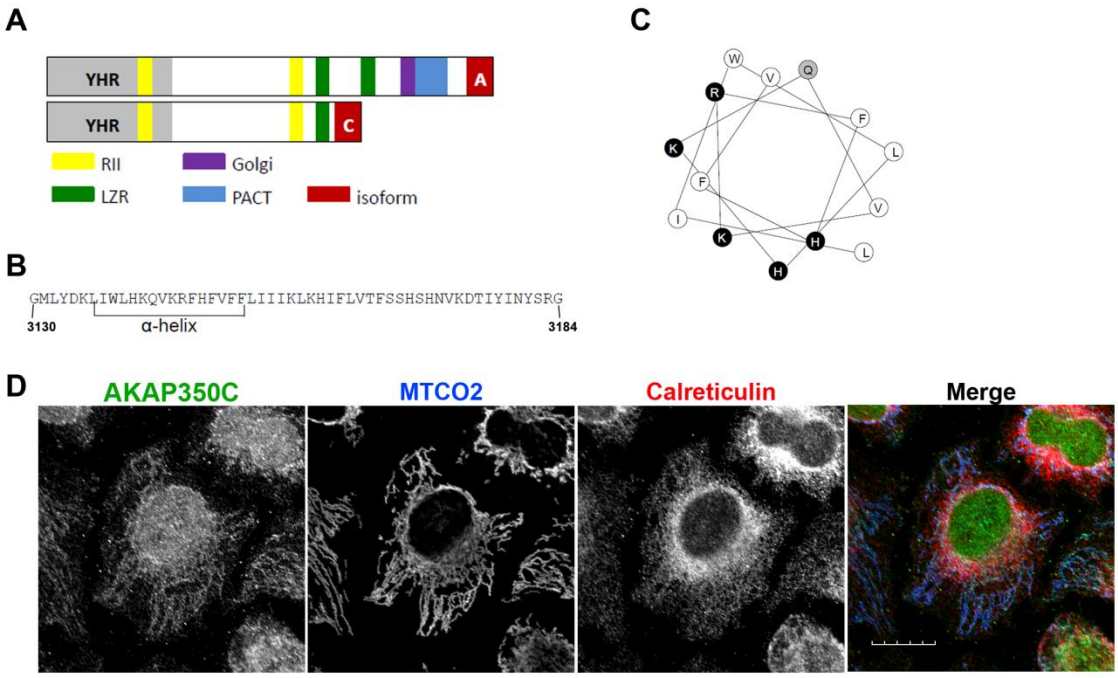

Figure 12. Characterization of AKAP350C. A) The AKAP350 splice variant is determined by the ending of the protein (red). Both variants contain two PKA $R_{II\alpha}$-binding domains (yellow). AKAP350A contains one leucine zipper region (green), while AKAP350C contains only one. Other domains include YHR (Yotiao homology region; grey), Golgi (Golgi-targeting domain; purple), and PACT (pericentrin and AKAP350 centrosomal-targeting domain; blue). **B)** AKAP350C has a unique 55-amino acid sequence, which contains a predicted alpha helix (Protean). **C)** The alpha helix predicted is amphipathic. **D)** HeLa cells were stained for edogenous AKAP350C (green), MTCO2 (mitochondria; blue), and calreticulin (ER; red). (Scale bars: 20 µm)

Results

Characterization of AKAP350C.

AKAP350C was previously identified using 3'-rapid amplification of cDNA ends (RACE) in a human lung cDNA (Schmidt *et al*., 1999; Shanks *et al*., 2002a). We have now completed cloning of AKAP350C from CaCo2 (human colorectal adenocarcinoma) RNA. The AKAP350C cDNA is 9.5 kb and codes for a protein of 3184 amino acids.

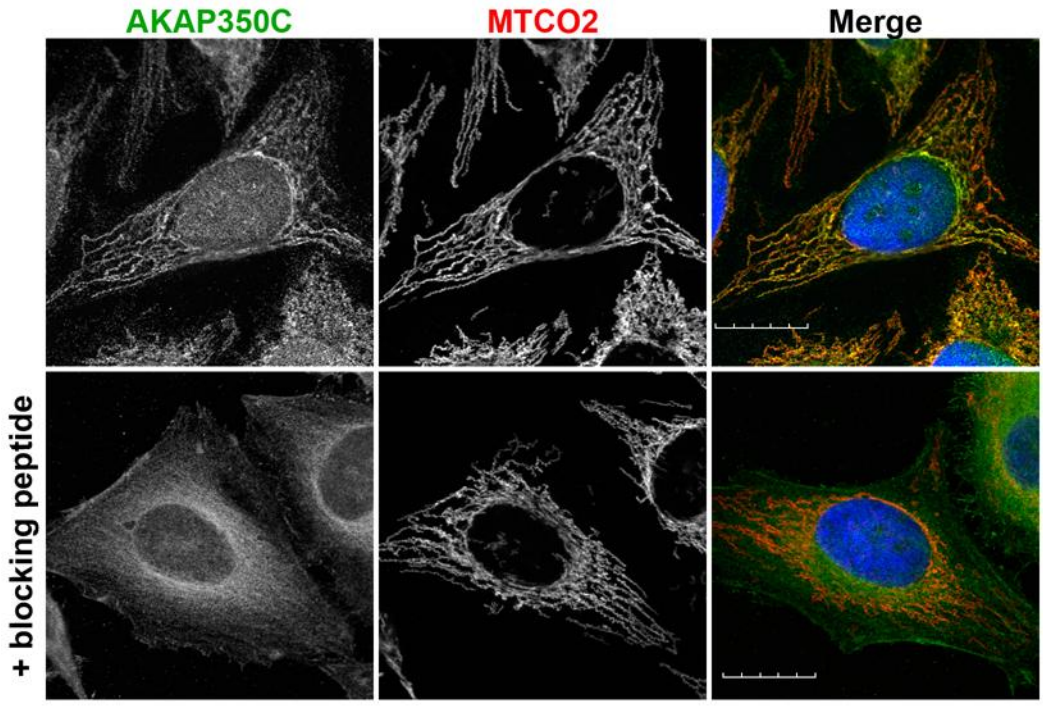

Figure 13. Specificity of AKAP350C antibodies. HeLas cells were grown on collagen-coated coverslips. Cells were stained for AKAP350C (green), mitochondria (MTCO2, red), and nuclei (DAPI, blue). The AKAP350C antibody was pre-incubated with either PBS or 20 µM blocking antigen peptide. (Scale bars: 20 µm)

AKAP350C is missing the carboxyl-terminal region containing centrosomal- and Golgi-targeting domains found in AKAP350A (Figure 12A) (Schmidt *et al*., 1999; Gillingham and Munro, 2000; Shanks *et al*., 2002a). Instead, the carboxyl terminus of AKAP350C contains a unique 55-amino acid sequence (Figure 12B). An amphipathic alpha helix is predicted in the first half of this sequence (Figure 12B and C). AKAP350C is ubiquitously expressed among tissues and cell lines (data not shown).

To examine the endogenous localization of AKAP350C, we made two isoform-specific antibodies against different epitopes in the AKAP350C-specific carboxyl terminal sequence and validated the specificity of these antibodies (Figure 13 and data

not shown). In immunofluorescence staining, both antibodies showed mitochondrial localization of AKAP350C in all cells and tissues we examined (Figure 13 and data not shown).

The amphipathic alpha helix is required and sufficient for targeting to mitochondria.

The AKAP350C sequence contains no known mitochondrial-targeting motifs, so determining its targeting domain could shed light on a previously unknown targeting motif or mechanism. The carboxyl-terminal 55 amino acids is the only sequence unique to AKAP350C, so we hypothesized that the mitochondrial-targeting domain is contained within that unique sequence. The only identifiable structural feature within the unique sequence was an amphipathic alpha helix (Figure 12B and C). Therefore, I evaluated whether the amphipathic alpha helix was required for mitochondrial localization of AKAP350C, using synthetic constructs to overexpress GFP-tagged AKAP350C fragments. I created several mutant constructs for GFP-chimeras of amino acids 2680-3184 of AKAP350C (AKAP350C-F3) and GFP-AKAP350C-C55 (the last 55 amino acids 3130-3184) following the schematic in Figure 14. The overexpressed GFP-AKAP350C-F3 (Figure 15) and GFP-AKAP350C-C55 (Figure 17) localize in a distribution that overlaps with mitochondria, suggesting that the carboxyl 55 amino acids can specify targeting.

Several truncation and point mutants were examined for their ability to target to mitochondria. The truncation mutant F3-L3136X, which only contains 6 of the 55 amino acids, abolished targeting to the mitochondria (Figure 15), supporting the importance of the unique AKAP350C carboxyl terminus in specifying mitochondrial targeting. Proline

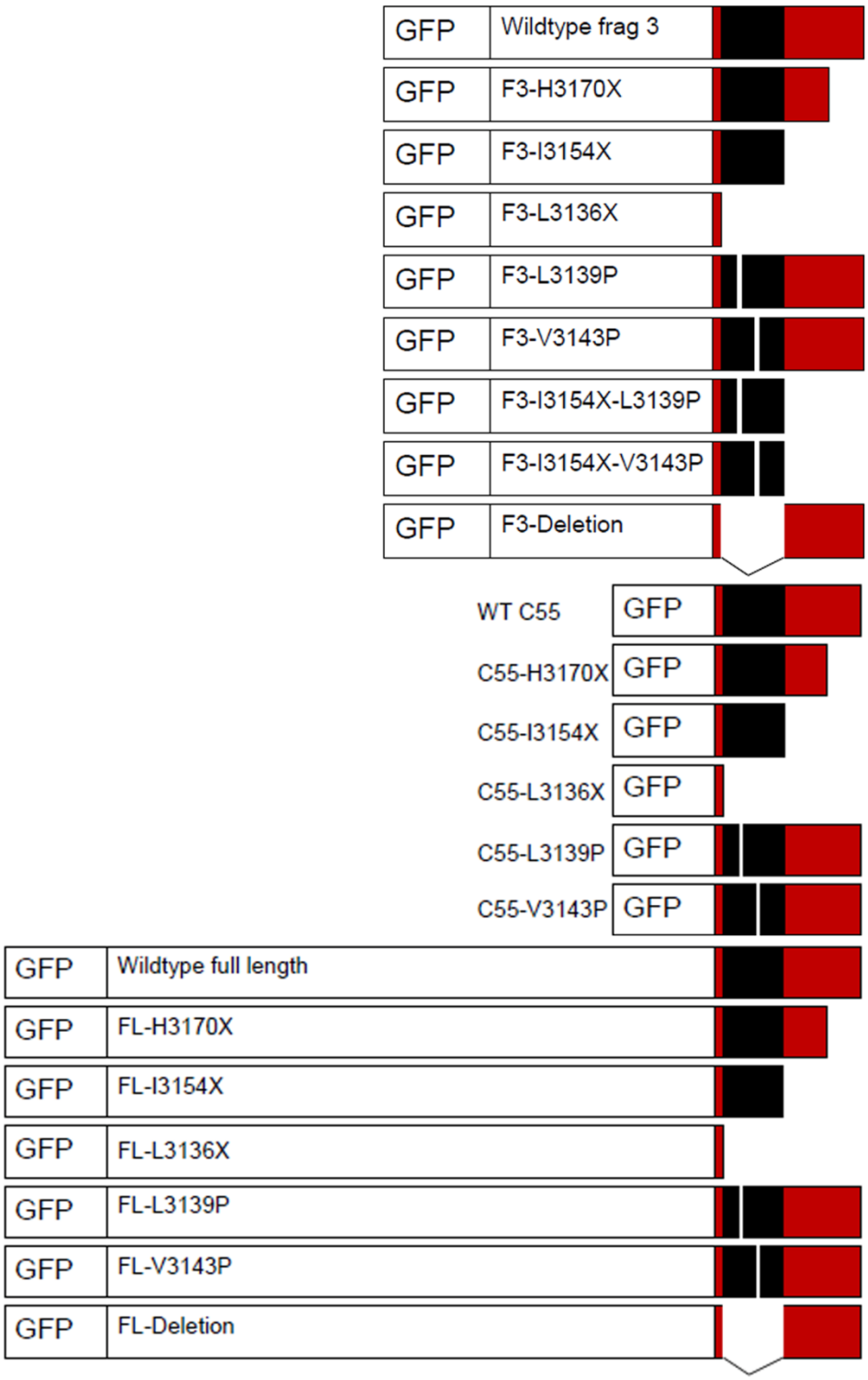

Figure 14. Schematic of GFP-AKAP350C constructs for mitochondrial targeting. Quickchange site-directed mutagenesis was used to create truncation and point mutants. Synthetic AKAP350C sequence was used as template.

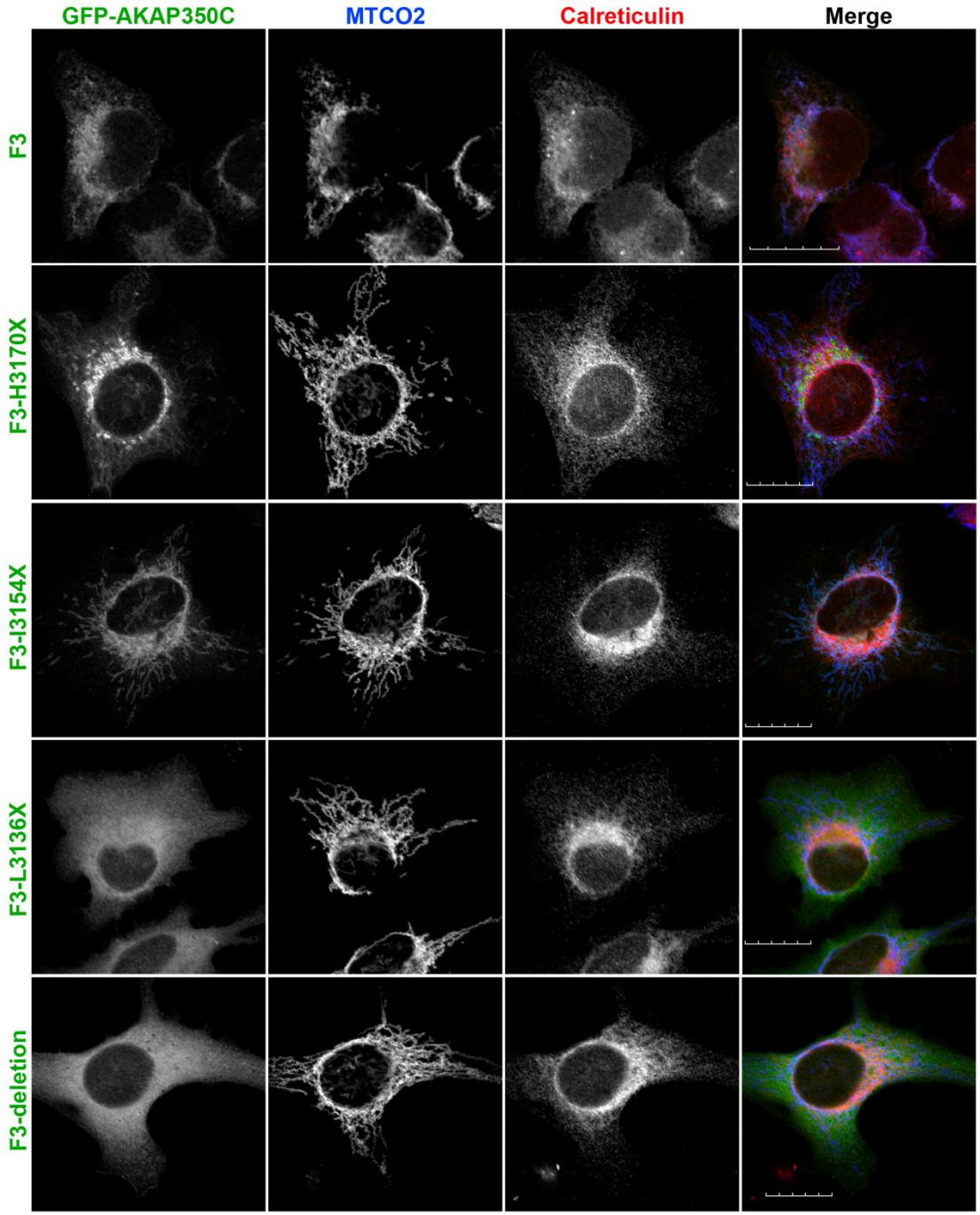

Figure 15. The AKAP350C carboxyl-terminal amphipathic alpha helix is required for targeting to mitochondria. HeLa cells were grown on collagen-coated coverslips. Cells were transfected with various AKAP350C constructs using Polyjet and stained for MTCO2 (mitochondria; blue) and calreticulin (ER; red). (Scale bars: 20 µm)

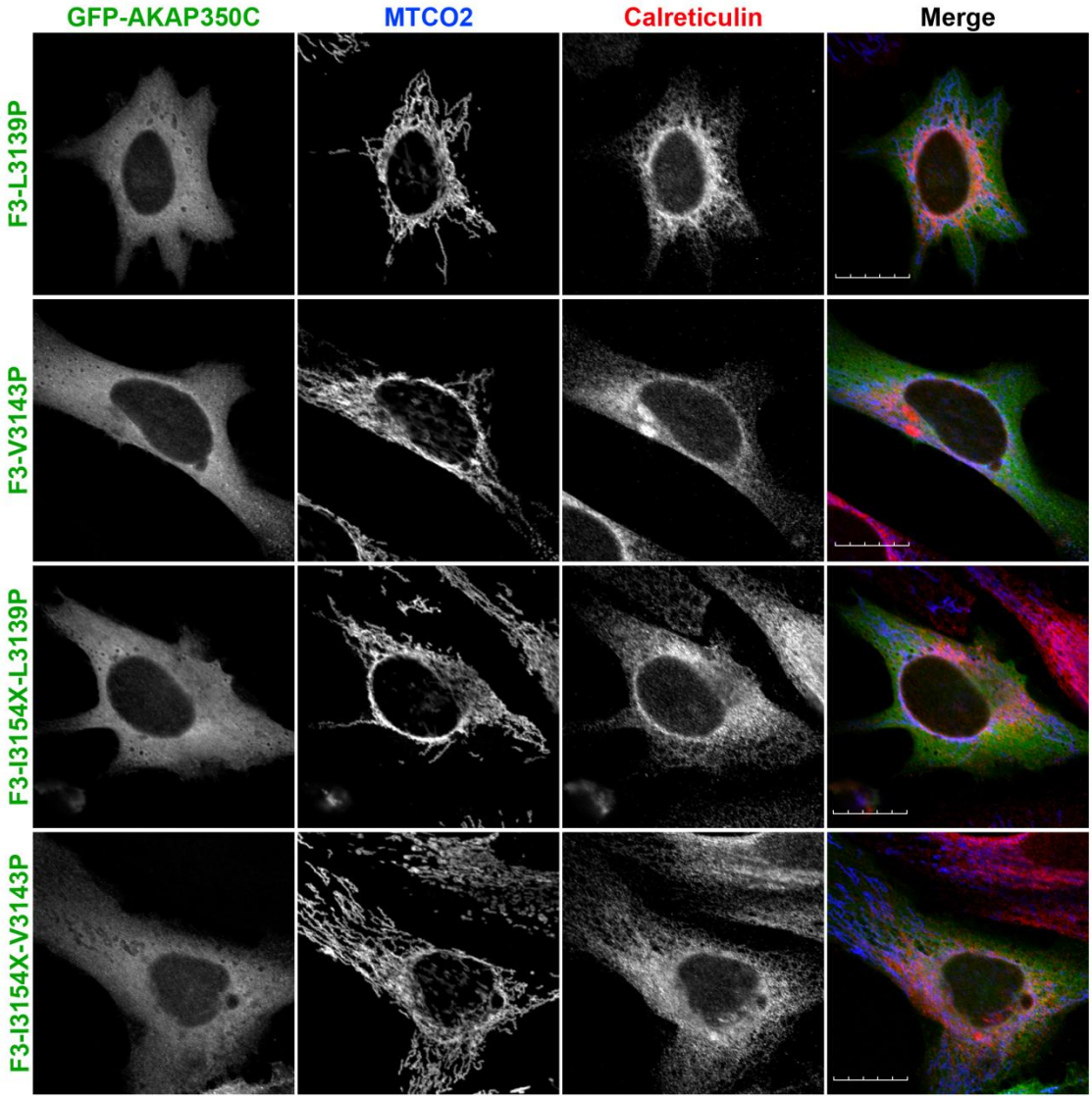

Figure 16. The structure of the AKAP350C carboxyl-terminal amphipathic alpha helix is required for targeting to mitochondria. HeLa cells were grown on collagen-coated coverslips. Cells were transfected with various AKAP350C point mutant constructs using Polyjet and stained for MTCO2 (mitochondria; blue) and calreticulin (ER; red). (Scale bars: 20 µm)

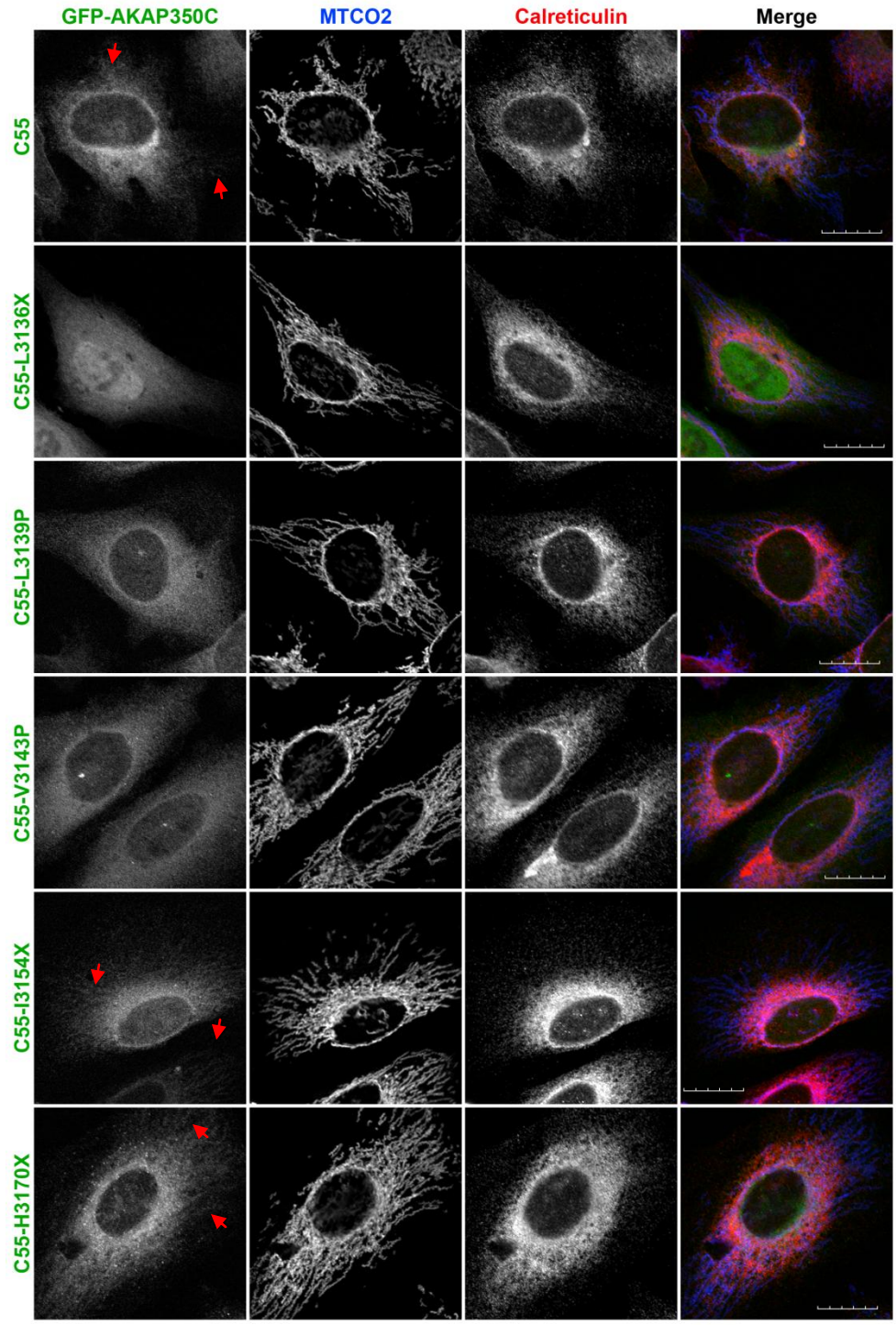

Figure 17. The AKAP350C carboxyl-terminal amphipathic alpha helix is sufficient for targeting to mitochondria. HeLa cells were grown on collagen-coated coverslips. Cells were transfected with various AKAP350C C55 constructs using Polyjet and stained for MTCO2 (mitochondria; blue) and calreticulin (ER; red). The red arrow indicates mitochondrial staining. (Scale bars: 20 μm)

substitution mutants F3-L3139P and F3-V3143P, which disrupt the alpha helical structure, also abolished mitochondrial targeting of AKAP350C (Figure 16). The truncation mutant F3-I3154X, which removes the amino acids after the alpha helix, retained mitochondrial targeting (Figure 15). This mutant appears to have enhanced targeting to the mitochondria when compared with wildtype. Double mutants F3-L3139P-I3154X and F3-V3143P-I3154X no longer targeted to the mitochondria (Figure 16). As expected, the proline disrupting the alpha helix abolishes the enhanced targeting seen in F3-I3154X. Interestingly, the truncation mutant F3-H3170X has a mixed localization, localizing partially to mitochondria and partially to the cytosol (Figure 15). This suggests the possibility of another domain in the last 30 amino acids that could target another organelle. Finally, removal of the alpha helix (F3-deletion) also blocked targeting to the mitochondria (Figure 15). Thus, any mutation that deleted or disrupted the alpha helix abolished mitochondrial targeting of AKAP350C.

Next, I examined whether the alpha helix is sufficient for targeting mitochondria. As mentioned above, C55-wildtype localized near the mitochondria, similar to F3-wildtype. The C55 constructs are small and do not target as well as the larger F3 constructs. However, a pattern can still be observed. As predicted, C55-L3136X, C55-L3139P, and C55-V3143P all have a cytosolic localization (Figure 17). The C55-H3170X has a mixed localization, similar to that of F3-H3170X (Figure 17). As shown in Figure 17, C55-I3154X localizes to the mitochondria. This 24 amino acid fragment, mostly comprised of the 17 amino acid amphipathic alpha helix, was sufficient to target GFP to the mitochondria. Therefore, the alpha helix is required and sufficient for mitochondrial targeting of AKAP350C.

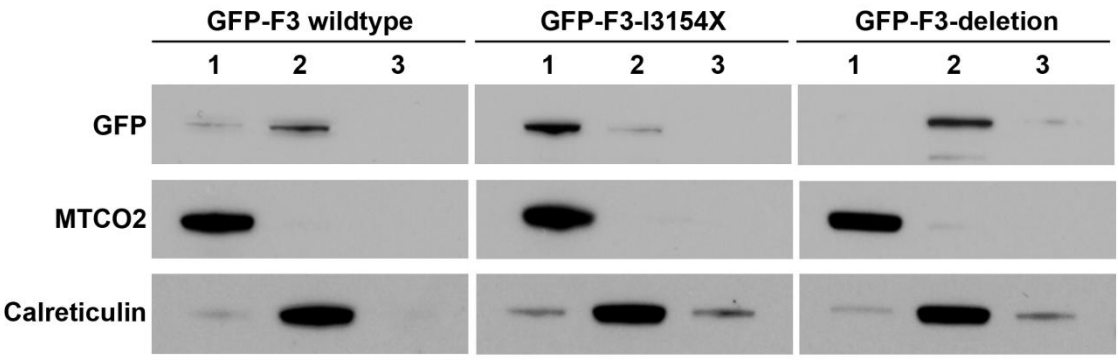

Figure 18. Biochemical confirmation that the amphipathic alpha helix is required for AKAP350C association with mitochondria. Mitochondria were isolated from HEK-293 cells transfected with GFP-AKAP350C constructs. In each case, Lane 1 contains the mitochondrial fraction; Lane 2 contains the microsomal fraction (pellet of 100,000 x g centrifugation); and Lane 3 contains the supernatant of the 100,000 x g centrifugation. In each lane, 12.5 µg of protein were loaded. Membranes were probed for MTCO2 (mitochondria), calreticulin (ER), and GFP (AKAP350C construct). The GFP westerns shown were taken at different exposures due to differences in level of expression.

Biochemical confirmation that the amphipathic alpha helix is required for association with mitochondria.

I next utilized a biochemical approach to evaluate the sub-cellular distribution of the various AKAP350C mutants. Mitochondria were isolated from cells expressing the AKAP350C mutants and compared with other sub-cellular fractions. As predicted based on data in Figure 15 and Figure 16, mutants which deleted or disrupted the amphipathic helix, including F3-L3136X, F3-L3139P, and F3-deletion, abolished association with mitochondria and these constructs partitioned in the microsomal fraction and 100,000 x g supernatant (Figure 18 and data not shown). AKAP350C constructs that retained an intact amphipathic helix localized with mitochondria, including F3 and F3-I3154X (Figure 18). Wildtype F3 localized in both mitochondrial and microsomal fractions, which may be due to the high level of overexpression of this construct. These

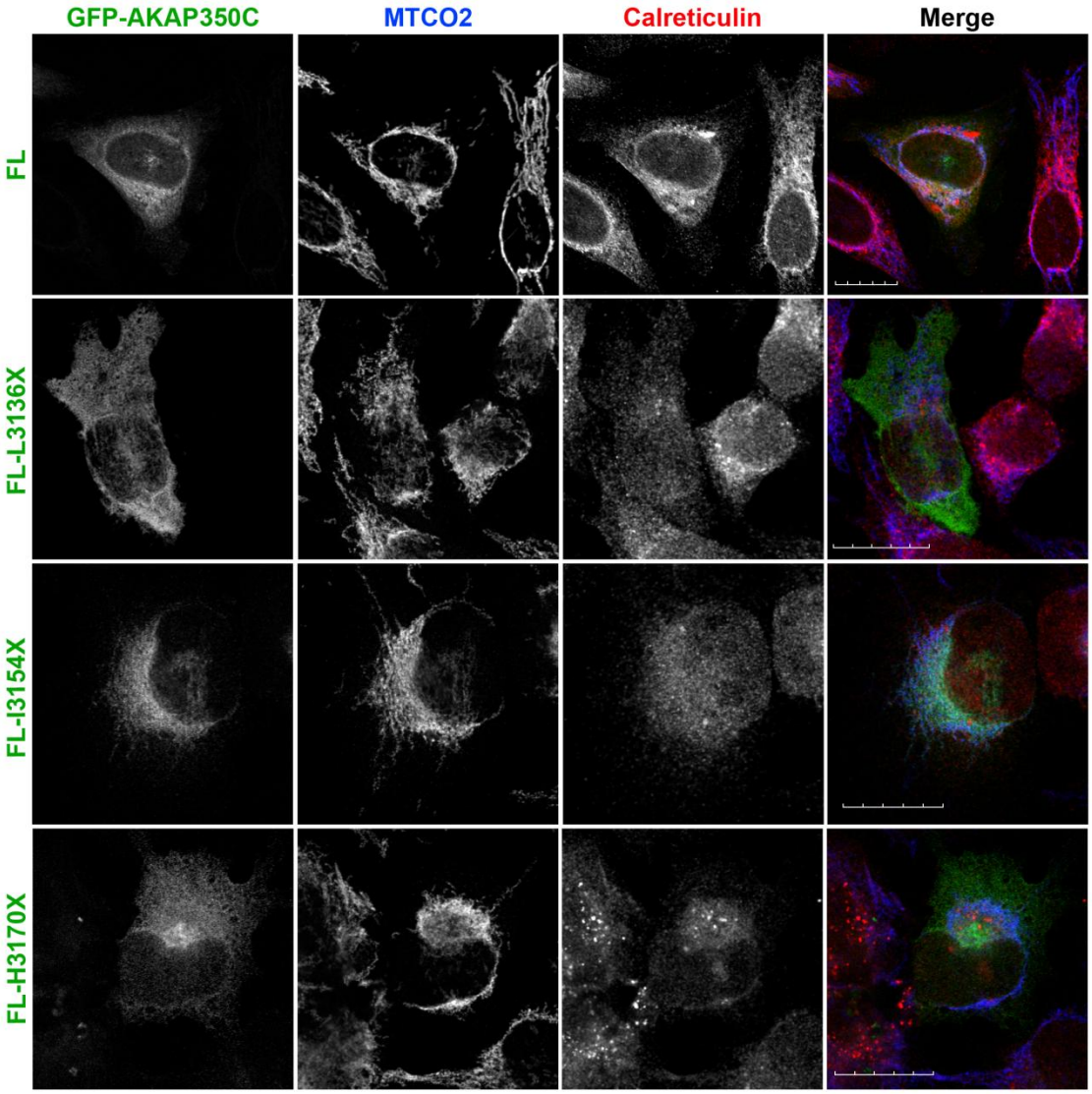

Figure 19. Overexpression of AKAP350C disrupts mitochondria morphology. HeLa cells were grown on collagen-coated coverslips. Cells were transfected with various AKAP350C constructs using Polyjet and stained for MTCO2 (mitochondria; blue) and calreticulin (ER; red). (Scale bars: 20 µm)

results confirm that the amphipathic alpha helix is required for AKAP350C association with the mitochondria.

Overexpression of AKAP350C localizing to mitochondria disrupts mitochondria morphology.

When full length AKAP350C protein (GFP-AKAP350C-FL) was overexpressed, the mitochondrial structure was disrupted and GFP-AKAP350C-FL localized in a distribution overlapping with mitochondria and the endoplasmic reticulum (Figure 19). This disruption of mitochondrial morphology was not observed with overexpression of GFP-AKAP350C-F3 (Figure 15). I next examined whether targeting-deficient mutants of AKAP350C-FL would have a similar affect. Overexpression of GFP-AKAP350C-FL-L3136X did not alter mitochondrial morphology as dramatically and distributed in the cytosol. In contrast, GFP-AKAP350C-FL-I3154X associated with mitochondria and caused mitochondrial collapse (Figure 19). Additionally, GFP-AKAP350C-FL-H3170X partially associated with mitochondria and caused mitochondrial collapse. These studies suggested that an increased amount of AKAP350C at mitochondria disrupted the mitochondrial morphology, causing a structural collapse.

To investigate further the nature of the mitochondrial morphology changes, I imaged cells using transmission electron microscopy. HEK-293T cells expressing GFP-AKAP350C-FL, GFP-AKAP350C-FL-I3154X, or GFP were flow-sorted for GFP-positive cells. The GFP-positive cells were then embedded and imaged. Control cells expressing only GFP exhibited normal mitochondria distributed throughout the cell (Figure 20). Cells expressing AKAP350C-FL or FL-I3154X displayed clustering of mitochondria in the perinuclear region. The mitochondria did not appear hyper-fused. Rather, a number of abnormal morphologies were observed including mitochondria with

membranous protrusions lacking internal cristae (Figure 20). Preliminary studies indicate this is not due to the process of mitophagy (data not shown). These differing morphologies suggested that AKAP350C plays a role in regulating mitochondrial dynamics and/or morphology.

AKAP350C does not target mitochondria by direct association with lipids.

Determining how the amphipathic alpha helix targets AKAP350C to mitochondria is important for understanding this new targeting domain. I examined whether AKAP350C associated with lipids through the amphipathic alpha helix. I made

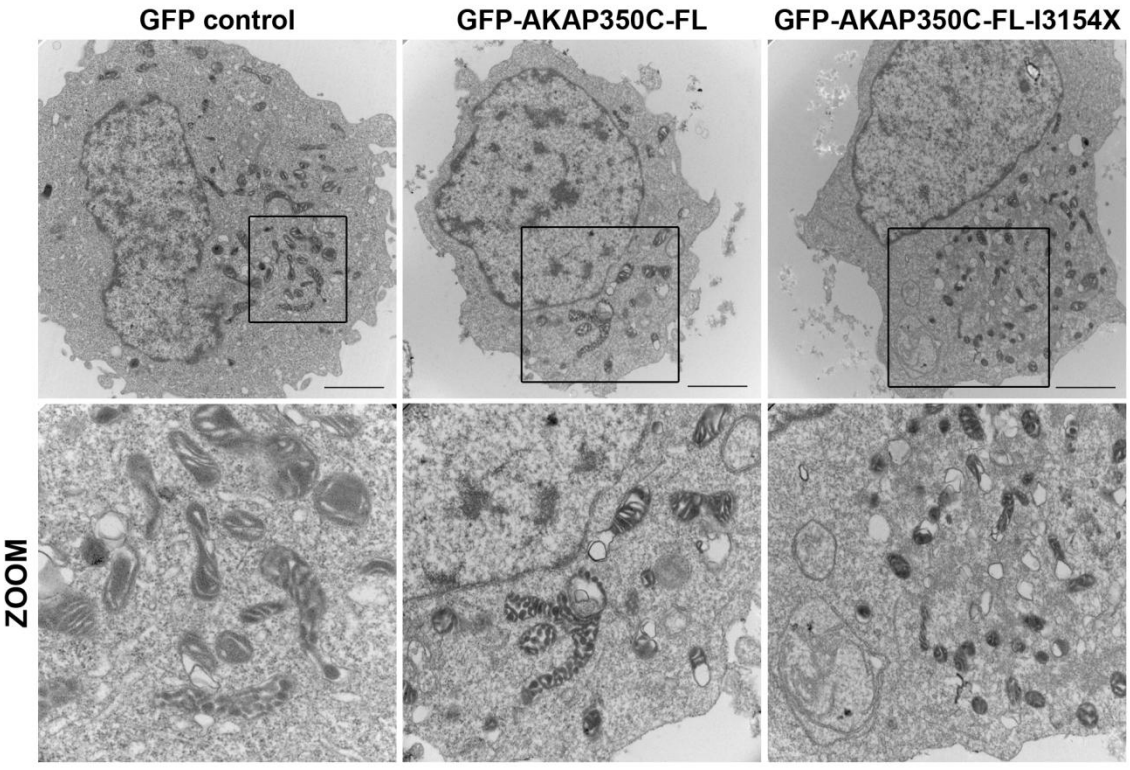

Figure 20. Overexpression of AKAP350C localizing to mitochondria induces clustering and disrupts mitochondria morphology. HEK-293T cells were transfected with various AKAP350C constructs or GFP-only control. Cells were flow-sorted and GFP-positive cells were collected. The cell pellets were fixed, embedded, and processed for imaging with transmission electron microscopy. (Scale bars: 2 microns)

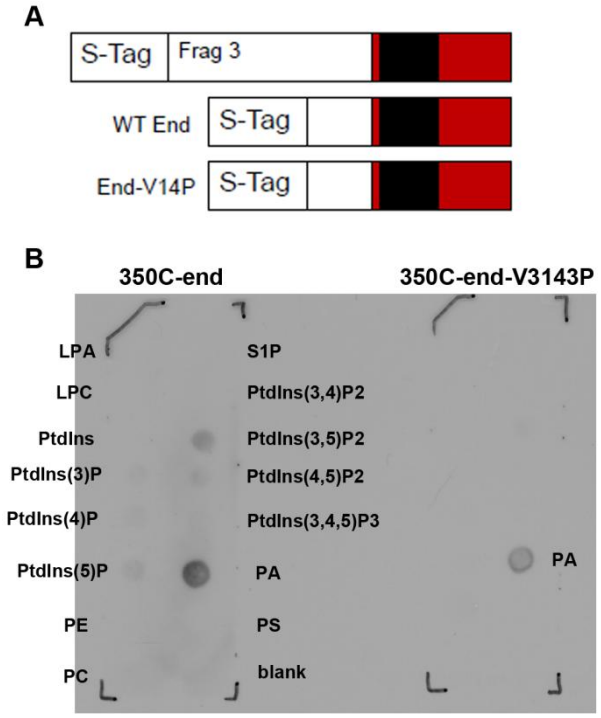

Figure 21. AKAP350C does not target mitochondria by direct association with lipids. A) Diagram of AKAP350C fragments in pET30a vectors. The End fragments are 102 amino-acids. **B)** PIP strips (lipid-dotted membranes) were probed with bacterially expressed, purified AKAP350C fragments. Protein was detected using S-protein antibodies conjugated to horseradish peroxidase (HRP) secondary.

constructs of the carboxy-terminal 102 amino acids of AKAP350C in bacterial expression vectors containing S-tags (Figure 21A). Purified protein was used to probe lipid-dotted membranes. Purified wildtype S-tag-End-C, S-tag-End-C-V3143P, and S-tag-End-C-deletion all show a positive interaction with phosphatidic acid (PA) (Figure 21B and data not shown). Because there is no difference between the wildtype interactions and those of the mutant proteins, it is not likely that AKAP350C targets mitochondria via direct lipid interaction.

AKAP350C associates with mitochondrial fission and fusion proteins.

Given that AKAP350C is scaffolding PKA, which is well known regulator of mitochondrial fission/fusion dynamics (Rambold and Lippincott-Schwartz, 2011), I sought to determine whether AKAP350C is associated with fission regulator proteins such as Mff and fusion regulator proteins such as Mfn1 and Mfn2. To examine those interactions, we overexpressed GFP-AKAP350C together with myc-Mff, myc-Mfn1 or myc-Mfn2 in HEK cells and then used GFP-binding protein-conjugated beads to isolate complexes (Rothbauer *et al*., 2006). We found that both GFP-AKAP350C-FL and GFP-AKAP350C-F3-I3154X specifically isolated Mff, Mfn1 and Mfn2 (Figure 22).

We next examined immunostaining of endogenous AKAP350C in HeLa cells, overexpressing mCherry-Mff, mCherry-Mfn1 or mCherry-Mfn2 (Figure 23). As described previously (Otera *et al*., 2010; Otera and Mihara, 2011), Mff overexpression resulted in short, fragmented mitochondria, whereas overexpression of mitofusins induced a spectrum of mitochondrial fusion leading to eventual mitochondrial collapse and formation of perinuclear clusters with enlarged mitochondria (Santel *et al*., 2003, Pich *et al*., 2005). We observed substantial co-localization of AKAP350C with Mff (Figure 23A), Mfn1 (Figure 23, B and C) and Mfn2 (Figure 23, D and E).

It should be noted that the extent of mitochondrial fusion, and therefore mitochondrial shape, varied depending on the level of mitofusin protein expression. Low levels of mitofusin over-expression resulted in an elongated, fused mitochondrial network

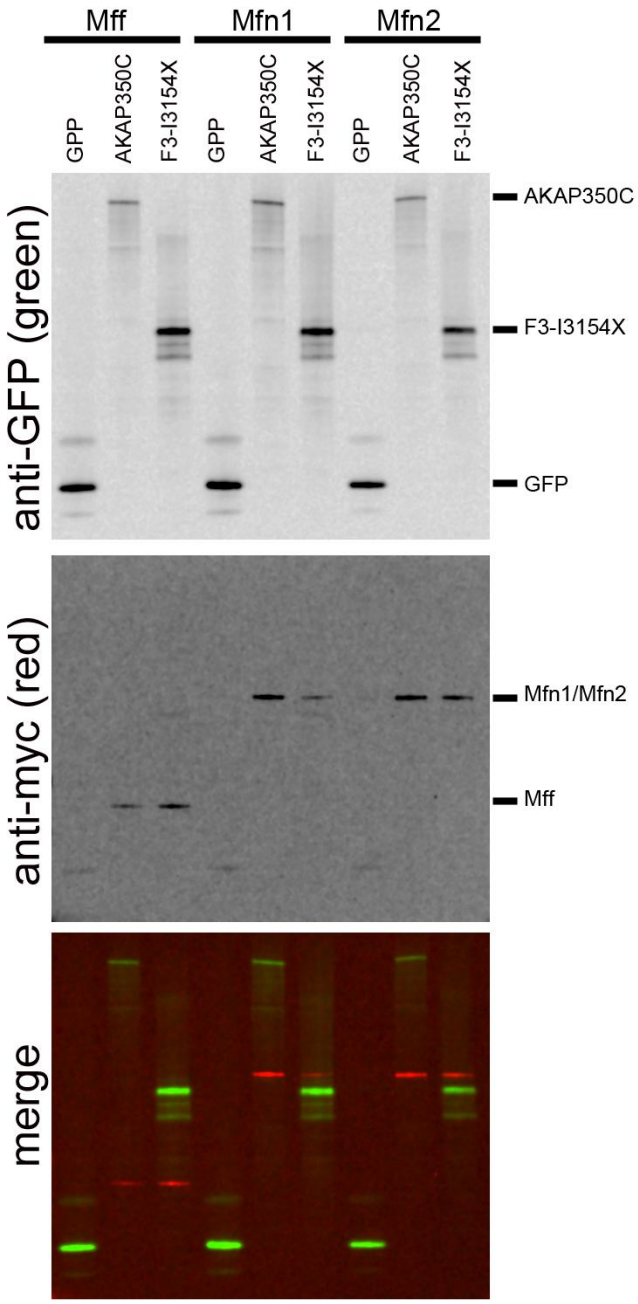

Figure 22. AKAP350C associates with mitochondrial fission and fusion proteins. GFP-tagged AKAP350C or empty pEGFP-C1 vectors were co-expressed with either myc-tagged Mff, myc-tagged Mfn1 or myc-tagged Mfn2 in HEK-293T cells. Proteins isolated using GFP-binding protein conjugated beads were probed for myc-tag (to detect Mff, Mfn1, Mfn2) and for GFP (to detect AKAP350C). Empty pEGFP-C1 vector was used as a negative control. Dual detection was performed on the same membrane for both GFP and myc using Odyssey Li-Cor system.

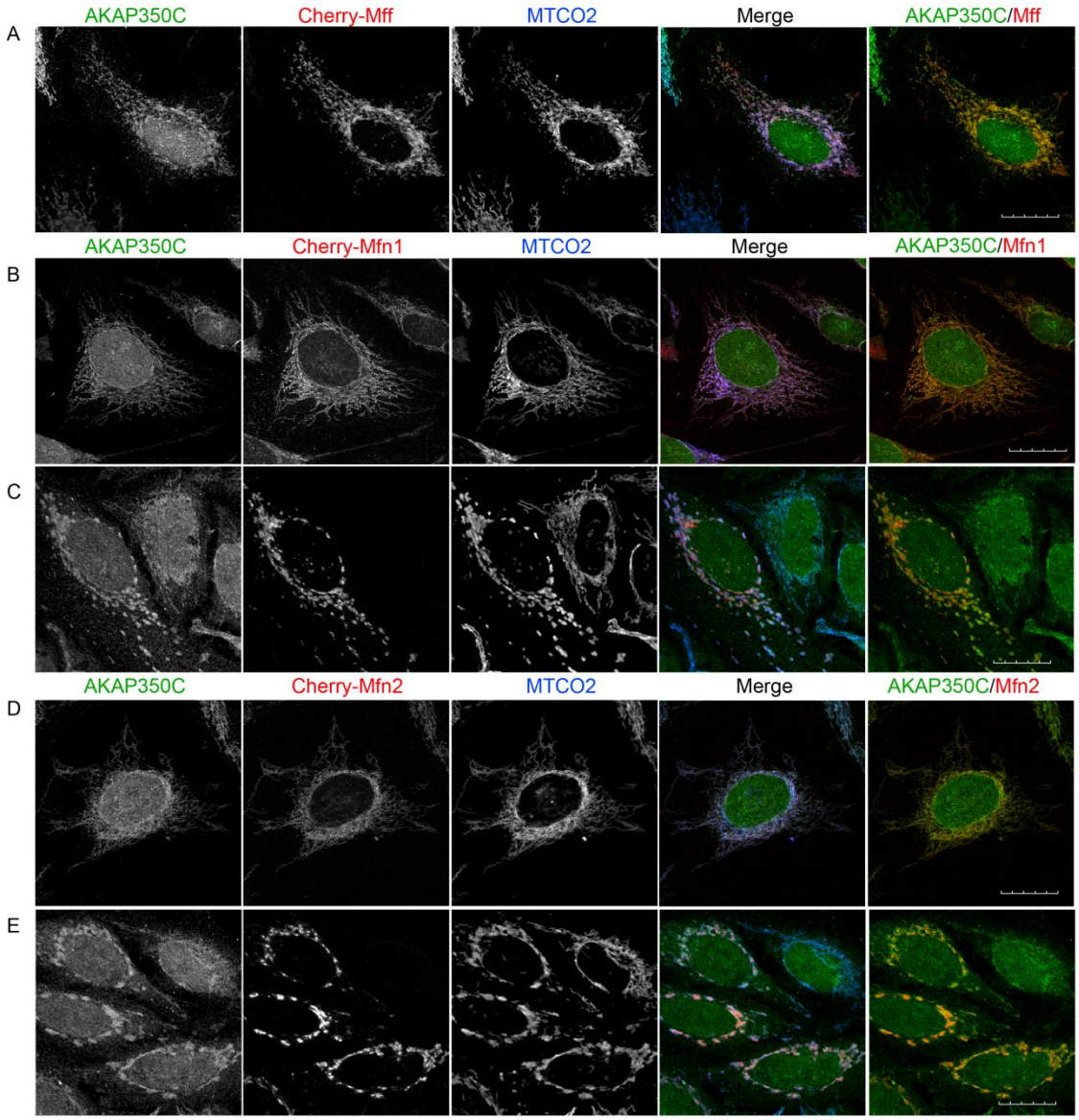

Figure 23. Endogenous AKAP350C co-localizes with overexpressed fission/fusion proteins (Mff/Mitofusins). HeLa cells were transfected with either Cherry-Mff **(A)**, Cherry-Mfn1 **(B, C)**, or Cherry-Mfn2 **(D, E)** and dual-stained for endogenous AKAP350C (green) and mitochondria marker MTCO2 (blue). Note, that higher levels of expression of mitofusins (C and E for Mfn1 and Mfn2, respectively) change the pattern of endogenous AKAP350C staining. The degree of co-localization between endogenous AKAP (green) and overexpressed Mff/Mfn1/Mfn2 (red) were quantified using Pearson's Correlation Coefficient (PCC). PCCs were determined using JACOP plug-in of ImageJ software. PCC: (A) 0.918; (B) 0.908; (C) 0.920; (D) 0.938; (E) 0.880. (Scale bars: 20 μm)

with extensive co-localization of endogenous AKAP350C (see Figure 23B and Figure 23D for Mfn1 and Mfn2, respectively).

Higher levels of mitofusins over-expression encouraged formation of further fused mitochondrial clusters (see Figure 23C and Figure 23E for Mfn1 and Mfn2, respectively) that eventually collapsed around perinuclear region (data not shown). We also noted that overexpression of mitofusins changed the pattern of endogenous AKAP350C staining, with endogenous AKAP350C accumulating with the fused mitochondria (Figure 23, C and E). The association of AKAP350C with both mitochondria fission and fusion proteins supports the concept of a dynamic organization of AKAP350C scaffolding complexes, which may scaffold fission/fusion proteins at the mitochondria.

Overexpressed GFP-AKAP350C-F3-I3154X construct also significantly overlapped with overexpressed Cherry-Mff, Cherry-Mfn1 and Cherry-Mfn2 and demonstrated the same spectrum of mithochondrial morphologies depending on levels of mitofusins overexpression that we observed with endogenous AKAP350C (Figure 24A). Finally, the GFP-AKAP350C-F3-I3154X construct also greatly overlapped with endogenous AKAP350C on mitochondria, whereas F3-deletion (the non-targeting mutant, see above) was completely cytosolic (Figure 24B).

Overexpression of AKAP350C induces apoptosis as well as potentiates both TRAIL- and NaBu-induced apoptosis onset.

Mitochondrial fission and fusion balance is highly related to the ability of cell to adapt to various cellular stresses and contributes in quality control by eliminating damaged material by mitophagy and apoptosis (Otera *et al*., 2013). Because of possible

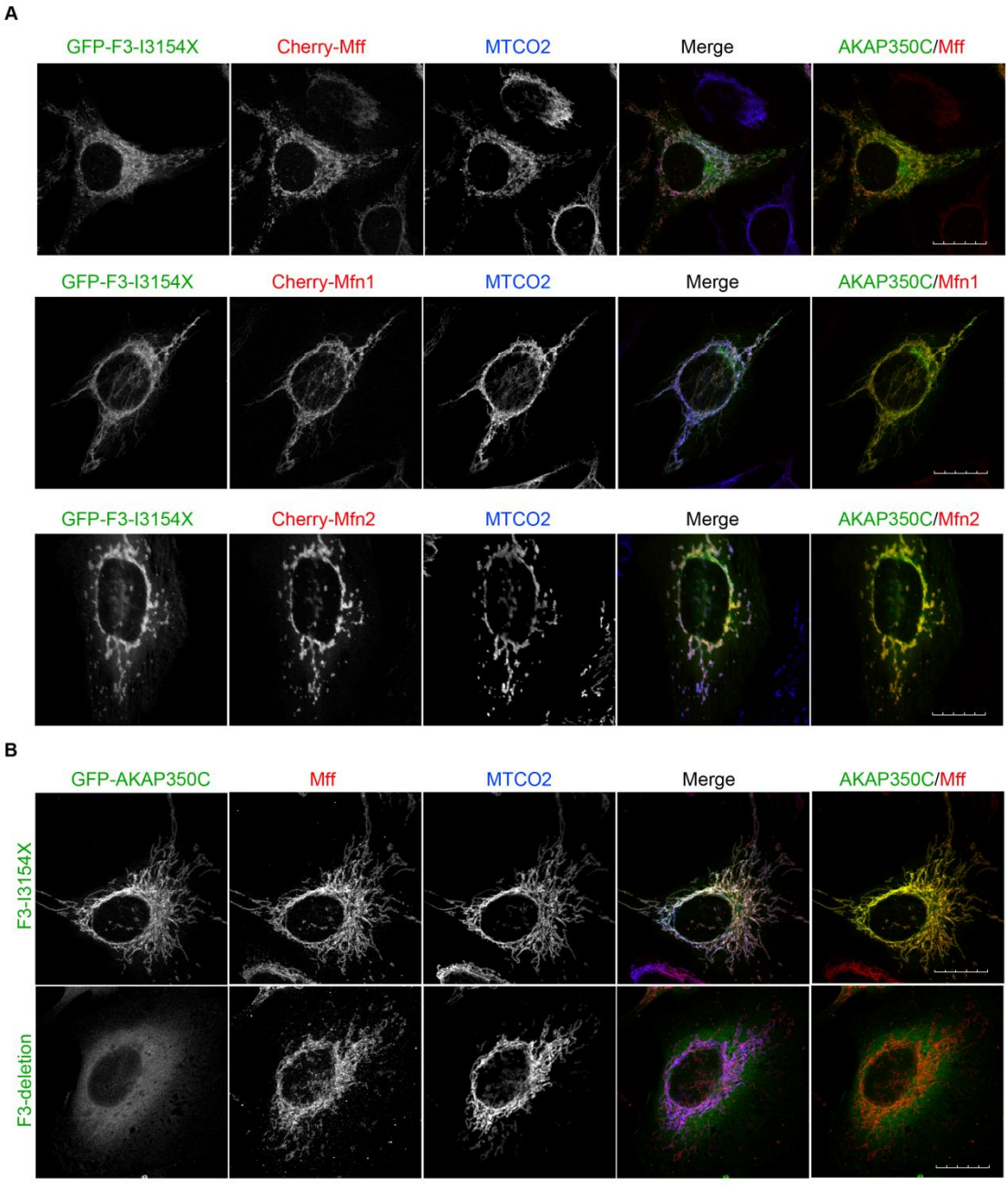
A
GFP-F3-I3154X
Cherry-Mff
MTCO2
Merge
AKAP350C/Mff
GFP-F3-I3154X
Cherry-Mfn1
MTCO2
Merge
AKAP350C/Mfn1
GFP-F3-I3154X
Cherry-Mfn2
MTCO2
Merge
AKAP350C/Mfn2
B
GFP-AKAP350C
Mff
MTCO2
Merge
AKAP350C/Mff
F3-I3154X
F3-deletion

Figure 24. Overexpressed AKAP350C co-localizes with fission/fusion proteins (Mff/Mitofusins). (A) HeLa cells were transfected with GFP-F3-I3154X (green) and either Cherry-Mff, Cherry-Mfn1, or Cherry-Mfn2 (red) and then stained for the mitochondrial marker MTCO2 (blue). **(B)** F3-I3154X, but not F3-delition mutant co-localizes with endogenous Mff. HeLa cells were transfected with GFP-AKAP360C (F3-I3154X or F3-delition)(green) and dual-stained with anti-Mff antibody (red) and mitochondrial marker MTCO2 (blue). The degree of co-localization between AKAP (green) and Mff/Mfn1/Mfn2 (red) were quantified using Pearson's Correlation Coefficient (PCC). PCCs were determined using JACOP plug-in of ImageJ software. PCC were 0.943 (GFP-F3-I3154X with Cherry-Mff), 0.775 (GFP-F3-I3154X with Cherry-Mfn1), 0.970 (GFP-F3-I3154X with Cherry-Mfn2), 0.932 (GFP-F3-I3154X with endogenous Mff, red), whereas F3-deletion mutant of AKAP350C exhibited uniform cytosolic staining. (Scale bars: 20 µm)

role of AKAP350C in fission/fusion balance, we evaluated if overexpression of full length of AKAP350C or F3-I3154X would influence apoptosis. To test this, we transfected HEK cells with full length GFP-AKAP350C, GFP-F3-I3154X or empty pEGFP vector. To induce apoptosis, cells were either treated with 500 ng/ml of TRAIL for 4 hours or with 5 mM Sodium Butyrate (NaBu) for 24 hours. After treatments cells were collected in SDS-containing lysis buffer and analyzed by western blot (Figure 25). We assessed PARP-cleavage as it is a reliable and established apoptosis indicator downstream of caspase activation. Overexpression of AKAP350C induced PARP-cleavage in untreated HEK cells as well as increased PARP-cleavage in both TRAIL- and NaBu-treated cells, which suggests increased levels of apoptosis (Figure 25). The increased PARP-cleavage in cells overexpressing GFP-F3-I3154X compared to full length AKAP350C may be due to the higher levels of expression of GFP-F3-I3154X compared to wild type (Figure 25). These results suggest that overexpression of

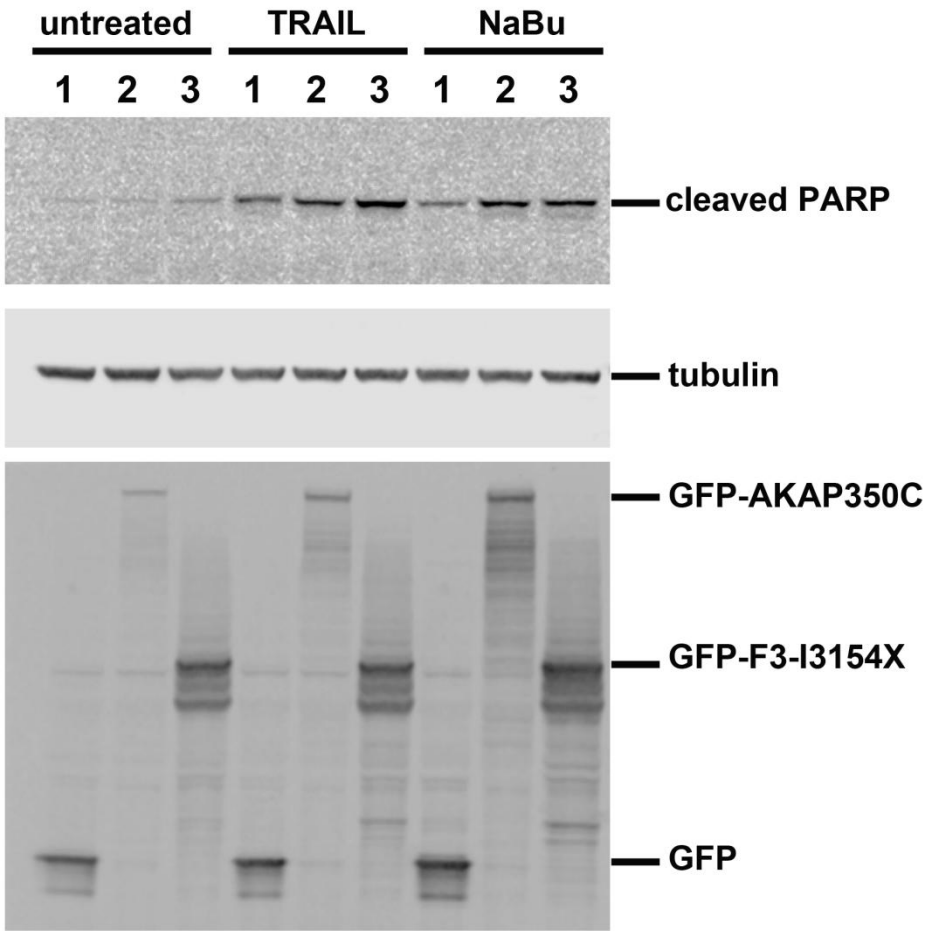

Figure 25. Overexpression of AKAP350C promotes apoptosis. HEK cells were transfected with empty pEGFP vector (1), full length GFP-AKAP350C (2) or GFP-F3-I3154X (3). After transfection cells were treated with either 500 ng/ml of TRAIL for 4h or 5 mM sodium butyrate (NaBu) for 24, harvested in lysis buffer, and then analyzed by Western blot for PARP activation. α-tubulin staining was used as an internal loading control. The same membrane was probed for cleaved PARP and for tubulin simultaneously, and then re-probed for GFP.

AKAP350C induces apoptosis as well as potentiates both TRAIL- and NaBu-induced apoptosis.

Discussion

In this study, we identified a novel AKAP350 splice variant, AKAP350C, which localizes to mitochondria and disrupts mitochondrial morphology. We completed cloning of AKAP350C, which contains 55 amino acids of unique protein sequence relative to other splice variants. This relatively small unique sequence greatly differentiates AKAP350C from AKAP350A in terms of subcellular distribution and role. I also identified a novel mitochondrial-targeting domain within AKAP350C. The carboxyl-terminal 55-amino acids contain an amphipathic alpha helix that is required and sufficient for mitochondrial targeting of AKAP350C. Since AKAP350C also associated with Mff and mitofusins, the results suggest that AKAP350C likely participates in regulation of mitochondrial fusion and fission dynamics.

While it is clear that the amphipathic alpha helix in the unique carboxyl terminal of AKAP350C is required for targeting to the mitochondria, the interacting partner for this helix remains unclear. We have determined that AKAP350C can associate with Mff and mitofusins, but these proteins cannot account for the targeting to the mitochondria. It is possible that AKAP350C can interact with lipids on the mitochondrial outer membrane through either hydrophobic interactions or electrostatic charge. In preliminary studies, I have not been able to identify any direct interactions with either phospholipids or phosphatidyl-inositides (Figure 21). Proteins such as hexokinase I contain domains of charged and hydrophobic regions that lay upon the surface of the outer membrane (Gelb

et al., 1992, Sui and Wilson, 1997). Additionally a similar complex binding mechanism has been proposed for D-AKAP1 localization to mitochondria (Ma and Taylor, 2002). Further investigations will be required to determine the discrete molecular mechanisms responsible for AKAP350C association with mitochondria.

Mitochondria are critical signaling integration centers, and AKAPs serve to scaffold many proteins in close proximity for sequestration of coordinated signaling within cells, thereby allowing greater spatial and temporal control of signaling cascades. Loss of an AKAP protein, and subsequently the signal integration it provides, is typically embryonic lethal in knockout mice (Carnegie *et al*., 2009). AKAP350C likely serves as a signaling focal point for the regulation of mitochondrial dynamics, scaffolding PKA and mitochondria fission and fusion proteins in close proximity. Upon Mfn1 or Mfn2 overexpression, AKAP350C colocalizes with mitofusins. This scaffolding could lead to local coordination of phosphorylation and dephosphorylation of fusion and fission proteins.

Interestingly, overexpression of full-length AKAP350C caused mitochondrial structural collapse. One possible explanation is that the increased recruitment of mitochondrial fission and fusion proteins associated with AKAP350C caused an imbalance between fission and fusion. Alternatively, the overexpression of AKAP350C may saturate a receptor protein on the mitochondrial surface. By electron microscopy, mitochondria in cells over-expressing AKAP350C showed abnormal morphologies with outer membrane blebbing without internal christae. These abnormal morphologies were not associated with any markers of miophagy (data not shown). Thus, it appears likely that AKAP350C may act as a regulator of mitochondrial structure.

Mitochondrial dynamics and the balance between fission and fusion is an important process in regulating cellular stress response (Youle and van der Bliek, 2012). Our data showed that AKAP350C associates with mitochondrial fission/fusion proteins and likely aids in regulating mitochondrial dynamics. Additionally, overexpression of AKAP350C exacerbated TRAIL-induced apoptosis. These results suggest that AKAP350C is involved in the regulation of mitochondrial dynamics under non-stress conditions, but also plays a role in the regulation of mitochondria during stress response. Another splice variant, AKAP350A, also serves dual roles, localizing to the Golgi apparatus (Shanks *et al*., 2002a) and centrosome (Schmidt *et al*., 1999) during non-stress conditions, while re-localizing to RNA stress granules during stress response (Kolobova *et al*., 2009).

Other AKAP proteins are known to localize to mitochondria, including AKAP149 and Rab32. Seemingly redundant, these AKAPs likely function uniquely under steady-state conditions. For example, AKAP149 is involved in mitochondrial RNA processing, but there is no known role for Rab32 or AKAP350C involving RNA. It is possible these mitochondria-targeted AKAPs are both redundant and distinct, meaning that they play different roles when all are present, but can compensate at least partially if one is lost. Mitofusins 1 and 2 are one example of this distinct and redundant strategy employed for mitochondrial dynamics (Chen *et al*., 2003). Mfn1 and Mfn2 are 60% homologous (Santel *et al*., 2003) and have shared functions, but each mitofusin also functions uniquely. When Mfn1 is knocked down or knocked out, Mfn2 can only partially compensate, and vice versa. Given the crucial role for mitochondria in cell survival, this redundancy could account for the localization of multiple AKAPs at mitochondria.

Since mitochondrial fission and fusion proteins participate in neurodegenerative, cardiovascular, and other diseases (Stetler *et al*. 2013, Joseph *et al*. 2012), AKAP350C as a signal integration center could provide an important future therapeutic target for regulation of mitochondrial function in stress and disease.

Methods

Cloning of AKAP350C

We previously cloned the 3'-end of AKAP350C from a 3'-RACE strategy using a human lung cDNA (Schmidt *et al*., 1999; Shanks *et al*., 2002a). To amplify the complete sequence, we synthesized a cDNA from 5 µg of CaCo-2 cell total RNA using an anti-sense primer specific for AKAP350C (AS1: CGTAGCTGTTTAAACCAATTAGACAATCCTC). The resulting cDNA was then used for as template for amplification using Advantage Taq polymerase (Clontech) of the AKAPA350C sequence with a nested AKAP350C anti-sense primer (AS2: CTAACCCCTAGAGTAATTAATATAGATTGTATC) and Sense primers from all 50 exons of the known AKAP9 gene. The largest polymerized fragment was obtained with a sense primer from Exon 5 (Exon 5-S: CTGAACAAGGAGCACAAGACAGTCCGAC) and AS2. To complete the 5' sequence, we performed created a 5'-RACE linkered RNA from CaCo-2 RNA (Ambion RLM-RACE) and synthesized cDNA primed with AS1. The 5' ends were then amplified with a universal primer from the linker region (5'-RACE inner) and an antisense primer against Exon 5. The resulting PCR fragments were cloned into pTOPO and sequenced to determine authentic 5' sequences. The complete DNA sequence was then assembled using DNASTAR software. The resulting sequence was

deposited in Genbank as an update of the original AKAP350C 3'-cDNA sequence AF247727.

Expression analysis

Tissue cDNAs used were supplied (Qiagen). Cell line cDNAs were made from total RNA extracted from cell pellets.

AKAP350C-specific antibodies

Two AKAP350C-specific antibodies were made. The first antibody was produced against SSHSHNVKDTIYINYSRG (Antibody Facility at the University of Georgia). The second antibody was produced against CDKLIWLHKQVKRFHFV (Covance). The peptide used for antibody production was used to block the antibody during staining to show specificity of antibodies.

Cell culture

HeLa cells (American Type Culture Collection, ATCC) were maintained at 37°C in 5% CO_2 using complete RPMI media supplemented with 10% fetal bovine serum (FBS). HEK-293 cells (American Type Culture Collection, ATCC) were maintained at 37°C in 5% CO_2 using complete DMEM media supplemented with 10% fetal bovine serum (FBS). Polyjet was used for transfections according to the manufacturer's protocol (SignaGen). To induce apoptosis cell were treated either with 500 ng/ml of TRAIL (Recombinant Human TRAIL/Apo2 ligand; BioVision). for 4 hours or with 5 mM Sodium Butyrate (NaBu) for 24 hours.

GFP-AKAP350C assembly

Synthetic constructs of AKAP350C fragments were ordered from GeneART. Amino acids 1-1400 were received as fragment 1 (F1) in a modified pEGFP vector

missing the HindIII site normally in the multicloning site. Amino acids 1360-2700 were received as fragment 2 (F2) in pMA vector. Finally, amino acids 2680-3184 were received as fragment 3 (F3) in pMA vector. AKAP350C-F3 was subcloned into pEFGP-C3 using XhoI and BamHI restriction site. Assembly of full length AKAP350C was achieved via triple ligation at 16C overnight using pEGFP-AKAP350C-F1 (cut with HindII and BamHI), AKAP350C-F2 (cut from pMA with HindIII and XhoI), and AKAP350C-F3 (cut with XhoI and BamHI).

Mutagenesis

Point mutations were created using Quickchange PCR techniques (Agilent Technologies). Primers were designed using the Quickchange primer design tool. The synthetic sequence of AKAP350C (GeneART) was used for all mutagenesis.

Plasmid construction

Human Mff was amplified from human heart tissue cDNA using primers 5'-GAGCGTCGACATGAGTAAAGGAACAAGCAGTGACAC-3' and 5'-GAGCGGATCC CTAGCGGCGAAACCAGAGC-3' and was ligated as a SalI/BamHI fragment into SalI/BamHI sites of pmCherry-C1 (a gift from Dr. Roger Tsien, University of California, San Diego) and pMyc-C1. Human Mfn1 and Mfn2 were also amplified from human heart tissue cDNA using primers 5'-GAGCGAATTC ATGGCAGAACCTGTTTCTCCACT-3' and 5'-GAGCGGATCC TTAGGATTCTTCATTGCTTGAAGG-3' (Mfn1) or 5'-GAGCGAATTCATGTCCCTGCTCTTCTCTCGATG-3' and 5'-GAGCGGATCCCTATCTGCTGGGCTGCAGGTACT-3' (Mfn2) and were ligated in EcoR1/BamH1 sites of pmCherry-C1 and pMyc-C2.

Fluorescence microscopy and analysis

HeLa cells grown on collagen-coated coverslips were fixed at room temperature for 15 minutes using 4% paraformaldehyde (PFA) supplemented with 0.1% Triton X-100, 80 mM K-PIPES pH 7.2, 1 mM EGTA, 1 mM $MgSO_4$, and 30% glycerol. Cells were permeabilized with 0.25% Triton X-100 and blocked with 5% normal serum for one hour at room temperature. The cells were incubated with primary antibodies for one hour at room temperature: rabbit-anti-AKAP350C serum (1:300), mouse-anti-MTCO2 (1:400, Abcam), chicken-anti-calreticulin (1:750, Abcam), mouse-anti-Mfn1 (1:200, Abcam), mouse-anti-Mfn2 (1:200, Abcam), and rabbit-anti-Mff (1:200, PTG Lab). This was followed by incubation at room temperature for one hour with species-specific fluorescent secondary antibodies (1:500; Invitrogen or Jackson Immunoresearch). Coverslips were mounted using Prolong Gold with DAPI (Invitrogen). Cells were imaged using a 60x oil immersion lens on Olympus FV-1000 confocal fluorescence microscope (Vanderbilt Cell Imaging Shared Resource).

Mitochondria preparation and analysis

HEK-293 cells were transfected with AKAP350C constructs. Mitochondria were isolated using the Qproteome Mitochondria Isolation Kit (Qiagen) following the protocol for high-purity preparations. An additional 100,000 x g centrifugation step was performed on the microsomal fraction from the kit to further separate the ER and cytosolic fractions. Proteins from the ER and cytosol fractions were precipitated using the protein precipitation method in the Qproteome Mitochondria Isolation kit handbook. Protein concentrations of each fraction were taken using the BCA Protein Assay kit (Pierce), and 12.5 µg protein from each fraction was run in a 10% polyacrylamide gel.

Proteins were transferred to nitrocellulose membrane. Primary antibodies used for western blotting were mouse-anti-MTCO2 (1:1,000; Abcam), rabbit-anti-calreticulin (1:1,000, Abcam), and rabbit-anti-GFP (1:5,000, Abcam). Secondary antibodies were donkey-anti-mouse-HRP (1:5,000) and donkey-anti-rabbit-HRP (1:5,000) from Jackson. Signal was detected using ECL Western Blotting Substrate (Pierce).

Flow-sorting and EM analysis

HEK-293T cells were transfected with GFP and GFP-AKAP350C constructs. Cells were flow-sorted and GFP-positive cells were collected (with assistance from Dr. Jim Higginbotham). The cell pellets were then given to the Vanderbilt Cell Imaging Shared Resource core for fixation, embedding, and processing (courtesy of Dr. Janice Williams). Transmission electron microscopy images were taken using a Philips/FEI T-12 electron microscope.

Protein expression and purification

AKAP350C fragments were cloned into pET30 vectors. Constructs were used to transform BL-21-DE3-RIL bacteria. Autoinduction media (Studier 2005) was used to induce protein expression in the bacteria during overnight growth. Bacteria were then pelleted and sonicated. Expressed protein was purified using Ni-NTA-agarose beads and eluted from the beads with high concentration of Imidazole.

Lipid-binding assay

Purified protein was used for overlay onto PIP strips (Echelon). The overlay was performed according to company protocol for blocking and protein incubation. After the protein incubation, the membranes were washed with PBS-T, as in the company protocol, but then also washed with TBS-T, as per protocol for the antibody used for detection.

Protein was detected using S-protein-HRP-conjugate antibody (Novagen) according to company protocol. Signal was detected using chemiluminescence.

GFP pull-down and western blotting

HEK-293T cells were co-transfected with GFP-tagged AKAP350C or empty pEGFP-C1 vectors with either myc-tagged Mff, Mfn1 or Mfn2. 24 h after transfection cells were lysed with co-IP buffer (1% digitonin, 120 mM NaCl, 50 mM HEPES, pH 7.5, supplemented with protease inhibitors and phosphatase inhibitors) for 15 min at 4°C and lysates were centrifugated at 16,000g for 10 min. Clarified lysates were diluted with lysis buffer lacking digitonin to bring final concentration of digitonin to 0.5%.The pull-downs were performed using GFP-binding protein-conjugated agarose beads for 2h at 4°C (Rothbauer *et al*., 2006). Beads were washed three times with co-IP buffer with 0.1% digitonin and once with co-IP buffer lacking digitonin and future analyzed by western bloting using an Odyssey imager (LiCor). The same membrane was probed for both GFP-tag and Myc-tag simultaneously. Memebrane was probed with the primary antibodies: 910-C2 mouse-anti-myc (1:1,000; Vanderbilt Molecular Recognition Shared Resource) and rabbit-anti-GFP (1:10,000; Abcam) followed by incubation with IRDye secondary antibodies: donkey-anti-Mouse IRDye680RD (1:40,000) and donkey-anti-Rabbit IRDye800CW (1:40,000) (LiCor).

For cleaved-PARP detection, HEK-293T cells were transfected with either GFP-tagged AKAP350C full-length, F3-I3154X or empty pEGFP-C1 vectors. Cells were lysed in SDS-containing lysis buffer and analyzed by Western blotting. The same membrane was simultaneously probed with primary antibodies rabbit-anti-cleaved PARP (Asp214/215) (1:1,000, Abcam) and mouse anti-alpha-tubulin (1:10,000, Sigma), and

later re-probed with rabbit anti-GFP (1:10,000, Abcam). Signal was detected using a LiCor Odyssey imager.

CHAPTER IV

IDENTIFICATION OF A NOVEL CAPRIN-1 PHOSPHORYLATION SITE AND KINASE, AND DISCOVERY OF A THIRD PKA-BINDING SITE IN AKAP9 PROTEINS

Introduction

All organisms experience stress at an organismal and cellular level, and proper stress response is crucial for survival (Jaggi *et al*., 2011). Cells have developed several stress responses and the capability to tailor the response depending on the type and level of stress (Fulda *et al*., 2010). All stress responses aim for protection of the basic cellular functions and components such as DNA repair and stability, cell cycle control, and protein quality control (Kültz, 2005). Cells initially employ response mechanisms to aid in cell recovery, but if the stressor persists or the damage is too great, cells then activate death signaling pathways to remove unhealthy cells (Fulda *et al*., 2010).

During inadequate stress response, cells can respond too strongly, not strongly enough, or inappropriately. First, if a cell survives a stress but fails to completely recover to normal status, a mutated gene or long-lived protein could remain within a cell causing it to develop into a disease (Fulda *et al*., 2010). Second, a strengthened stress response could have detrimental effects such as cancer cells being more resistant to treatment (Lowe and Lin, 2000; Hanahan and Weinberg, 2000; Lowe *et al*., 2004). Third, a weakened stress response could have detrimental effects such as diseased neurons with a weakened stress response dying upon even a weak stress episode (Wolozin, 2012; Roussel et al., 2013; Lagouge and Larsson, 2013). The importance of proper stress

response is apparent in the high degree of conservation of basic stress response pathways throughout evolution (Fulda *et al*., 2010).

Because stress response literally can determine the difference between life and death, cellular stress response is a highly regulated process. Phosphorylation is one key protein modification highly involved in the regulation of cellular homeostasis, stress response, autophagy, the cell cycle, and many other aspects of cellular function (Karve and Cheema, 2011). The human genome encodes roughly 500 protein kinases and 200 protein phosphatases, and over 30% of proteins are phosphorylated at some time in their existence (Cohen, 2001). Major areas of study include determining phosphorylation sites, discerning kinase-substrate dynamics, and identifying temporal and spatial regulation of phosphorylation events. The phosphorylation state of a protein can alter its function in many ways, including activation, deactivation, marking for degradation, alteration of interacting partners, and sub-cellular localization (Cohen, 2001). Dysregulation of protein phosphorylation has been implicated in many diseases including cancer, neurodegenerative disease, and metabolic disorders (Fulda *et al*., 2010; Karve and Cheema, 2011). Many pathogens and toxins utilize alterations in protein phosphorylation as their mechanism of action (Cohen, 2001). Therefore, the integration and regulation of signaling cascades is critical for appropriate stress response.

One way to integrate these signaling pathways is through scaffolding proteins in close proximity. A-Kinase Anchoring Proteins (AKAPs) are a large, diverse family of functionally similar scaffolding proteins that associate with a variety of signaling proteins (Tröger *et al*., 2012). AKAPs were discovered as PKA (Protein kinase A) anchors that provide localized cAMP (cyclic AMP)/PKA signaling, but it has since been shown they

play many other roles as well (Theurkauf and Vallee, 1982; Lohmann *et al*., 1984). AKAPs function as anchors for targeting proteins to specific sub-cellular locations, and the localization and composition of AKAP complexes is dynamic. AKAPs associate with both signaling enzymes and their substrates to bring the components of signaling cascades in close proximity (Michel and Scott, 2002). This allows AKAPs to provide spatiotemporal regulation of cAMP/PKA signaling, as well as serve as signal integration centers (Tröger *et al*., 2012). AKAPs comprise a very diverse family of proteins, and over 50 AKAPs have been identified to date (Wong and Scott, 2004; Tröger *et al*., 2012). The importance of AKAP function is evident in the embryonic lethality of most AKAP knockout mice (Carnegie *et al*., 2009). At least one AKAP is found in every tissue in the body (Welch *et al*., 2010).

AKAP9 gene products are integral for many cellular stress responses. The AKAP9 gene has four known products: yotiao, AKAP350A, AKAP350B, and AKAP350C. Yotiao is important for repolarization of cardiomyocytes, and its dysregulation can lead to chronic heart failure (Tröger *et al*., 2012). Disrupting the anchoring of KCNQ1 by yotiao leads to long QT syndrome, a potentially fatal heart arrhythmia (Chen *et al*., 2007). Therefore, yotiao is an important regulator in cardiac stress response. AKAP350A is also involved in cellular stress response, specifically stress granule formation (Kolobova *et al*., 2009). Upon cellular stress, AKAP350A localizes to stress granules and associates with mRNAs. AKAP350A also associates with other stress granule proteins, such as CCAR1 (cell cycle and apoptosis regulatory protein 1) and caprin-1 (cytoplasmic activation/proliferation-associated protein-1) (Kolobova *et al*., 2009). The previous chapter shows AKAP350C plays a role in regulation of

mitochondrial dynamics, a highly adaptive process involved in many aspects of cellular stress response. It remains to be seen in which stress response AKAP350B participates.

Cellular stress response is an intricate network of pathways, and any additional information discovered could be a key piece of the puzzle. This chapter contains several puzzle pieces that may help make connections when added to the large body of literature currently available. I discovered caprin-1 is phosphorylated on a serine residue *in vitro*, most likely by casein kinase II. This phosphorylation could regulate the function of caprin-1 during stress as well as its function when stress is not present. Also, a third $R_{II\alpha}$-binding site was identified in AKAP350C, with homology to other AKAP9 gene products. Further investigations detailing the exact mechanisms involved in these phenomena are needed and could open new avenues for research.

Results

AKAP350A associates with Caprin-1 and its kinase, Casein Kinase 2.

AKAP350A has been shown to associate with mRNAs (Kolobova *et al*., 2009), but whether AKAP350A interacts with mRNAs directly or through an intermediate protein remains unknown. I initially sought to determine which proteins in the AKAP350A complex associates with mRNAs by using the CLIP method (Ule *et al*., 2005). Briefly, this method involves using ultra-violet light to crosslink proteins and RNA. This is followed by cell lysis and an immunoprecipitation of your protein of interest. The immunoprecipitate is incubated with polynucleotide kinase (PNK) and ^{32}P-gamma-ATP.

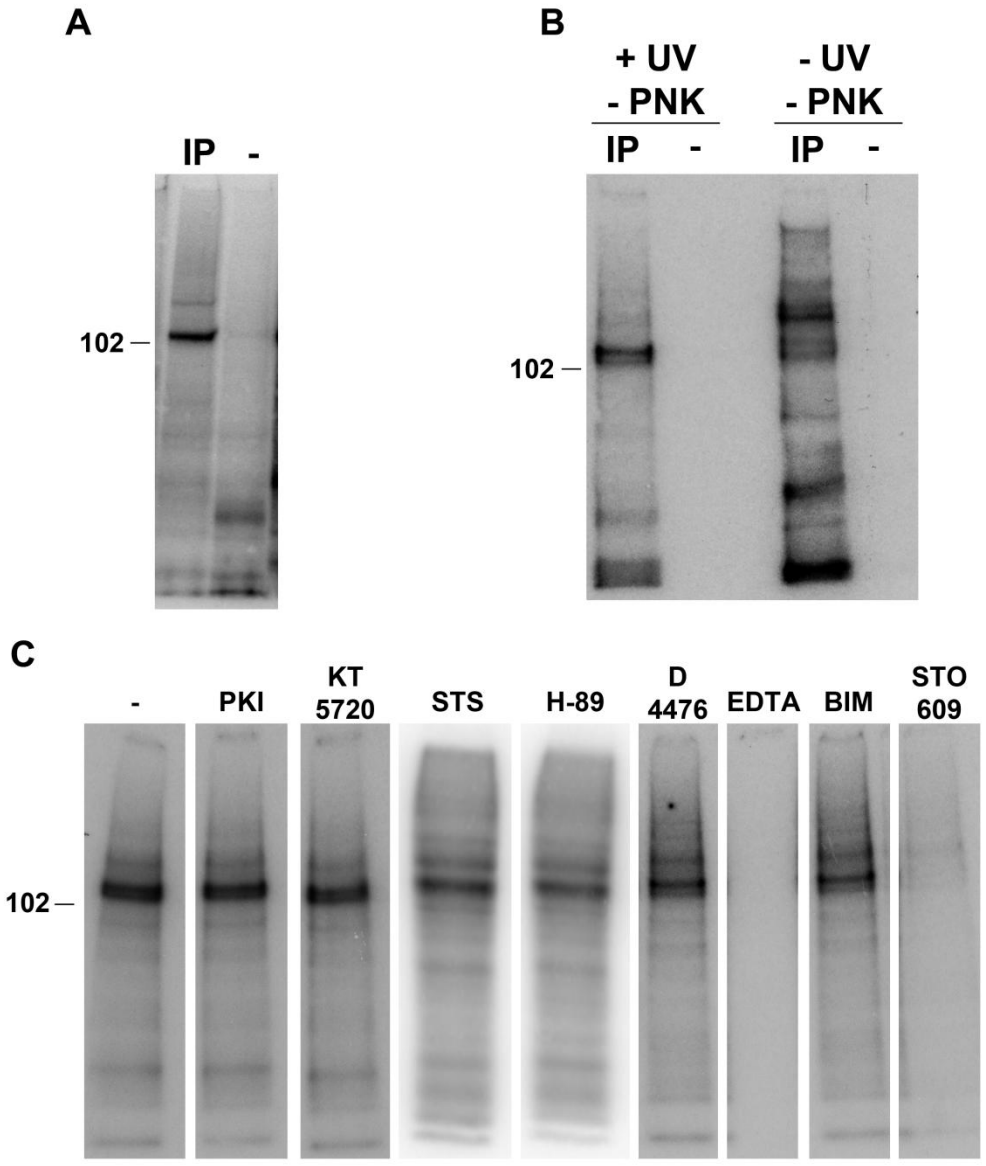

Figure 26. AKAP350A associates with Caprin-1 and its kinase, Casein Kinase II. UV crosslinked HEK-293T lysates were used for AKAP350A immunoprecipitations. Immunoisolates underwent *in vitro* phosphorylation with ^{32}P-ɣ -ATP. **A)** One major band is radiolabeled. Subsequent analyses show this band contains Caprin-1. **B)** Controls show protein, not RNA, is being phosphorylated. One control omits polynucleotide kinase (PNK; kinase for RNA), and another control omits PNK and UV crosslinking (crosslinks RNA to proteins). **C)** Several kinase inhibitors were added during the *in vitro* phosphorylation step and were compared to the signal seen with no inhibitor (-).

This is then run on a gel and the radiolabel is detected. A single major band was seen upon detection of the radiolabeled signal (Figure 26A). This band was cut from the gel and sent for proteomics analysis, and was determined to be caprin-1 (data not shown). As mentioned, AKAP350A associates with caprin-1 (Kolobova *et al*., 2009), a stress granule protein, and caprin-1 is known to associate with mRNAs during stress granule formation (Solomon *et al*., 2007). I then decided to perform a control experiment with one sample excluding the protein-RNA crosslinking, and another sample excluding the PNK that phosphorylates the RNA. When RNA is not present or when RNA cannot be phosphorylated, there is still a band of phosphorylation that contains caprin-1 (Figure 26B). This suggested that a protein is being phosphorylated instead of RNA. Since caprin-1 is the protein contained in the labeled band, it can be concluded that caprin-1 phosphorylation was being detected. When UV light and PNK were excluded, a second band was seen around 150 kDa, but proteomics analysis did not reveal the protein contained in this band.

This *in vitro* phosphorylation event also suggested that AKAP350A associates with the kinase responsible for phosphorylating caprin-1 in this system. To address which kinase phosphorylates caprin-1, I repeated the CLIP protocol but included various kinase inhibitors during the *in vitro* phosphorylation step (Figure 26C). The inhibitor STO-609 was the only inhibitor that blocked phosphorylation of caprin-1 (Figure 26C). This inhibitor has been shown to inhibit casein kinase II (CK2), among other kinases (Bain *et al*., 2007). CK2 has been identified in several proteomic analyses of AKAP350 immunoisolates and was found to be co-immunoprecipitated by AKAP350A (data not shown). Other inhibitors tested were PKI (protein kinase A inhibitor), KT5720 (inhibits

PKA, Aurora B, and many others), staurosporine (inhibits PKC, PDK1, AMPK, and others), H-89 (inhibits PKA, PKB, ROCK-II and others), D4476 (inhibits CK1 and PKD1), and BIM-1 (inhibits PKCα, β1, β2, γ, δ, ε) (Davies *et al*., 2000; Bain *et al*., 2003; Bain *et al*., 2007). Magnesium is required for oxidative phosphorylation (Sacktor, 1954), so a sample with no additional magnesium and EDTA to chelate residual magnesium was used as a negative control for phosphorylation (Figure 26C).

Caprin-1 is phosphorylated on a serine residue *in vitro*.

Caprin-1 has many predicted phosphorylation sites (C-Phos software). I next wanted to determine whether caprin-1 is phosphorylated on a serine, threonine, or tyrosine residue. To address this question, I performed phospho-amino acid analysis using two-dimensional thin layer chromatography. The samples for this were obtained from the ^{32}P-labeled band that contains caprin-1. Comparing the image for amino acid

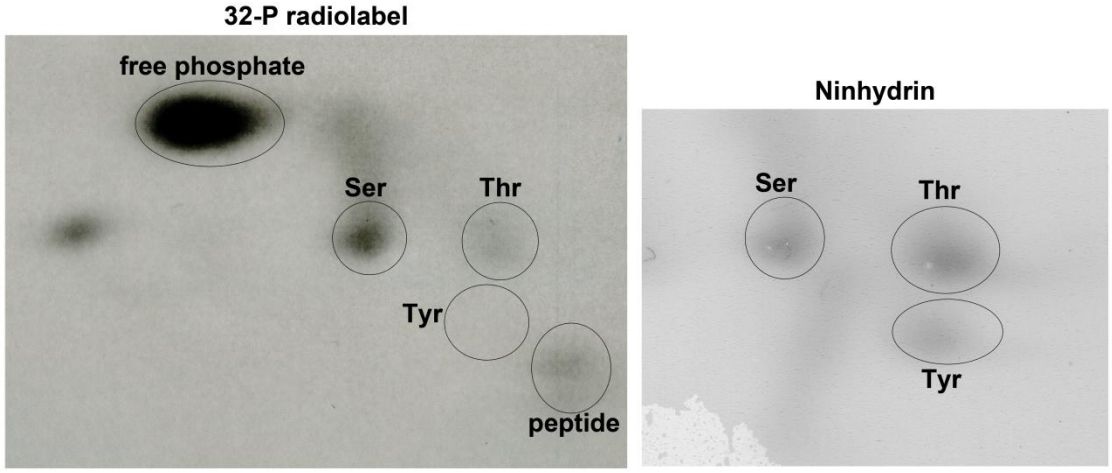

Figure 27. Caprin-1 is phosphorylated on a serine residue in vitro. The radiolabeled band containing caprin-1 was excised from the gel and then digested to obtain single residues. This sample was used for two-dimensional thin layer chromatography. Radiolabel was detected using a phosphor-imager screen. Amino acid residues were detected using a ninhydrin spray.

labeling (ninhydrin spray) to the radiolabel detection shows that the main radiolabeled component in the caprin-1 band is a serine residue (Figure 27). There is a slight signal for phosphorylated threonine as well, so it is possible there is a second, less prominent phosphorylation event occurring *in vitro*. Caprin-1 contains a predicted CK2 phosphorylation site at serine-179 (C-Phos software).

Phosphorylation of caprin-1 by CK2 is not affected by sodium arsenite- or Darinaparsin-treatment.

As discussed previously, caprin-1 localizes to stress granules upon cellular stress. The exact mechanism triggering caprin-1 relocalization remains unknown. I investigated whether the phosphorylation of caprin-1 by CK2 is altered upon the induction of stress granule formation. Cells were pre-treated with either sodium arsenite or Darinaparsin prior to UV crosslinking; the rest of the CLIP protocol was followed as described previously with the addition of phosphatase inhibitors. Pre-treatment of cells with sodium arsenite or Darinaparsin did not affect the *in vitro* phosphorylation of caprin-1 (data not shown). This suggests the change in the phosphorylation state of caprin-1 is unique to UV-induced stress.

AKAP350 contains a third PKA-binding site.

As evidenced by the name, AKAPs are most well-known for their ability to scaffold PKA. Among its many roles within the cell, PKA is a key player in the regulation of cellular stress response (Diviani *et al*., 2013). AKAPs associate with PKA via its regulatory (R) subunits, and AKAP350A binds regulatory subunit type II alpha ($R_{II\alpha}$). Two $R_{II\alpha}$-binding sites have been identified in AKAP350A (Schmidt *et al*., 1999;

Witczak *et al*., 1999; Takahashi *et al*., 1999) within a region of homology between AKAP350A and AKAP350C.

To investigate the importance of PKA-binding to AKAP350A and AKAP350C function, I created single and double mutants of AKAP350C with one or both $R_{II\alpha}$-binding sites mutated (Figure 28A). However, I found that the double mutant, GFP-AKAP350C-R1R2, still bound to $R_{II\alpha}$ (data not shown). This led to an examination of the rest of the AKAP350C sequence to look for other potential $R_{II\alpha}$-binding sites, which have a secondary structure of an amphipathic alpha helix. An additional amphipathic alpha helix (helix number 3) was found from amino acids 1197 to 1216 (Figure 28B). A proline-substitution point mutation was used to disrupt this alpha helix and test whether the disruption abolished association with ^{32}P-$R_{II\alpha}$. Another alpha helix (helix number 4) was also mutated to control for specificity of helix 3. I performed an overlay experiment with a recombinant fragment of AKAP350C and recombinant $R_{II\alpha}$ radiolabeled with ^{32}P. The fragment of AKAP350C used for the overlay assay contains helices 1, 3, and 4 (350C-H134). Recombinant Rab14 served as a negative control for $R_{II\alpha}$ binding. The association of wildtype 350C-H134 with $R_{II\alpha}$ is greatly decreased upon mutation of the known $R_{II\alpha}$- binding site, helix 1 (350C-H134-R1) (Figure 28C). The association of 350C-H134-R1 with $R_{II\alpha}$ was abolished by the additional mutation of the third helix (350C-H134-R1R3) (Figure 28C). The additional mutation of helix 4 (350C-H134-R1R4) did not have an effect on the amount of $R_{II\alpha}$ binding compared to 350C-H134-R1.

To further verify helix 3 as an additional third $R_{II\alpha}$-binding site in the AKAP350 proteins, I next examined the ability of the mutant constructs to associate with $R_{II\alpha}$ compared to wildtype. GFP-binding protein-conjugated beads (Rothbauer *et al*., 2006)

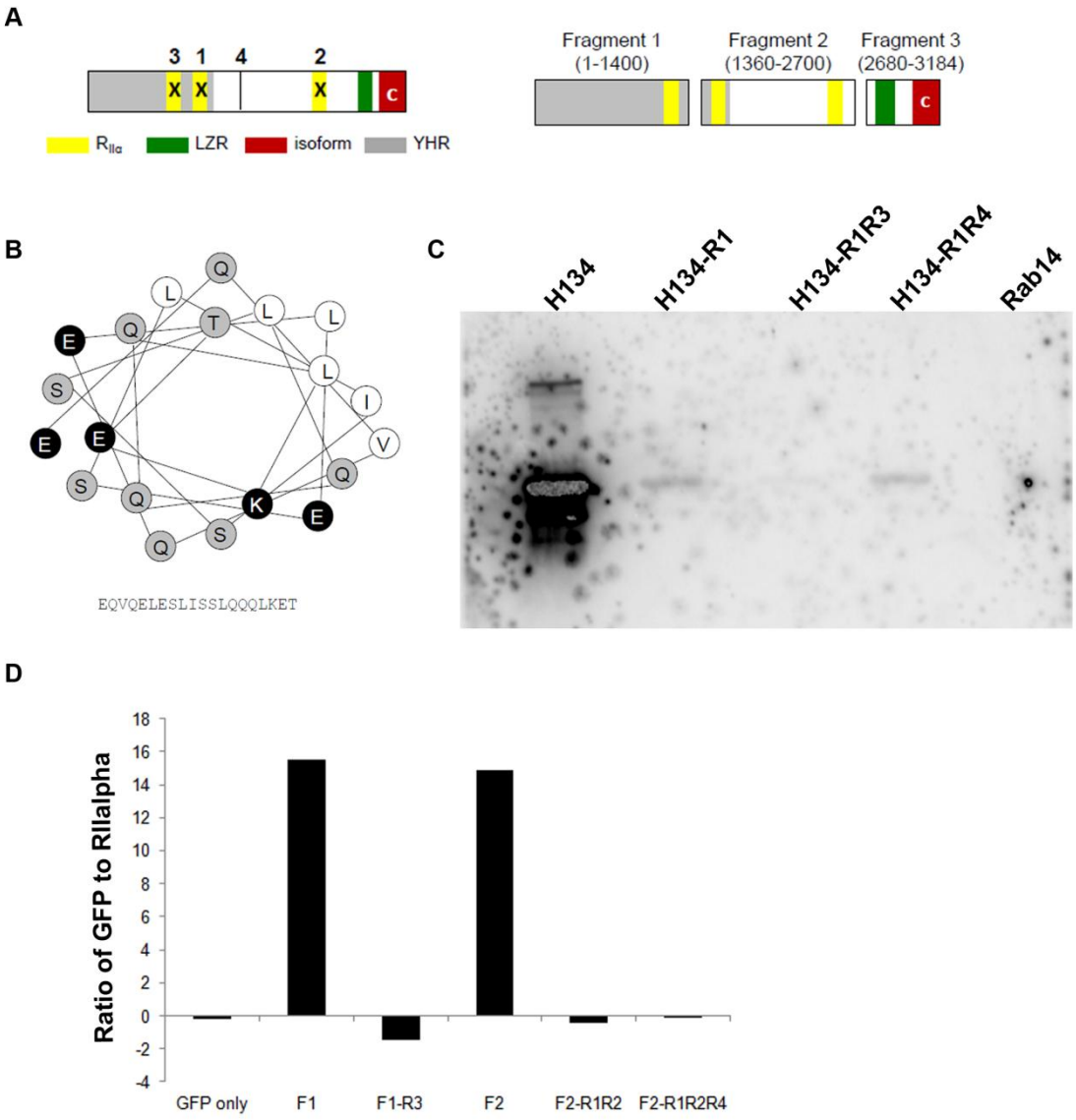

Figure 28. AKAP350 proteins contain a third PKA-binding site. A) Diagram of AKAP350C with two original $R_{II\alpha}$-binding sites (1 and 2) and new third site (3). **B)** Third site is an amphipathic alpha helix. White circles are hydrophobic residues, black are charged, and grey are polar. **C)** Recombinant AKAP350C fragments containing helices 1, 3, and 4 (control helix) and Rab14 (PKA-binding negative control) were used for overlay with ^{32}P-$R_{II\alpha}$. **D)** HEK-293T cells were transfected with various AKAP350 fragments. Lysates were used for GFP pull-downs, and the samples were run in a 10% gel and transferred to nitrocellulose. Membranes were probed for $R_{II\alpha}$ and GFP. Film was scanned and signal was quantified using LiCor Odyssey software.

were utilized for GFP pull-downs with lysates from HEK-293T cells overexpressing AKAP350C fragments (Figure 28A). Wildtype AKAP350C-F1 (amino acids 1-4200) and wildtype AKAP350C-F2 (amino acids 1360-2700) both associate with $R_{II\alpha}$ (Figure 28D). AKAP350C-F1-R3 does not bind $R_{II\alpha}$, verifying that mutating helix 3 abolishes the ability of fragment 1 to bind $R_{II\alpha}$ (Figure 28D). AKAP350C-F2-R1R2 and AKAP350C-F2-R1R2R4 do not associate with $R_{II\alpha}$ (Figure 28D), which suggests there are no additional $R_{II\alpha}$-binding sites within fragment 2. Mutation of helix 4 has no affect on $R_{II\alpha}$-binding.

Discussion

In these studies, I discovered two pieces of information that will add to the body of knowledge for the puzzle of cellular stress response regulation. First, I discovered that caprin-1 is phosphorylated on a serine residue by casein kinase II (CK2) *in vitro* (Figure 26). Caprin-1 has many potential phosphorylation sites and much work is being done to determine its phosphorylation state under various conditions. It is important to know the site of phoshorylation, the kinase, and when that phosphorylation occurs in order to better elucidate where this data fits in the overall network of stress response regulation. My data shows caprin-1 and CK2 are both co-immunoprecipitated by AKAP350A, so they are both present in the AKAP350A complex. Also, Figure 27 shows that the site of phosphorylation in this system is likely a serine residue. Further work to determine the exact phosphorylation site and the function of this phosphorylation *in vivo* is needed.

Phosphorylation of caprin-1 does not seem to be affected by the induction of stress granule formation. Exposure to UV rays, like those used for crosslinking in these

experiments, is a stressor for cells (Latonen and Laiho, 2005; Fulda *et al*., 2010). UV irradiation triggers stress response pathways and DNA damage checkpoints (Latonen and Laiho, 2005), and prolonged or severe UV irradiation can induce apoptosis (Fulda *et al*., 2010). It is possible that the changes in the phosphorylation of caprin-1 by CK2 are a response to the specific stressor of UV irradiation. Indeed, CK2 has been shown to phosphorylate p53 after cells are stressed with UV light (Keller *et al*., 2001).

This new phosphorylation information could also impact research regarding the function of caprin-1 outside of cellular stress response. Caprin-1 also plays roles in disease and regular cell functions. Caprin-1 interacts with Fragile-X Mental Retardation protein (FMRP) and functions to transport neuronal RNA granules (El Fatimy *et al*., 2012). When FMRP does not function properly, this can result in numerous neurological sequelae in Fragile X Syndrome (Kolobova *et al*., 2009; El Fatimy *et al*., 2012). Phosphorylation could affect the interaction of caprin-1 with FMRP or RNAs. Indeed, FMRP has been found in proteomic analyses of AKAP350A immunoisolates (data not shown). Caprin-1 was initially discovered as a protein regulating lymphocyte proliferation (Grill *et al*., 2004), and knockdown or knockout of caprin-1 greatly reduces cell proliferation (Wang *et al*., 2005). It has also previously been shown that caprin-1 is phosphorylated, but the phosphorylation site and kinase were not identified (Grill *et al*., 2004).

My discovery of a third $R_{II\alpha}$-binding site within the AKAP350 proteins is a major development in the PKA scaffolding literature. PKA is a critical regulatory kinase within the phosphorylation literature (Kanamaru *et al*., 2012; Diviani *et al*., 2013). We can now use $R_{II\alpha}$-binding deficient mutants, with all three sites mutated, to study the functionality

of AKAP350 proteins independently of their PKA scaffolding. These mutants could possibly be used as dominant negatives when overexpressed in order to determine the effects of loss of temporal and spatial regulation of PKA by AKAP350 proteins. In AKAP350 knock-down cell lines, these constructs would be especially powerful to rescue all functions of the AKAP350 protein with the exception of PKA-scaffolding.

The location of the new $R_{II\alpha}$-binding site is in a region that is homologous between AKAP350A, AKAP350C, and yotiao. The discovery of this new site could impact research from the past two decades involving PKA regulation by AKAP9 gene products. Any previous studies performed with $R_{II\alpha}$-binding mutants may need to be repeated using truly $R_{II\alpha}$-binding-deficient mutants. Yotiao and AKAP350A were discovered during a time when protein structure prediction computer programs were not available, and the prediction of amphipathic alpha helices ($R_{II\alpha}$-binding sites) was done by eye. This greatly increased the chances of missing a binding site. Indeed, of the three research groups that discovered AKAP350, only one group identified two binding sites (Takahashi *et al*., 1999) while the others only identified one (Schmidt *et al*., 1999; Witczak *et al*., 1999). Though protein structure prediction programs have been available for some time, nothing has instigated the need to investigate the possibility of additional $R_{II\alpha}$-binding sites until now. The impact of the discovery of an additional $R_{II\alpha}$-binding site remains to be seen.

The phosphorylation of Caprin-1 by CK2 and the discovery of an additional $R_{II\alpha}$-binding site in AKAP9 gene products are two critical pieces of the stress response-regulation puzzle. All cells experience various stressors throughout their existence, and it is critical for cells to be capable of responding to each stress. The cellular stress response

is a highly regulated complex integration of signaling pathways (Fulda *et al*., 2010). Protein phosphorylation is one of the key components in this regulation (Cohen, 2001; Karve and Cheema, 2011). Studies are ongoing in every area of phosphorylation, including determining phosphorylation sites, discerning kinase-substrate dynamics, and identifying temporal and spatial regulation of phosphorylation events. Phosphorylation or dephosphorylation can alter the function of a protein in many ways, including activation, deactivation, mark for degradation, change interacting partners, and alter sub-cellular localization (Cohen, 2001). Every additional piece of information is added to the puzzle to find its appropriate place within the regulation of cellular stress response.

Methods

Cell culture

HeLa cells (American Type Culture Collection, ATCC) were maintained at 37°C in 5% CO_2 using complete RPMI media supplemented with 10% fetal bovine serum (FBS). HEK-293T cells (American Type Culture Collection, ATCC) were maintained at 37°C in 5% CO_2 using complete DMEM media supplemented with 10% fetal bovine serum (FBS). Effectene was used for some transfections according to the manufacturer's protocol (Qiagen). Polyjet was used for some transfections according to the manufacturer's protocol (SignaGen).

CLIP

I adapted the CLIP protocol from the Darnell Laboratory (Ule *et al*., 2005). HEK-293T were grown to about 80% confluency. After washing, cells were crosslinked with 400 mJ/cm^2 ultraviolet light. Cells were then pelleted and lysed with M-PER

(Thermo Scientific) with protease inhibitors (Sigma). Lysates were treated with RQ1 DNase (Promega) and RNase A (USB). Protein concentration was determined using the BCA protein assay (Pierce). Equal amounts of protein from each lysate were used for the immunoprecipitation. AKAP350A was immunoprecipitated using the rabbit-anti-AKAP350A antibody we developed, and magnetic sheep-anti-rabbit Dynabeads (Invitrogen). Beads were resuspended in reaction buffer (70 mM Tris-Cl, pH 7.5; 10 mM $MgCl_2$; 5 mM DTT), and inhibitors were added at this step, if applicable. Polynucleotide Kinase (PNK, New England Biolabs) was then added, if applicable. Then, 3000 Ci/mM ^{32}P-gamma-ATP was added, and the mix was incubated at 37°C for 10 minutes while shaking. The supernatant was disposed of, and the beads were washed with ice-cold PBS then resuspended in sample buffer. The samples were run in a polyacrylamide gel. The gel was then dried and exposed to film or a phosphoimager screen. The inhibitors were used at the following final concentrations: 10 µM H-89 (Sigma), 10 µM KT5720 (Sigma), 10 µM PKI (Sigma), 100 nM Staurosporine (Sigma), 10 µM STO-609 (Calbiochem), 200 nM BIM-1 (Cayman Chemical), and 10 µM D 4476 (Cayman Chemical). For stress pre-treatment, cells were incubated at 37°C for 45 minutes with a final concentration of either 0.5 mM sodium arsenite (Riedel de Haen) or 0.05 mM darinaparsin (Ziopharm) prior to UV crosslinking. Lysates were treated with phosphatase inhibitors (Sigma).

Phospho-amino acid sample preparation

The radiolabled samples from the CLIP protocol (above) were run in a polyacrylamide gel, which was then stained with colloidal coomassie. The gel was then dehydrated and exposed to phospho-imaging screen. The coomassie-stained and

radiolabeled band was cut from the gel and put in a glass dish. The gel piece was incubated with 100 mM ammonium bicarbonate (AmBic) for 15 minutes at room temperature. The gel was diced, and then put into screw-top 1.5 mL tube. Then, 500 µL fresh 100 mM AmBic was put in the tube and incubated overnight at room temperature. Fresh AmBic was placed in the tube and incubated at room temperature for 15 minutes. The AmBic was discarded and replaced with a 1:1 solution of acetonitrile to 100 mM AmBic and incubated at room temperature for 15 minutes. This was repeated as necessary to destain the gel. Next, I added 100% acetonitrile, and incubated the sample at room temperature for 15 minutes, repeating until gel was dehydrated. To the dry samples, I then added 300 µL of 0.01 µg/µL trypsin in 25 mM AmBic, and incubated this overnight at 37 °C. The supernatant was placed in a new tube. Then, 200 µL 60% acetonitrile/0.1% formic acid was added to the gel pieces and incubated at room temperature for 15 minutes. This supernatant was added to the previous supernatant, and then dried in a vacuum until no liquid remained. The pellet was washed with 100 µL water and dried in a vacuum a total of three times. Then, 100 µL 6N HCl was added and heated at 100°C for two hours. The HCl was diluted with 900 µL water, and then dried in a vacuum. This was washed with water and dried in a vacuum two times.

Phospho-amino acid analysis thin-layer chromatography

The running buffer (2.5% formic acid, 8% acetic acid at pH 1.9) was used to make the standards: 2 mg phosphoserine, 2 mg phosphothreonine, and 2 mg phosphotyrosine into 1 mL running buffer. The running control was running buffer containing phenol red and xylene cyanole. The dried samples were resuspended in 10 µL running buffer, and 2 µL standards were added to each sample. First, 2 µL control was

spotted on the nitrocellulose plate about 2 cm from left and bottom of the plate. Then, 2 µL sample was spotted about 2 cm from bottom, centered in the plate. The plate was carefully wetted using an overlayed filter paper with holes cut out around the spots, taking care to approach the spots evenly from all directions. The filter paper was removed and plate was placed samples-down into the running apparatus, with the samples at the negative electrode. This was covered with a glass plate and run at 500V until dye reached about half way across the plate. The plate air dried overnight.

Next, the plate was rotated 90° counterclockwise. The plate was wetted with the second dimension running buffer (1% pyridine, 10% acetic acid at pH 3.5) using filter paper strips, careful to approach the line the sample ran evenly from all directions. This was run as before, at 500V, and the plate was air dried overnight. The plate was sprayed with ninhydrin to image amino acids. The plates were exposed to a phospho-imager screen to detect ^{32}P radiolabeling.

Protein expression and purification

AKAP350C fragments were cloned into pET30 vectors. Constructs were used to transform BL-21-DE3-RIL bacteria. Autoinduction media (Studier 2005) was used to induce protein expression in the bacteria during overnight growth. Bacteria were then pelleted and sonicated. Expressed protein was purified using Ni-NTA-agarose beads and eluted from the beads with high concentration of Imidazole.

Radiolabeling

The radiolabeling reaction buffer contains 0.1 µg PKA, 50 mM MOPS, pH 6.8, 50 mM NaCl, 2 mM $MgCl_2$, 1 mM DTT, 0.1 mg/mL BSA, and water to a final volume of 300 µL. Then, add 2 µg $R_{II\alpha}$ and 50 µCi ^{32}P -gamma-ATP. Mix well, and incubate on

ice for 1.5 hours. The ^{32}P-$R_{II\alpha}$ is cleaned using spin desalting columns according to the manufacturer's protocol (Thermo Scientific).

Overlay

Bacterially expressed and purified AKAP350C fragments were run in a 10% polyacrylamide gel. The proteins were then transferred to nitrocellulose and blocked with 5% milk in TBS-T (0.1% Tween-20). The ^{32}P-$R_{II\alpha}$ was added to milk until it was 100,000 counts per minute. This mixture was incubated with the membrane at room temperature for 3.5 hours while rocking. The membrane was then washed for 15 minutes three times with TBS-T. The membrane was then wrapped in plastic and exposed to film or a phosphoimager screen.

GFP pull-down and western blotting

HEK-293T cells were transfected with various AKAP350C constructs. Cells were lysed with M-PER (Thermo Scientific). The pull-downs were performed using GFP-binding protein-conjugated agarose beads for 2h at room temperature (Rothbauer *et al*., 2006). Samples were run in a 10% polyacrylamide gel, and proteins were transferred to nitrocellulose membrane. Primary antibodies used for western blotting were mouse-anti-$R_{II\alpha}$ (1:1000; BD) and rabbit-anti-GFP (1:5000, Abcam). Secondary antibodies were donkey-anti-mouse-HRP (1:5000) and donkey-anti-rabbit-HRP (1:5000) from Jackson. Signal was detected using ECL Western Blotting Substrate (Pierce). Film was scanned and signal quantified using LiCor Odyssey software.

CHAPTER V

DEVELOPMENT AND INITIAL CHARACTERIZATION OF AKAP9-KNOCKOUT AND CONDITIONAL AKAP9$^{F/F}$ MICE

Introduction

Animal models have become an integral part of modern scientific research. These systems allow the study of a particular protein in the *in vivo* niche as opposed to the artificial environments of laboratory plastic and glassware (Gama Sosa *et al*., 2010). *In vivo* animal studies also provide scientists with an avenue for broadening their *in vitro* studies into systemic studies. Genetically modified mice are the most common *in vivo* model used for studying human disease (Gama Sosa *et al*., 2010). The use of animal models in stress response is very prominent and necessary given that often the whole organism, not just an isolated cell type, experiences the stress. A study in whole animals is necessary to better understand the complexities of an organism's response to a stressor.

One common method of utilizing animal models to study stress is to use genetically modified, or transgenic, animals to examine the role of a specific protein or family of proteins in stress response. For example, researchers have used transgenic mouse models of Parkinson's disease to study the effects of oxidative stress on the progression of the disease (Varçin *et al*., 2012). Many of these models of Parkinson's disease involve the genetic mutation of individual proteins or protein families, such as Parkin or the PARK proteins, that are involved in or increase susceptibility to oxidative stress (Varçin *et al*., 2012). Mice expressing a mutant form of Parkin, an E3 ubiquitin ligase, exhibit the hallmark features associated with Parkinson's disease (Hart and Xu,

2009). Importantly, mitochondria isolated from Parkin-deficient mice have decreased respiration, and the mice exhibit widespread metabolic issues (Palacino *et al*., 2004). Parkin-deficient mice also express lower numbers of stress response proteins and are more susceptible to oxidative stress (Palacino *et al*., 2004). Additionally, many of the genetic knockout mouse models of Parkinson's disease exhibit mitochondrial dysfunction and/or increased levels of oxidative stress. From these *in vivo* studies, mitochondrial dysfunction and oxidative stress have been strongly linked to Parkinson's disease pathogenesis (Varçin *et al*., 2012).

Transgenic mouse models are also used to identify previously unknown roles of stress response in the pathogenesis of diseases. Researchers studying *Osteogenesis imperfecta* (OI) developed a mouse model of the disease, and they discovered the unfolded protein response is involved in the pathogensesis of OI (Lisse *et al*., 2008). The mice have a mutation in procollagen 1, type 1 (COL1A1), which causes the collagen to misassemble and not be secreted, resulting in accumulation in the endoplasmic reticulum (ER). This triggers ER stress, specifically the unfolded protein response. If this stress is prolonged, it induces apoptosis in osteoblasts, thereby contributing to the disease progression (Lisse *et al*., 2008). This suggests that ER stress-mediated apoptosis is a key player in the pathogenesis of *Osteogenesis imperfecta*, and has fueled a new avenue for research on this disease.

Proper stress response is a critical element in development and disease prevention. AKAP9 gene products, which include yotiao, AKAP350A, AKAP350B, and AKAP350C, are involved in various stress responses. Thus, it is important to determine the role these proteins play on a whole tissue and organism level. Yotiao, the shortest

AKAP9 splice variant, is important for repolarization of cardiomyocytes. Dysregulation of yotiao can lead to chronic heart failure (Tröger *et al*., 2012). Furthermore, disrupting the anchoring of the potassium channel subunit, KCNQ1, by yotiao leads to long QT syndrome, a potentially fatal heart arrhythmia (Chen *et al*., 2007). Therefore, yotiao is a critical regulator of the cardiac stress response.

AKAP350A is also involved in cellular stress response, specifically stress granule formation (Kolobova *et al*., 2009; Mason *et al*., 2011). Upon cellular stress, AKAP350A localizes to stress graules and associates with mRNAs and other stress granule proteins (Kolobova *et al*., 2009). Stress granule formation is induced by many stressors including viral infection, during which some viruses suppress while others hijack the stress response (White and Lloyd, 2012). Irradiation also induces stress granule formation in tumor cells following whole animal radiotherapy (Moeller *et al*., 2004). During stress granule formation, protein and mRNA components of stress granules aggregate (Anderson and Kedersha, 2006). Misregulation of this aggregation process has been implicated in several diseases, especially neurodegenerative disorders (Wolozin, 2012). More specifically, aberrant aggregation of stress granule proteins is implicated in the pathogenesis of amyotrophic lateral sclerosis (ALS) (Li *et al*., 2013).

As seen in Chapter III, another splice variant, AKAP350C, targets to mitochondria and is involved in the regulation of mitochondrial fission and fusion. Knockout of mitochondria fission and fusion proteins typically results in embryonic lethality (Kanamaru *et al*., 2012). The balance between the processes of fission and fusion is a key component in the ability of mitochondria to respond to cellular stress (Fulda *et al*., 2010). As described above, inadequate mitochondrial stress response is a

key feature in many neurodegenerative and other diseases. Therefore, investigations of these AKAP9 gene products on a whole animal scale will provide novel insight into their role in stress response and possibly numerous diseases

In this chapter, I describe the development of AKAP9-knockout ($AKAP9^{-/-}$) and conditional knockout ($AKAP9^{F/F}$) mice, as well as fibroblasts derived from null mouse tissue. The development of $AKAP9^{-/-}$ mice is significantly impaired, resulting in death by 13 days of age. This death presumably results from the severe lung impairment. The $AKAP9^{-/-}$ mice would possibly develop a liver phenotype if they were able to age (as is possible with $AKAP9^{F/F}$ mice). The fibroblasts from $AKAP9^{-/-}$ mice proved to be useful because they led to the discovery of tissue-specific preferential splicing. This splicing prompted the development of conditional knockout $AKAP9^{F/F}$ mice so that AKAP9 can be removed at varying time points. These AKAP9 mouse models now allow for investigations into the role of AKAP9 in a variety of tissues and diseases.

Results

Generation of $AKAP9^{-/WT}$ and $AKAP9^{WT/WT}$ genetic chimeras.

AKAP9 knockout-first, conditional-potential embryonic stem (ES) cells were purchased from Knockout Mouse Project (KOMP). The cells were heterozygous with one wildtype allele and one knockout-first, conditional-potential mutant allele (Figure 29A). The knockout-first allele has a LacZ reporter and Neomycin-resistance cassette flanked by Flp recombinase target (Frt) sites inserted between exons 7 and 8 of the AKAP9 gene, which contains a total of 51 exons (Figure 29). This cassette also has a

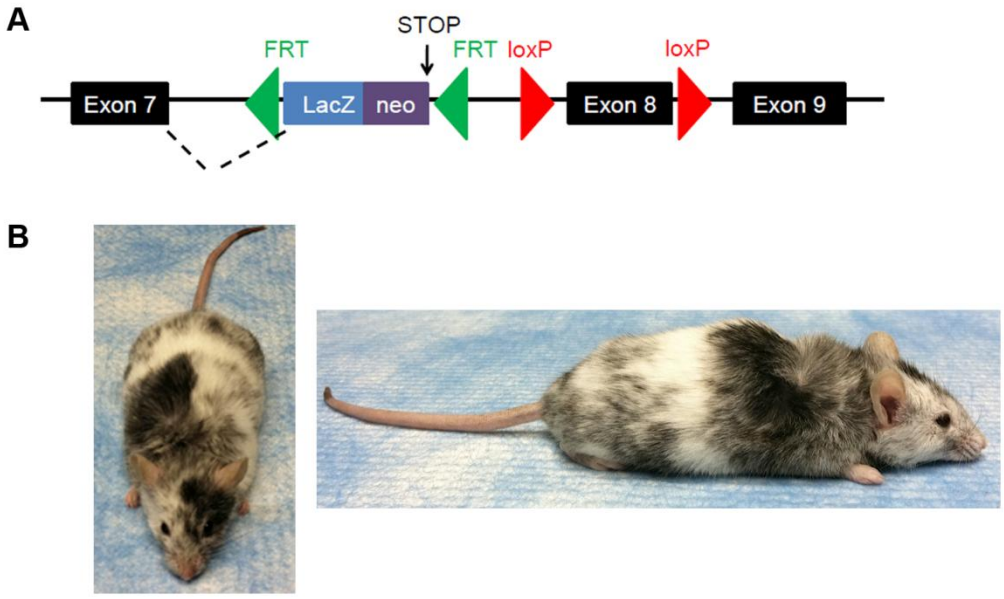

Figure 29. Generation of AKAP9$^{-/-}$ knockout-first chimeras. A) Diagram of mutant allele in embryonic stem cells purchased from KOMP. A LacZ/Neo cassette is inserted between exons 7 and 8, so that exon 7 will splice into the cassette which contains a stop codon. Frt-recombination sites flank the LacZ/Neo cassette, and LoxP-recombination sites flank exon 8. **B)** One of the male chimeras estimated to be 80% derived from the injected ES cells (the black coat color).

splice site acceptor, so exon 7 was designed to splice into the LacZ/Neo cassette, which contains a stop codon. The result would be a severely truncated, presumably non-functional AKAP9 protein. This truncation mutant would be less than one-fifth of the full length protein. This would effectively knock out all known splice variants of AKAP9: yotiao, AKAP350A, AKAP350B, and AKAP350C.

The AKAP9 knockout-first, conditional-potential ES cells from a C57BL/6 background were injected into albino C57BL/6 embryos. The embryos were then transferred to an albino C57BL/6 female to generate chimera offspring. In total, 3 male chimeras and one female chimera were generated, identified by black and white coat color (Figure 29B). The female and two males were estimated to be 80% derived from

the injected cells, and the other male was estimated to be 10% derived from the injected cells. The resulting chimeras were crossed to albino C57BL/6 mice, with one chimera resulting in germline transmission. When a black pup is born from the albino mother, this indicates the pup received an allele from the injected ES cell DNA as the black coat color is dominant over the recessive albino allele. Because the ES cells were heterogenous, these black pups must then be genotyped to determine the presence of the wildtype or mutant allele. After genotyping, nine black pups were obtained with four pups having the mutant allele. Once AKAP9 knockout-first heterozygous ($AKAP9^{-/WT}$) mice were obtained, they were crossed to each other to generate AKAP9 knockout-first homozygous ($AKAP9^{-/-}$) mice.

$AKAP9^{-/-}$ mice have a severe lung phenotype.

$AKAP9^{-/-}$ mice survive birth but suffer a severe phenotype after birth. Interestingly, the eight AKAP9-/- mice obtained thus far have been male. All of the mice that were born had died or had to be euthanized by 13 days of age due to failure to thrive, with the exception of one. Compared to their littermates, the $AKAP9^{-/-}$ mice were less than half the size (Figure 30A). Additionally, they appeared to have stunted hair growth initially. The pups also appeared lethargic when compared to littermates. Atrophied testes were observed in the $AKAP9^{-/-}$ mouse that lived longer than 13 days of age (data not shown). Upon analysis of the $AKAP9^{-/-}$ organs, the lungs appeared large for the body size when compared to a littermate. Histology showed the lungs to be the only grossly affected tissue. In the $AKAP9^{-/-}$ mice, the walls of the alveoli appear very thin when compared to wildtype age-matched mice (Figure 30B). The single-cell squamous

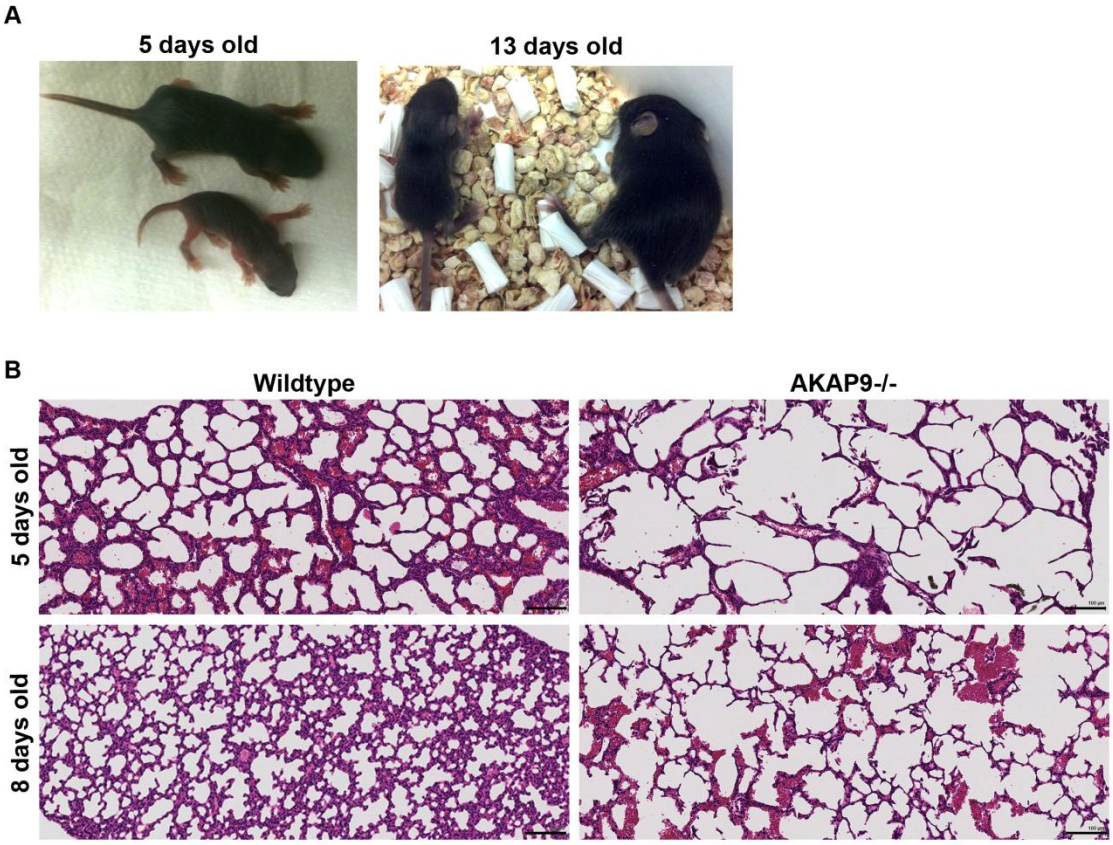

Figure 30. AKAP9$^{-/-}$ mice have a severe size and lung deficiency. A) AKAP9$^{-/-}$ pups are less than half the size of their littermates. B) Hematoxylin and eosin stain of AKAP9$^{-/-}$ lungs. Tissues were fixed in 4% paraformaldehyde overnight at 4°C. (Scale bars: 100 µm)

epithelial walls of the alveoli in the AKAP9$^{-/-}$ mice appear to be stretched and occasionally appear to have ruptured. From the histological examination of all tissues, the lung phenotype is presumably the cause of death.

AKAP9$^{-/-}$ mice have a liver phenotype.

By gross analysis of AKAP9$^{-/-}$ tissues, it was noted there may be a gross liver phenotype, though one was not seen during histological examinations. An AKAP9$^{-/-}$ pup

that was euthanized at five days old had pale spots throughout the liver. The spots were evenly distributed, similar in size, and affected all lobes. Furthermore, the entire liver was pale in the AKAP9$^{-/-}$ pup euthanized at 8 days old. When the 13-day-old AKAP9$^{-/-}$ pup was examined, the liver was almost completely white. This pattern suggests a progressive phenotype in the liver that may become a health issue in aged mice. Further investigation into the liver phenotype is warranted.

Characterization of AKAP9$^{-/-}$ and AKAP9$^{-/WT}$ fibroblasts.

The severe phenotype seen in the AKAP9$^{-/-}$ pups prompted me to devise another way to study the effects of knocking out AKAP9. For this, I isolated skin fibroblasts from tail tissues of AKAP9$^{-/-}$, AKAP9$^{-/WT}$, and wildtype littermates. AKAP9$^{-/-}$ fibroblasts propagated much slower than the AKAP9$^{-/WT}$ and wildtype fibroblasts. Therefore, it was not possible to characterize the AKAP9$^{-/-}$ fibroblasts as fully as the other lines.

Surprisingly, the AKAP$^{-/-}$ fibroblasts still expressed at least one of the AKAP9 gene products. When stained with an antibody against an epitope in AKAP350A and AKAP350C, immunostaining was observed in the AKAP9$^{-/-}$ fibroblasts. This antibody was previously characterized and verified, so these results suggest at least one AKAP9 splice variant is still present in the AKAP9$^{-/-}$ fibroblasts. This led us to test cDNA made from skin and lung total RNA for the presence of AKAP350A. We found wildtype AKAP350A message is still expressed in the skin, comparable to wildtype tissue, but not in the lung. We hypothesize there is tissue-specific preferential splicing around the inserted cassette, thereby splicing around the inserted stop codon, producing full length protein. Further investigation is needed to determine which tissues lack AKAP9 expression.

Upon further examination of the fibroblasts, the AKAP350 immunostaining appears to label the Golgi apparatus (Figure 31A and B). In some cells, the Golgi structure appears to be fragmented (Figure 31A), while in other cells the Golgi appears intact (Figure 31B). AKAP350A localizes to the Golgi (Shanks *et al*., 2002a) and centrosome (Schmidt *et al*., 1999) under non-stress conditions. AKAP9$^{-/WT}$ and wildtype fibroblasts show similar staining patterns with the AKAP350 antibody (Figure 31C and D, respectively). All three genotype groups also exhibited centrosomal staining. Using a commercially available antibody to the N-terminus of the AKAP9 gene products, I verified localization of an AKAP9 protein on the Golgi (Figure 31E). AKAP350 has been shown to play a role in ciliogenesis (Hurtado *et al*., 2011), so I sought to determine if fibroblasts isolated this way could be utilized to study this process. These fibroblasts do make primary cilia, though some cells exhibit multiple primary cilia (Figure 31F).

Developing the conditional AKAP9$^{F/F}$ mice.

Due to the issue of preferential splicing around the cassette, I developed the conditional knockout mouse line. AKAP9$^{-/WT}$ mice were bred with mice with flippase recombinase (Flp). When Flp is present in an AKAP9$^{-/WT}$ mouse, recombination occurs between the Frt sites, removing the LacZ/Neo cassette and the early stop codon, producing an AKAP9F/WT mouse (Figure 32A). This recombination removes exon 8. The splicing from exon 7 to exon 9 will result in nonsense mutations and early termination, effectively knocking out all full length AKAP9 proteins. AKAP9$^{F/WT}$ mice were then crossed to obtain AKAP9$^{F/F}$ mice, homozygous for the conditional knockout allele. All tissues appear normal and these mice were phenotypically wildtype as

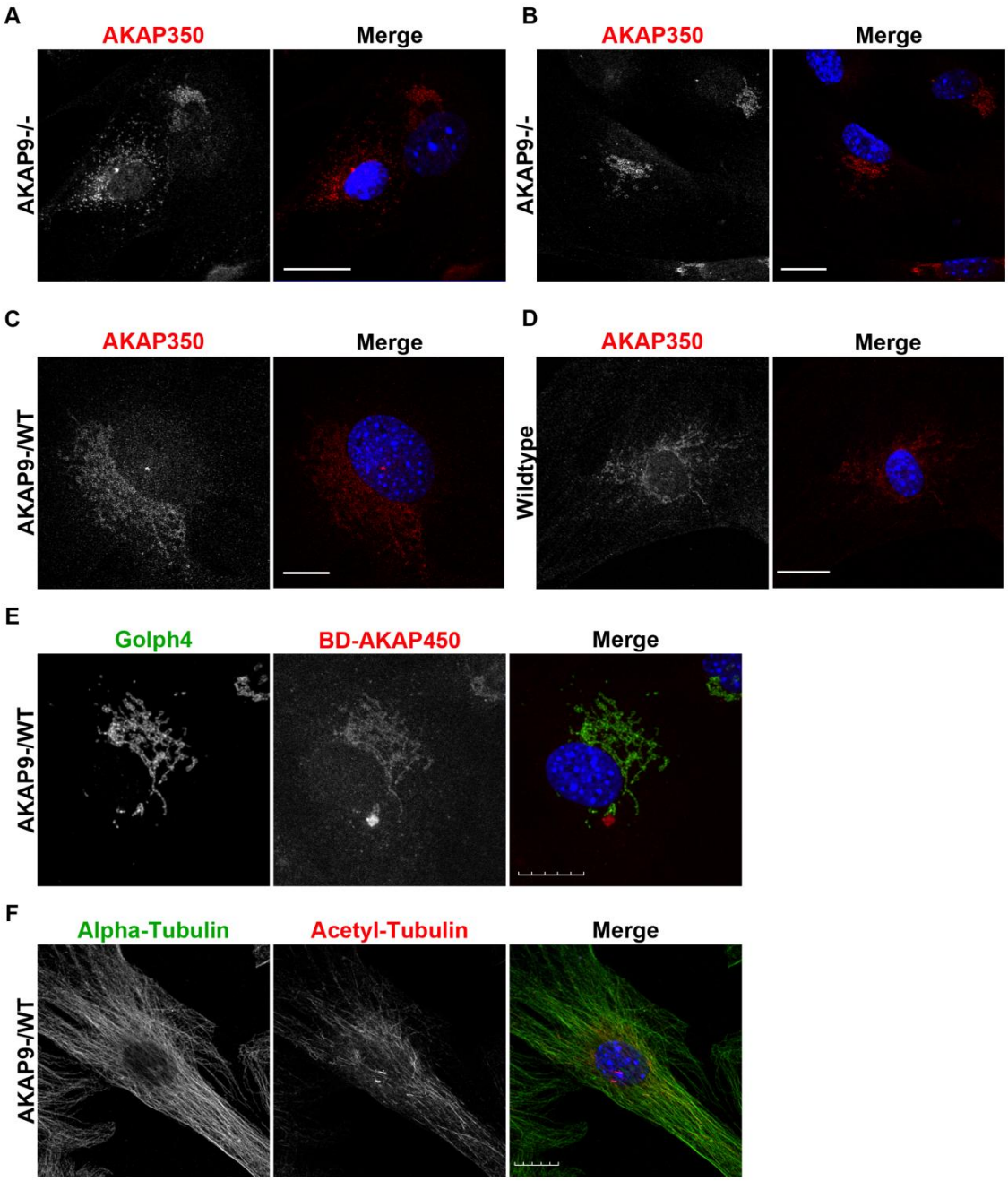

Figure 31. Characterization of AKAP9$^{-/-}$, AKAP9$^{-/WT}$, and wildtype fibroblasts. Skin fibroblasts were isolated from tail tissue. Fibroblasts were grown on poly-lysine-coated coverslips and were fixed with 4% paraformaldehyde. **A, B, C, D)** AKAP9$^{-/-}$ (A, B), AKAP9$^{-/WT}$ (C), and wildtype (D) cells were stained with our AKAP350 antibody (red). **E)** AKAP9$^{-/WT}$ cells were stained with Golph4 (Golgi, green) and the commercial antibody BD-AKAP450 (AKAP9 N-terminus, red). **F)** AKAP9$^{-/WT}$ cells were stained with alpha-tubulin (green) and acetylated-tubulin (red). All cells were also stained with DAPI (nuclei, blue). (Scale bars: 20 µm)

expected. The AKAP9$^{F/F}$ mice can then be bred to various mice expressing Cre recombinase to cause recombination between the LoxP sites (Figure 32B). Both global and tissue-specific, such as lung and liver, Cre-driver mice are of interest.

Discussion

I have developed AKAP9$^{-/-}$ mice using ES cells purchased from KOMP (Figure 29A and Figure 30). These mice have a dramatically shortened lifespan, living up to 13 days of age. The apparent cause of death is a lung defect, but more research is needed to determine the exact cause (Figure 30). The stretched appearance and rupturing of the

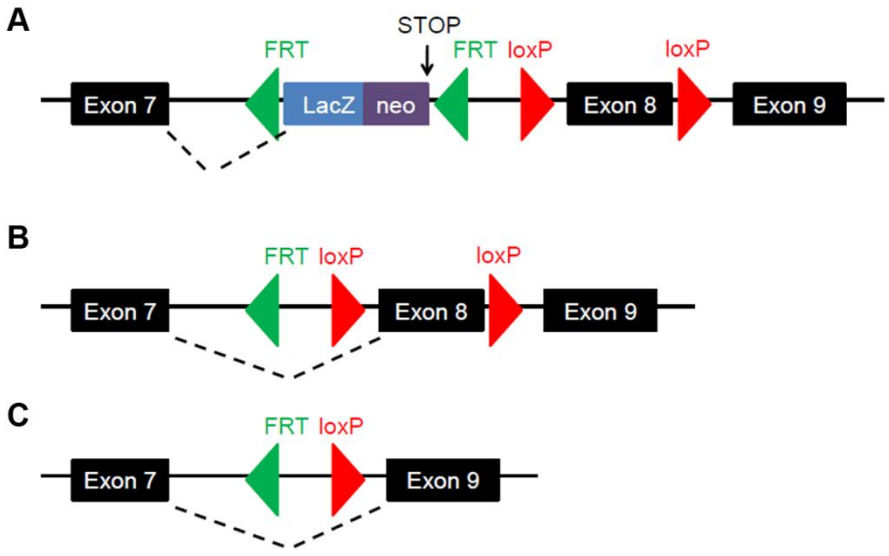

Figure 32. Schematic of AKAP9 conditional alleles. A) Diagram of mutant allele in embryonic stem cells purchased from KOMP. A LacZ/Neo cassette is inserted between exons 7 and 8, so that exon 7 will splice into the cassette which contains a stop codon. Frt-recombination sites flank the LacZ/Neo cassette, and LoxP-recombination sites flank exon 8. **B)** When Flp is expressed, recombination occurs between Frt sites, deleting the LacZ/Neo cassette. Splicing occurs normally. **C)** Upon Cre expression, recombination occurs between the LoxP sites, removing exon 8. Splicing from exon 7 to exon 9 results in nonsense mutations and early termination.

alveoli walls suggests hyperinflation of the lungs. An AKAP9 splice variant could regulate cellular organelle dynamics and be required for the lungs to return to a deflated state. AKAP9-mediated regulation of lung function is likely, as PKA regulates many aspects of the pulmonary endothelial barrier (Sayner, 2011). Many alveolar ion channels and proper fluid clearance from the alveoli are highly regulated by PKA, and the dysregulation can lead to pulmonary edema (Maron *et al*., 2005; Sayner, 2011). AKAP9 splice variants also serve as regulators for various stress responses. It is possible the stress of birth and beginning to breath requires a response regulated by an AKAP9 variant. Continued dysregulation of AKAP9-mediated stress response could induce a diseased state in the lungs, ultimately causing death.

AKAP9$^{-/-}$ mice are less than half the size of their littermates and have phenotypically abnormal liver and testes. Fibroblasts from tail tissues were able to be cultured for eight weeks (Figure 31). From these cultures, I found that AKAP9$^{-/-}$ mice have tissue-specific splicing around the inserted transgene. Due to viability and splicing issues, I also developed the conditional knockout AKAP9$^{F/F}$ (Figure 32). These mice are ready to be bred to mice expressing Cre recombinase to obtain tissue-specific AKAP9 knockout.

In a recent study, researchers investigated the role of AKAP9 gene products in spermatogenesis using an AKAP9 knockout mouse derived concurrently with our mice, from ES cells purchased at KOMP (Schimenti *et al*., 2013). They discovered delayed maturation and mislocalization of cells involved in spermatogenesis. Indeed, I also noted atrophied testes in our AKAP9$^{-/-}$ mice. In contrast to our breeding scheme, they opted to

breed AKAP9$^{-/WT}$ mice directly with constitutive Cre-expressing mice and, thus forgoing the conditional potential (Schimenti *et al*., 2013). These mice were then crossed with other mice containing a second mutation in exon 13 in the AKAP9 gene. Also, this study only examined the effects of AKAP9 knockout in the testes, and no other tissues were investigated. Interestingly, the researchers mention overall animal viability was not affected in their mice past 100 days of age (Schimenti *et al*., 2013), which is in stark contrast to our findings of the mice living less than two weeks after birth. Whether the different breeding strategies or additional mutations, caused this discrepancy remains to be investigated.

The AKAP9$^{-/-}$ mice remain a powerful tool for future studies. The dramatically shortened lifespan of AKAP9$^{-/-}$ mice suggests at least one AKAP9 gene product is important in development and possibly disease. Further characterization of the lung defect in AKAP9$^{-/-}$ mice at the cellular and sub-cellular level is needed to determine the exact defect and whether these mice could serve as a disease model. One possible explanation is a defect in the development or maintenance of the lung smooth muscle. The smooth muscle is responsible for the contractility of the lungs (Low and White, 1998), and the hyperinflated lungs seen in the AKAP9-/- mice could be due to a defect in smooth muscle contraction. Hyperinflation of the lungs is also seen in various disease states, such as chronic obstructive pulmonary disease (COPD) (Ferguson, 2006). A decrease in connective tissues in the alveoli, commonly seen in COPD, could also be an explanation for the hyperinflation in the AKAP9$^{-/-}$ mice, as connective tissue also affects contractility.

The conditional AKAP9$^{F/F}$ mouse is an especially powerful tool that will allow knockout of AKAP9 proteins in adult mice, something not possible with the AKAP9$^{-/-}$ mice. This would allow the investigation of the roles of AKAP9 proteins in maintaining homeostasis and in aging, as well as development and progression of disease. The AKAP$^{F/F}$ mice could be crossed with a liver-specific Cre-expressing mouse to investigate, in adults, the potential liver phenotype seen developing in the AKAP9$^{-/-}$ pups. AKAP350A plays a role in bile secretion in the liver by regulating the polarity of hepatocytes constituting the canaliculi (Mattaloni *et al*., 2012). Progressive familial intrahepatic cholestasis (PFIC) is a disease resulting from the inability to secrete bile, and is partially characterized by metabolic and nutrition deficiencies (Nicolaou *et al*., 2012). The progressive nature of this disease is similar to the progressive nature of the liver phenotype seen in AKAP9$^{-/-}$ mice. Also, metabolic and nutrition deficiencies could account for the small size of the AKAP9$^{-/-}$ mice.

As demonstrated above, studying an AKAP9 genetic mutant mouse model could provide insight into novel roles for AKAP9 proteins during development, aging, and the development and progression of disease. The involvement of an AKAP9 protein in development appears likely since the AKAP9$^{-/-}$ mice have a severe lung phenotype (Figure 30) which was not expected to be the primary phenotype based on current literature. This could potentially lead to the use of these mice in the development of therapeutics. The mice can also be used to study the effects of stress on development and disease. Also, studying the effects of the absence of these proteins within a whole organism may possibly elucidate novel roles of the proteins within signaling pathways or in specific cell types.

Methods

Animal Care and Use

All animal care, maintenance, and treatment of animals in these studies was done in strict accordance with protocols approved by the Institutional Animal Care and Use Committee of Vanderbilt University.

Generation of genetic chimeras

Knockout-first, conditional potential AKAP9$^{-/WT}$ embryonic stem (ES) cells from a C57BL/6 background (clone number EPD0033_5_B01) were purchased from Knockout Mouse Project (KOMP; Davis, CA). These ES cells were microinjected into wildtype albino C57BL/6 embryos in the Vanderbilt Transgenic Mouse/Embryonic Stem Cell Shared Resource (TMESCSR). The embryos were then transferred to recipient wildtype albino C57BL/6 females. Genetic chimeras were identified by black and white fur color.

Genotyping AKAP9$^{-/WT}$, AKAP9$^{-/-}$, AKAP9$^{F/WT}$, and AKAP9$^{F/F}$ mice

The AKAP9 gene was detected in all mice using the sense primer GTAATGTTTACATGTTCACTGGGAAATG and the anti-sense primer GTGTGCACGAACCTGATCCGCAT. Upon PCR, the band sizes are different depending on the allele: wildtype is about 500 nucleotides, knockout-first (Figure 29A) is 6,147 nucleotides, and the conditional allele (Figure 32A) is 700 nucleotides. For the AKAP9 PCR reactions, Advantage Taq II (Qiagen) was used with an extension time of one minute. The LacZ cassette was detected using the sense primer TGCCGCTCATCCGCCACAT and the anti-sense primer CACCGATCGCCCTTCCCAACAGT. Upon PCR using RedTaq (Sigma), a band of

about 600 nucleotides is seen in AKAP9 $^{-/WT}$ and AKAP9$^{-/-}$ mice. The presence of Flp recombinase was detected following the protocol from Jackson Laboratory (mouse stock # 003800). A band of 725 nucleotides was detected in all first-generation AKAP$^{F/WT}$ mice.

Tissue fixation, embedding, and sectioning

Immediately upon harvest, tissues were submerged in 4% paraformaldehyde for fixation overnight at 4°C with gentle agitation. Tissues were then washed three times with 70% ethanol for a minimum of 30 minutes each time at 4°C. Tissues were paraffin-embedded and 5 µm sections were used for all staining.

Tissue staining

Hematoxylin and eosin staining was performed by the Translational Pathology Shared Resource at Vanderbilt University.

Developing mouse fibroblasts

Fresh mouse tails from one-day-old pups were incubated in 0.04% bleach at room temperature rotating for 15 minutes, then washed twice with 1x Hank's balanced saline solution (HBSS). Tails were then put fresh HBSS and diced, then placed in a clean tube. Collagenase was added to a final volume of 1000 u/µL (collagenase blend type H, Sigma), and incubated at 37°C for 25 minutes. Samples were centrifuged at 2000 rpm for five minutes, and the supernatant discarded. After washing once with 1x HBSS, 0.05% trypsin was added. The samples were vortexed and incubated at 37°C for 20 minutes. Samples were then centrifuged at 2000 rpm for 5 minutes, and the supernatant discarded. The pellet was resuspended in 500 µL fibroblast media, pipetted to break up aggregates. For the fibroblast media, 10% fetal bovine serum, 1% MEM nonessential amino acids,

and 1% penicillin/streptomycin was added to DMEM media. The resuspensions were plated in a 3-cm dish, and 2 mLs fibroblast media was added. These were incubated at 37°C with humidity and 5% CO_2, disturbing dish as little as possible for 4-8 days.

Fluorescence microscopy

Fibroblasts were grown on poly-lysine-coated coverslips and were fixed at room temperature for 15 minutes using 4% paraformaldehyde (PFA) supplemented with 0.1% Triton X-100, 80 mM K-PIPES pH 7.2, 1 mM EGTA, 1 mM MgSO4, and 30% glycerol. Cells were permeabilized with 0.25% Triton X-100 and blocked with 5% normal serum for one hour at room temperature. The cells were incubated with primary antibodies for one hour at room temperature: mouse-anti-acetylated-tubulin (1:200, Sigma), rabbit-anti-gamma-tubulin (1:1000, Sigma), mouse-anti-AKAP350 (1:250), mouse-anti-AKAP450 (1:200, BD), and rabbit-anti-GOLPH4 (1:400, Abcam). The cells were then incubated with secondary antibodies for one hour at room temperature: goat-anti-mouse-Alexa-568 (1:500) and goat-anti-rabbit-Alexa-488 (1:500), both from Jackson. Coverslips were mounted using Prolong Gold plus DAPI (Invitrogen). Cells were imaged using a 60x oil immersion lens on Olympus FV-1000 confocal fluorescence microscope (Vanderbilt Cell Imaging Shared Resource).

Preparation of cDNA

Total RNA was isolated from frozen tissue with Trizol (Invitrogen) following the manufacturer's protocol. RNA was then treated with RNase-free RQ1 DNase (Promega). The High Capacity Reverse Transcription kit (Applied Biosystems) was used for making cDNA following the manufacturer's protocol using oligo dT primers for AKAP9$^{-/-}$ RNA.

CHAPTER VI

CONCLUSIONS AND FUTURE DIRECTIONS

Conclusions

Every cell experiences stress at some point, and how the cell responds to stress is critical to cell function (Fulda *et al*., 2010). Improper stress response can result in the survival of unhealthy cells that could result in progression to disease, resistance of disease cells to treatments, or erroneous cell death as seen in cardiovascular and neurodegenerative diseases (Fulda *et al*., 2010). Stress response can literally determine the difference between life and death, and, therefore, cellular stress response is a highly regulated process. The integration of numerous signaling pathways is central to this complex regulation.

A-kinase anchoring proteins (AKAPs) are large scaffolding proteins that serve as signal integration centers (Tröger *et al*., 2012). AKAPs act to scaffold kinases and their substrates as well as many other signaling proteins in close proximity to one another (Michel and Scott, 2002). This allows greater spatial and temporal control of the activation, deactivation, and integration of signaling cascades (Tröger *et al*., 2012). Many AKAPs have been identified, with each AKAP serving a unique function, and every cellular process is associated with at least one AKAP in some way (Table 1). Our lab is specifically interested in proteins encoded by the AKAP9 gene. There are several AKAP9 gene splice variants, including yotiao, AKAP350A, AKAP350B, and AKAP350C (Figure 5). Of these splice variants, AKAP350A (also known as

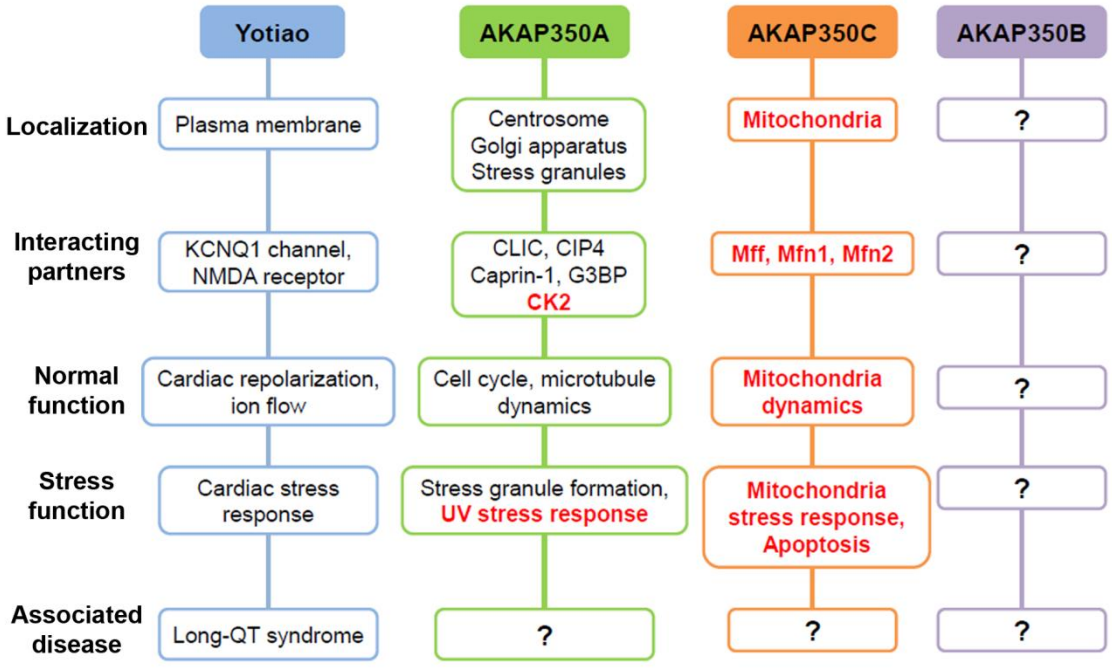

Figure 33. Summary of additional knowledge for AKAP9 gene products. AKAP9 gene products include yotiao, AKAP350A, AKAP350B, and AKAP350C. For each, this diagram lists the sub-cellular localization, the interacting partners, the normal function during non-stress conditions, the function during stress, and diseases associated with mutations and/or misregulation of the protein. Bold, red text indicates new knowledge obtained in this body of work.

AKAP450/AKAP9/CG-NAP) (Schmidt *et al*., 1999; Witczak *et al*., 1999; Takahashi *et al*., 1999) and yotiao are the most well-studied (Figure 6).

Without prior stress, AKAP350A localizes to the centrosome (Schmidt *et al*., 1999) and the Golgi apparatus (Shanks *et al*., 2002a) (Figure 33 and Figure 34). During non-stressed conditions, AKAP350A has roles in several cellular processes, including cell cycle regulation (Schmidt *et al*., 1999), canalicular development (Mattaloni *et al*., 2012), and microtubule organization (Larocca *et al*., 2006). Upon cellular stress, AKAP350A relocalizes from the Golgi to stress granules (Kolobova *et al*., 2009) (Figure 33 and Figure 34). AKAP350A associates with mRNAs and stress granule proteins both

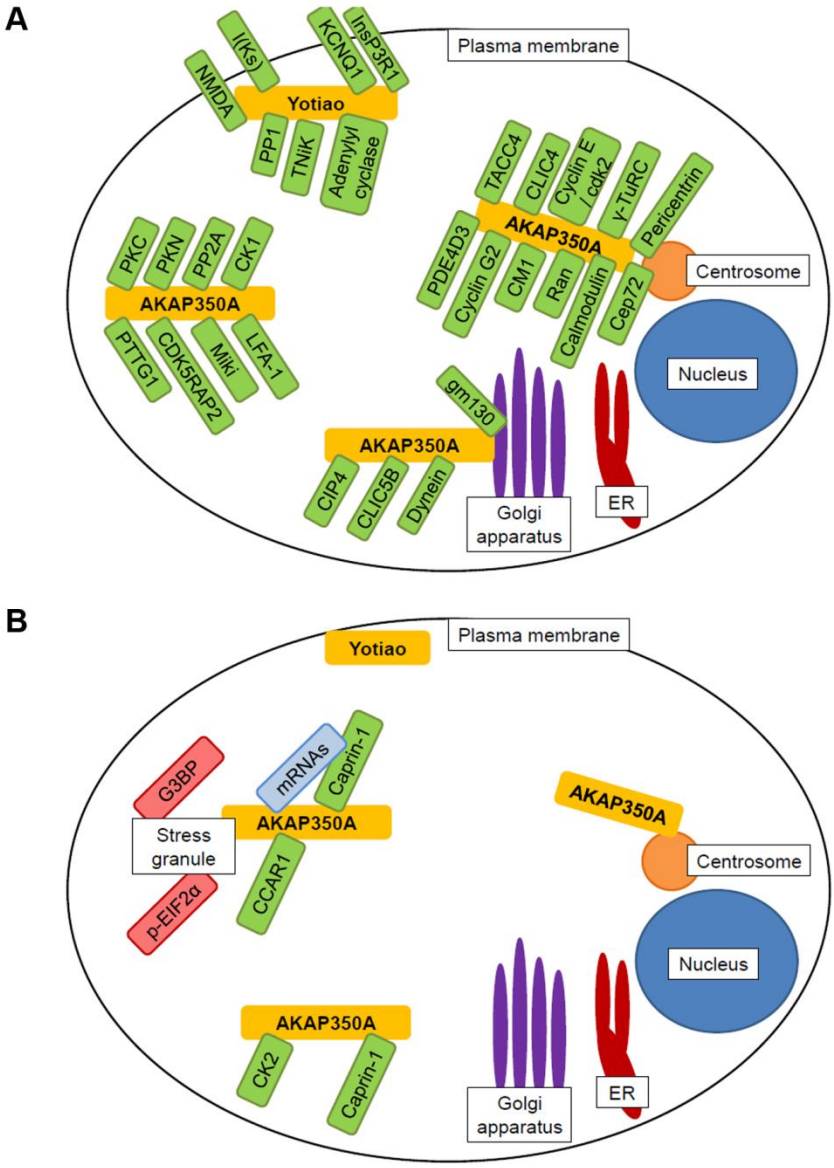

Figure 34. Schematic of AKAP350A and yotiao in a cell. AKAP350A- and yotiao-interacting proteins are green. PKA associates with yotiao and AKAP350A at all sub-cellular locations. **A)** Under normal conditions, yotiao localizes to the plasma membrane, and AKAP350A localizes to the Golgi apparatus, centrosome, and cytosol. For more information, see Chapter I. **B)** Upon stress, AKAP350A is dispersed from the Golgi and localizes to stress granules. There, AKAP350A associates with proteins and either directly or indirectly with mRNAs. AKAP350A may associate with other stress granule proteins, such as G3BP or p-EIF2α. AKAP350A also associates with caprin-1 and CK2, but it is unclear where this interaction occurs. AKAP350A at the centrosome and yotiao at the plasma membrane remain unchanged. For more information, see Chapters I, II, and IV.

during stress and during non-stress conditions (Kolobova *et al*., 2009), and the trigger for AKAP350A relocalization is unknown.

In this study, we used darinaparsin-treatment as a tool to better understand the temporal dynamics of stress granule formation, maintenance, and dispersal. Darinaparsin is an organic arsenical chemotherapeutic currently in Phase II clinical trials (Campàs and Castañer, 2009; Wu *et al*., 2010). Understanding the mechanism of action of a drug is crucial to understanding cell susceptibility and potential development of resistance. During our studies on the mechanism of action of darinaparsin, we discovered that darinaparsin induces stress granule formation but also stalls the completion of the stress response (Mason *et al*., 2011). Darinaparsin effectively acts similar to the combination treatment of sodium arsenite and nocodazole, as it induces a stress response while simultaneously destabilizing microtubules (Mason *et al*., 2011). Using darinaparsin-treatment as a tool for studying stress granule dynamics, we were able to show that stress granules must complete formation before they are able to disperse (Mason *et al*., 2011). Darinaparsin-induced stress granules are smaller, more numerous, and do not contain all components when compared to sodium arsenite-induced stress granules. AKAP350A only localized to a sub-set of darinaparsin-induced stress granules (Mason *et al*., 2011). A greater understanding of the formation, maintenance, and dispersal of stress granules will allow further targeting of these processes for therapeutics.

During these studies, I also discovered that AKAP350A potentially scaffolds casein kinase II (CK2), which phosphorylates caprin-1 (Figure 34). Previous studies show AKAP350A associates with mRNAs and caprin-1 during stressed and non-stress conditions (Kolobova *et al*., 2009), but it is not known if AKAP350A associates with

mRNAs directly or through a mediator. While investigating the mRNA-binding protein in the AKAP350A complex, I found that caprin-1 was phosphorylated *in vitro*. Caprin-1 contains many potential phosphorylation sites, and though it has previously been shown that caprin-1 is phosphorylated (Grill *et al.*, 2004), the kinase and phosphorylation site were not known. Understanding the phosphorylation states of caprin-1 could provide insight into the roles caprin-1 plays in stress granule formation and other cellular processes, such as proliferation. Subsequently, I discovered that CK2 is also part of the AKAP350A immunoisolate complex and is responsible for the *in vitro* phosphorylation of a serine residue in caprin-1 (Figure 33). Further investigation is needed to validate this phosphorylation event *in vivo* and to determine the function of this phosphorylation. Knowing the kinase for caprin-1 phosphorylation is critical for understanding the regulation of caprin-1 function, and possibly the regulation of stress granule dynamics.

Because AKAP350A potentially scaffolds caprin-1 and CK2, investigations into the functions of these proteins ultimately provides insight into the function of AKAP350A. Indeed, I identified a possible role for AKAP350A in ultraviolet (UV) light-induced stress response (Figure 33). Caprin-1 was only phosphorylated *in vitro* using lysates of cells that were stressed with UV light. Darinaparsin- and sodium arsenite-induced stress response did not alter the phosphorylation state of caprin-1. Further investigations are needed to fully determine the role of AKAP350A in UV-induced stress response.

Another AKAP9 gene product, AKAP350C, was previously identified as a potential splice variant (Shanks *et al.*, 2002a), but remained uncharacterized for almost a decade. In this present study, we completed cloning of AKAP350C and identified it as a

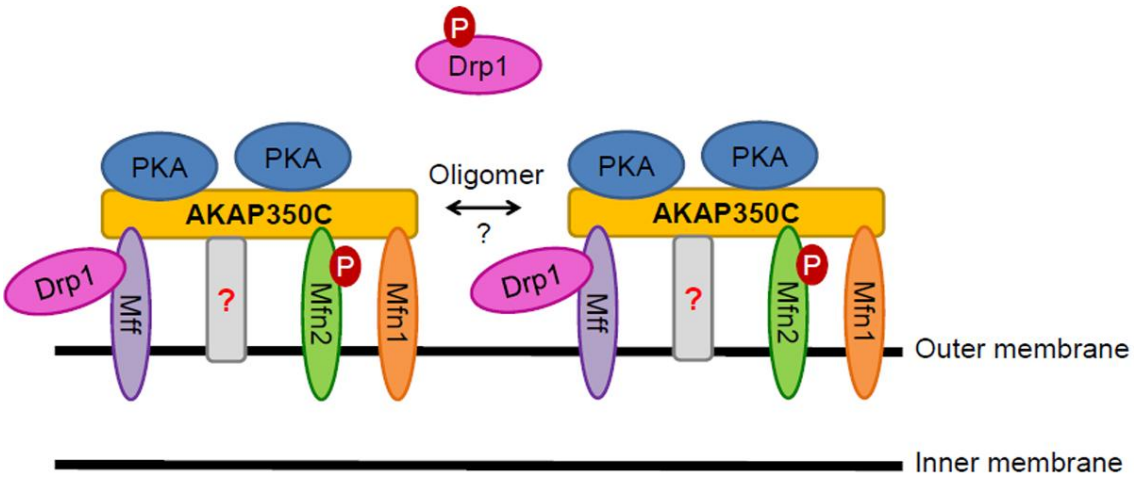

Figure 35. Schematic of AKAP350C at the mitochondria. AKAP350C scaffolds PKA, Mff, Mfn1, and Mfn2 in close proximity at the mitochondria outer membrane. Mff anchors Drp1 to the outer membrane, and when Drp1 is phosphorylated by PKA it becomes cytosolic. Mfn2 is also phosphorylated by PKA, though the function is unclear. AKAP350C is anchored to the mitochondria by an unknown entity. AKAP350C possibly oligomerizes, creating a signaling hub for mitochondrial dynamics.

mitochondria-targeted AKAP (Figure 33). AKAP350C lacks the centrosome- and Golgi-targeting domains found in AKAP350A (Figure 5) but contains a unique mitochondrial targeting sequence in the carboxyl terminus consisting of an amphipathic alpha helix. This is a novel targeting domain, and the alpha helix is necessary and sufficient for mitochondrial localization of AKAP350C. Alpha helices typically interact with proteins or membranes through either hydrophobic or electrostatic interactions with residues or phospholipids, respectively (Ma and Taylor, 2002). However, it does not appear that the amphipathic alpha helix in AKAP350C targets to mitochondria through electrostatic interactions with lipids. Other lipid or protein interactions remain possibilities and need to be investigated (Figure 35). Overexpression of full-length AKAP350C induced a collapse of mitochondria towards the perinuclear region. This suggests AKAP350C serves as a signaling center for the regulation of mitochondrial structural dynamics

(Figure 33 and Figure 35). Indeed, AKAP350C interacts with Mff (mitochondria fission factor), a mitochondrial fission protein, and mitofusins 1 and 2, mitochondrial fusion proteins (Figure 33 and Figure 35). The importance of these interactions and the mechanism of mitochondrial collapse remain to be investigated. Mitochondrial dynamics and the balance between fission and fusion is an important process in regulating cellular stress response (Youle and van der Bliek, 2012). We found that overexpression of AKAP350C is associated with increased apoptosis and exacerbates TRAIL- and sodium butyrate-induced apoptosis. The exact mechanism for regulation of apoptosis by AKAP350C remains to be elucidated. AKAP350C can potentially dimerize or oligomerize, allowing it to bring together many copies of the mitochondrial regulatory proteins (data not shown) (Figure 35). These combined results suggest that AKAP350C is responsible for coordination of mitochondrial structural dynamics and stress response (Figure 33 and Figure 35).

AKAPs associate with PKA via binding of the PKA regulatory (R) subunits. More specifically, the AKAP9 gene products bind regulatory subunit type II alpha ($R_{II\alpha}$). Two $R_{II\alpha}$-binding sites have been previously identified in AKAP350A (Schmidt *et al*., 1999; Witczak *et al*., 1999; Takahashi *et al*., 1999), with one of these sites also found in yotiao and both found in AKAP350C. During my AKAP350C studies, I also discovered a third, novel $R_{II\alpha}$-binding site in an area of homology between yotiao, AKAP350A, AKAP350C, and possibly AKAP350B. The newly identified $R_{II\alpha}$-binding is an amphipathic alpha helix similar to other known $R_{II\alpha}$-bindings. This third PKA-binding site is an amphipathic alpha helix, similar to other known PKA-binding sites. The identification of a third $R_{II\alpha}$-binding site has significant ramifications on the field.

Studies using mutants of AKAP9 proteins previously considered PKA-deficient may need to be re-examined.

To study the roles of the AKAP9 gene products *in vivo*, I developed AKAP9-knock out ($AKAP9^{-/-}$) and AKAP9-conditional knock out ($AKAP9^{F/F}$) mouse lines. $AKAP9^{-/-}$ mice are significantly impaired, resulting in death by 13 days of age. This death presumably results from the severe lung impairment, the most obvious, major phenotype. Additionally, the $AKAP9^{-/-}$ mice appear to develop a liver phenotype that seems to progress with age. The progression and severity of this phenotype is of interest to investigate in older mice (as is possible with $AKAP9^{F/F}$ mice). Investigations into fibroblast lines isolated from $AKAP9^{-/-}$ mice proved to be useful because they led to the discovery of tissue-specific preferential splicing. This splicing prompted the development of conditional knockout $AKAP9^{F/F}$ mice so that AKAP9 can be removed at varying time points and in various tissues.

The use of animal models in stress response is very prominent and necessary given that often the whole organism, not just an isolated cell type, experiences the stress. As shown in Figure 33, the associations between AKAP9 splice variants and disease remain relatively unknown. Misregulation of yotiao is linked to long QT syndrome, but that is the only known association. The dramatically shortened lifespan of $AKAP9^{-/-}$ mice suggests at least one AKAP9 gene product is important in development and possibly disease. The conditional $AKAP9^{F/F}$ mouse is an especially powerful tool that will allow knockout of AKAP9 proteins in adult mice, something not previously possible. The $AKAP9^{-/-}$ and $AKAP9^{F/F}$ mice will aid in identifying other diseases associated with AKAP9 proteins.

This body of work strengthens the concept that AKAP9 gene products have dual roles in cells with functions during non-stressed conditions and also during cellular stress response. Currently, three of the four known splice variants have been characterized and found to have dual roles (Figure 33). Yotiao functions normally in the repolarization of cardiomyocytes, but also serves as a regulator of cardiac stress response (Tröger *et al*., 2012). AKAP350A has several roles during non-stressed conditions, including regulation of cell cycle progression (Schmidt *et al*., 1999), microtubule dynamics (Larocca *et al*., 2006), and development of canaliculi (Mattaloni *et al*., 2012). During stress, AKAP350A functions in the regulation of stress granule formation (Kolobova *et al*., 2009), and possibly UV-induced stress response (Figure 33). I have shown now that AKAP350C is involved in the regulation of mitochondrial dynamics under non-stress conditions, as well as plays a role in the regulation of mitochondria during stress response (Figure 33). The $AKAP9^{-/-}$ and $AKAP9^{F/F}$ mouse lines that I developed are powerful tools that will be utilized to determine the consequences of losing the dual-regulation complexes, formed by the AKAP9 proteins, in the development and progression of disease.

Future directions

Examine stress granule dynamics.

Darinaparsin-treatment is a useful tool for further investigating the dynamics of stress granule formation, maintenance, and dispersal. Using darinaparsin-treatment, it was discovered that stress granules must complete formation before they can disperse (Mason *et al*., 2011). Darinaparsin-induced stress granules are smaller, more numerous, and are incomplete. Though the composition of stress granules is becoming increasingly known, the exact mechanisms of formation, maintenance, and dispersal remain largely unknown.

Darinaparsin-induced stress granules do not complete formation (Mason *et al*., 2011). Interestingly, these incomplete stress granules are heterogenous and do not contain all of the known stress granule components. Determining the assembly of stress granule components in a temporal manner would allow further elucidation of the mechanisms required for the process of formation. It would be interesting to investigate which stress granule components associate with one another before becoming part of the complete stress granule. If one protein is found to be present in all incomplete stress granules, this protein would be a likely candidate for a regulator of stress granule formation. If this master recruiting protein is discovered, it would be an excellent target for future therapeutics.

For incomplete stress granules, the stressor must be removed and then stress granule formation completed before the stress granules can disperse (Mason *et al*., 2011). This suggests not all components are required to initiate stress granule formation, but all components may be required to initiate dispersal. Defining which component(s) is (are)

last to enter complete stress granules could aid in determining the trigger for dispersal. For example, if AKAP350A is the last component in stress granule formation, then it would be the first component examined as the dispersal trigger. Another approach is to examine post-translational modifications of stress granule components and determine if any of those modifications are required for stress granule dispersal. The phosphorylation of eIF2α triggers stress granule formation, so it is likely a similar mechanism is used to trigger dispersal.

Elucidate role of CK2-mediated caprin-1 phosphorylation.

These studies show caprin-1 is phosphorylated on a serine reside by CK2 *in vitro,* but this data requires further validation and characterization. Caprin-1 contains a predicted CK2 phosphorylation site at serine-179 (C-Phos software). Once CK2-mediated phosphorylation of caprin-1 is verified, a phospho-deficient mutant of caprin-1 at this residue could serve to validate caprin-1 phosphorylation at this site.

Once the CK2-mediated phosphorylation of caprin-1 is characterized, the *in vivo* role of that phosphorylation is the next step in investigations. Phospho-deficient and phosphomimetic mutants of caprin-1 can be utilized for these experiments, possibly performing rescue experiments caprin-1-null (Wang *et al*., 2005) or caprin-1 knock-down cells. The phosphorylation state of caprin-1 in AKAP9-deficient mouse fibroblasts or knock-down cells is also of interest. Because caprin-1 localizes to stress granules and can induce stress granule formation upon overexpression, determining the role of caprin-1 phosphorylation in stress granule formation is critical. Depending on the results of

these experiments, another possible avenue of research is the role of AKAP350A in the regulation of UV-induced stress response.

Further characterize AKAP350C targeting.

AKAP350C targets to mitochondria via a novel targeting domain that is an amphipathic alpha helix. This targeting domain is contained within the first half of the carboxyl-terminal 55-amino acid sequence unique to AKAP350C. However, as shown in Chapter III, GFP-AKAP350C-F3-H3170X targets only partially to the mitochondria, with the remaining population localizing to the cytosol or ER. This suggests a second targeting domain is contained in the other half of the carboxyl-terminal 55-amino acid sequence. Further characterization of this potential second targeting domain could provide insight into an entirely new function for AKAP350C. AKAP350A has dual localizations to the centrosome and Golgi during non-stressed conditions, so the same could also apply to AKAP350C.

One obvious gap in AKAP350C knowledge is what the amphipathic alpha helical targeting domain is associating with. Though interacting proteins have been identified, they cannot account for the targeting of AKAP350C to mitochondria. The possibility remains that AKAP350C is interacting with lipids. We show the helix does not associate with phospholipids or inositides directly through electrostatic interactions. However, hydrophobic interactions between phospholipids and the alpha helix remain a possibility. Proteins such as hexokinase I contain domains of charge and hydrophobic regions that lay upon the surface of the outer membrane (Gelb *et al*., 1992, Sui and Wilson, 1997). Additionally a similar complex binding mechanism has been proposed for D-AKAP1

localization to mitochondria (Ma and Taylor, 2002). This must be examined as a possible mechanism for AKAP350C mitochondrial targeting.

Further define AKAP350C-regulated mitochondrial dynamics.

We know AKAP350C associates with the mitochondrial fission and fusion proteins, but we do not know whether this is a direct interaction. It is also not known if this interaction is constitutive or dynamic. Determining the intricacies of AKAP350C interaction with Mfn1, Mfn2, and Mff could shed light on the exact mechanism for AKAP350C regulation of mitochondrial dynamics.

All AKAPs serve as anchors for cAMP/PKA signaling, so the role of AKAP350C-anchored PKA in the regulation of mitochondrial dynamics should be investigated. This may prove difficult given the fact that other AKAPs localize to the mitochondria as well, and perhaps partially compensate for changes in AKAP350C-mediated PKA signaling. One way to circumvent this issue is performing *in vitro* experiments so other AKAPs are not present. Possible *in vitro* experiments to conduct include measuring changes in phosphorylation states of proteins such as Drp1 and Mfn2 and the association of mitochondrial proteins with AKAP350C following treatments such as forskolin, an activator of cAMP/PKA signaling.

Investigate AKAP350C regulation of apoptosis.

Mitochondrial dynamics and the balance between fission and fusion is an important process in regulating cellular stress response (Youle and van der Bliek, 2012). Overexpression of AKAP350C induces apoptosis and enhances TRAIL- and sodium

butyrate-induced apoptosis. Further investigation is needed to determine the mechanism of AKAP350C-induced apoptosis. AKAP350C potentially regulates apoptosis through two different pathways, the first being the same mechanism utilized for AKAP350C-mediated regulation of mitochondrial dynamics. Another possibility is that AKAP350C regulates apoptosis through a mechanism completely independent of that for regulation mitochondrial dynamics. Being such a large protein, AKAP350C likely interacts with more than just four proteins: PKA, Mfn1, Mfn2, and Mff.

Characterize AKAP350B.

AKAP350B is the last AKAP9 splice variant that is known to exist but is not characterized, which is an obvious gap in knowledge. Given what is known of the other splice variants (Figure 33), AKAP350B likely has a role in both normal cell physiology and cellular stress response. AKAP350B hypothetically has a small segment of unique sequence, as is the case for AKAP350A and AKAP350C, and it would be interesting to examine the purpose of that unique sequence.

Investigate PKA-independent roles of AKAP9 splice variants.

The PKA-independent roles of AKAP9 proteins have not been very well characterized. The identification of a third $R_{II\alpha}$-binding site warrants reexamining any previous investigations of binding-deficient AKAP9 protein constructs. AKAPs have more functions than just anchoring PKA, so it is important to investigate the functions of full-length, completely $R_{II\alpha}$-binding-deficient mutants of AKAP350A and AKAP350C. It is possible the overexpression of these mutants could act as dominant negatives by out-

competing endogenous protein. Compensation by other AKAPs could be an issue so *in vitro* studies may be required.

Investigate oligomerization of AKAP9 splice variants.

Interestingly, the proline substitution mutations in GFP-AKAP350C-C55-V3143P and GFP-AKAP350C-C55-L3139P abolished mitochondrial targeting but also caused relocalization to the centrosome. One possibility is that a centrosomal-targeting domain is also within the carboxyl-terminal 55 amino acids of AKAP350C. The more likely explanation is that the proline substitution somehow enhanced oligomerization of the construct with AKAP350A, which localizes to the centrosome.

Preliminary data suggests that AKAP350A and AKAP350C oligomerize with each other. Peptides specific to AKAP350A were identified in proteomics analyses of AKAP350C isolates. Also, overexpressed GFP-AKAP350C pulls down an endogenous AKAP350 protein, though it is not clear whether the endogenous protein is AKAP350A or AKAP350C. Further characterization of the dimerization or oligomerization of the AKAP9 splice variants is needed.

Fully characterize AKAP9$^{-/-}$ mice.

With the exception of yotiao, the role of AKAP9 splice variants in development and disease remain unknown. The AKAP9$^{-/-}$ mice could prove an invaluable tool for these investigations. The most important next step is to determine which tissues have preferential splicing around the transgene. Currently, only the lung and skin have been investigated, with the skin exhibiting preferential splicing. Learning which tissues are

affected by the transgene, like the lung, could provide insight into the differential splicing of AKAP9 in different tissues.

The AKAP9$^{-/-}$ mouse lung phenotype requires further examination. Deciphering whether the exact defect in the lung is smooth muscle, connective tissue, or something else will shed light on a previously unknown role of an AKAP9 gene product in lung development. This could also lead to the discovery of a link between a lung disease and the dysfunction or misregulation of an AKAP9 splice variant.

If investigations of preferential splicing indicate the liver and testes are affected by the transgene, the phenotypes in those tissues should be further examined. There appeared to be a liver phenotype developing, with the liver becoming increasingly pale, but this requires closer inspection at the tissue and cellular level. The possible testes phenotype is also an area of interest as all AKAP9$^{-/-}$ mice have been male, and the one surviving male appeared to have atrophied testes. Another study concluded AKAP9 splice variants are critical for spermatogenesis, and loss of AKAP9 resulted in atrophied testes (Schimenti *et al*., 2013). However, the splice variant responsible and the exact mechanism have not been identified.

Utilize AKAP9$^{F/F}$ mice.

Due to preferential splicing and viability issues in the AKAP9$^{-/-}$ mice, the AKAP9$^{F/F}$ mice have the greatest potential for providing insights into the roles of AKAP9 proteins *in vivo*. One experimental approach would be to cross AKAP9$^{F/F}$ mice with a mouse expressing an inducible global Cre recombinase, such as a tubulin-Cre mouse. This would allow the AKAP9$^{F/F}$ mouse to reach adulthood, and the effects of

losing AKAP9 proteins at a later time point can be investigated. A more targeted approach is crossing AKAP9$^{F/F}$ mice with mice expressing tissue-specific Cre recombinase. An obvious choice is a lung-specific Cre, but the liver, heart, and brain are also interesting possibilities given the possible phenotype in the liver and the importance of yotiao in the heart and brain. Investigating the role of AKAP9 proteins in the heart is also of interest given the importance of proper mitochondrial function in cardiomyocytes. AKAP350C regulates mitochondrial dynamics and stress response, and therefore, may cooperate with yotiao in the regulation of cardiomyocyte function.

REFERENCES

Abrenica B, AlShaaban M, and Czubryt MP. (2009) The A-kinase anchor protein AKAP121 is a negative regulator of cardiomyocyte hypertrophy. *J Mol Cell Cardiol*, **46**, 674-681.

Affaitati A, Cardone L, de Cristofaro T, Carlucci A, Ginsberg MD, Varrone S, Gottesman ME, Avvedimento EV, and Feliciello A. (2003) Essential role of A-kinase anchor protein 121 for cAMP signaling to mitochondria. *J Biol Chem*, **278**, 4286-4294.

Akakura S, Huang C, Nelson PJ, Foster B, and Gelman IH. (2008) Loss of the SSeCKS/Gravin/AKAP12 gene results in prostatic hyperplasia. *Cancer Res*, **68**, 5096-5103.

Akakura S and Gelman IH. (2012) Pivotal Role of AKAP12 in the Regulation of Cellular Adhesion Dynamics: Control of Cytoskeletal Architecture, Cell Migration, and Mitogenic Signaling. *J Signal Transduct*, **2012**, 529179.

Akileswaran L, Taraska JW, Sayer JA, Gettemy JM, and Coghlan VM. (2001) A-kinase-anchoring protein AKAP95 is targeted to the nuclear matrix and associates with p68 RNA helicase. *J Biol Chem*, **276**, 17448-17454.

Alto NM, Soderling J, and Scott JD. (2002) Rab32 is an A-kinase anchoring protein and participates in mitochondrial dynamics. *J Cell Biol*, **158**, 659-668.

Ambrosio AL, Boyle JA, and Di Pietro SM. (2012) Mechanism of platelet dense granule biogenesis: study of cargo transport and function of Rab32 and Rab38 in a model system. *Blood*, **120**, 4072-4081.

Anderson P and Kedersha N. (2006) RNA granules. *Cell Biol*, **172**, 803-808.

Arachchige Don AS, Dallapiazza RF, Bennin DA, Brake T, Cowan CE, and Horne MC. (2006) Cyclin G2 is a centrosome-associated nucleocytoplasmic shuttling protein that influences microtubule stability and induces a p53-dependent cell cycle arrest. *Exp Cell Res*, **312**, 4181-4204.

Arimura T, Hayashi T, Terada H, Lee SY, Zhou Q, Takahashi M, Ueda K, Nouchi T, Hohda S, Shibutani M, Hirose M, Chen J, Park JE, Yasunami M, Hayashi H, and Kimura A. (2004) A Cypher/ZASP mutation associated with dilated cardiomyopathy alters the binding affinity to protein kinase C. *J Biol Chem*, **279**, 6746-6752.

Ashrafi G and Schwarz TL. (2013) The pathways of mitophagy for quality control and clearance of mitochondria. *Cell Death Differ*, **20**, 31-42.

Asirvatham AL, Galligan SG, Schillace RV, Davey MP, Vasta V, Beavo JA, and Carr DW. (2004) A-kinase anchoring proteins interact with phosphodiesterases in T lymphocyte cell lines. *J Immunol*, **173**, 4806-4814.

Bain J, McLauchlan H, Elliott M, and Cohen P. (2003) The specificities of protein kinase inhibitors: an update. *Biochem J*, **371**, 199-204.

Bain J, Plater L, Elliott M, Shpiro N, Hastie CJ, McLauchlan H, Klevernic I, Arthur JS, Alessi DR, & Cohen P. (2007) The selectivity of protein kinase inhibitors: a further update. *Biochem J*, **408**, 297-315.

Banerjee R, Starkov AA, Beal MF, and Thomas B. (2009) Mitochondrial dysfunction in the limelight of Parkinson's disease pathogenesis. *Biochim Biophys Acta*, **1792**, 651-663.

Bao X, Faris AE, Jang EK, and Haslam RJ. (2002) Molecular cloning, bacterial expression and properties of Rab31 and Rab32. *Eur J Biochem*, **269**, 259-271.

Bauman AL, Michel JJ, Henson E, Dodge-Kafka KL, and Kapiloff MS. (2007) The mAKAP signalosome and cardiac myocyte hypertrophy. *IUBMB Life*, **59**, 163-169.

Beauchamp EM, Ringer L, Bulut G, Sajwan KP, Hall MD, Lee YC, Peaceman D, Ozdemirli M, Rodriguez O, Macdonald TJ, Albanese C, Toretsky JA, and Uren A. (2011) Arsenic trioxide inhibits human cancer cell growth and tumor development in mice by blocking Hedgehog/GLI pathway. *J Clin Inves*, **121**, 148-160.

Beavo JA and Brunton LL. (2002) Cyclic nucleotide research -- still expanding after half a century. *Nat Rev Mol Cell Biol*, **3**, 710-718.

Benson MA, Tinsley CL, and Blake DJ. (2004) Myospryn is a novel binding partner for dysbindin in muscle. *J Biol Chem*, **279**, 10450-10458.

Berryman MA and Goldenring JR. (2003) CLIC4 is enriched at cell-cell junctions and colocalizes with AKAP350 at the centrosome and midbody of cultured mammalian cells. *Cell Motil Cytoskeleton*, **56**, 159-172.

Bhatia N, Maiti PP, Choudhary A, Tuli A, Masih D, Masih M, Khan U, Ara T, and Jaggi AS. (2011) Animal models in the study of stress: a review. *NSHM J Pharm Healthcare Manag*, **2**, 42-50.

Boveri, Theodor. (1929) *The origin of malignant tumors*. Williams and Wilkins Company.

Bui QT, Golinelli-Cohen MP, and Jackson CL. (2009) Large Arf1 guanine nucleotide exchange factors: evolution, domain structure, and roles in membrane trafficking and human disease. *Mol Genet Genomics*, **282**, 329-350.

Bui M, Gilady SY, Fitzsimmons REB, Benson MD, Lynes EM, Gesson K, Alto NM, Strack S, Scott JD, and Simmen T. (2010) Rab32 modulates apoptosis onset and mitochondria-associated membrane (MAM) properties. *J Biol Chem*, **285**, 31590-31602.

Bultema JJ, Ambrosio AL, Burek CL, and Di Pietro SM. (2012) BLOC-2, AP-3, and AP-1 proteins function in concert with Rab38 and Rab32 proteins to mediate protein trafficking to lysosome-related organelles. *J Biol Chem*, **287**, 19550-19563.

Burgers PP, Ma Y, Margarucci L, Mackey M, van der Heyden MA, Ellisman M, Scholten A, Taylor SS, and Heck AJ. (2012) A small novel A-kinase anchoring protein (AKAP) that localizes specifically protein kinase A-regulatory subunit I (PKA-RI) to the plasma membrane. *J Biol Chem*, **287**, 43789-43797.

Calabi F and Cilli V. (1998) CBFA2T1, a gene rearranged in human leukemia, is a member of a multigene family. *Genomics*, **52**, 332-341.

Campàs C and Castañer R. (2009) Darinaparsin. *Drugs Future*, **34**, 97-100.

Carlucci A, Lignitto L, and Feliciello A. (2008a) Control of mitochondria dynamics and oxidative metabolism by cAMP, AKAPs and the proteasome. *Trends Cell Biol*, **18**, 604-613.

Carlucci A, Adornetto A, Scorziello A, Viggiano D, Foca M, Cuomo O, Annunziato L, Gottesman M, and Feliciello A. (2008b) Proteolysis of AKAP121 regulates mitochondrial activity during cellular hypoxia and brain ischaemia. *EMBO J*, **27**, 1073-1084.

Carnegie GK, Means CK, and Scott JD. (2009) A-kinase anchoring proteins: From protein complexes to physiology and disease. *IUBMB Life*, **61**, 394-406.

Carré M, Carles G, André N, Douillard S, Ciccolini J, Briand C, and Braguer D. (2002) Involvement of microtubules and mitochondria in the antagonism of arsenic trioxide on paclitaxel-induced apoptosis. *Biochem Pharmacol*, **63**, 1831-1842.

Castermans D, Wilquet V, Parthoens E, Huysmans C, Steyaert J, Swinnen L, Fryns JP, Van de Ven W, and Devriendt K. (2003) The neurobeachin gene is disrupted by a translocation in a patient with idiopathic autism. *J Med Genet*, **40**, 352-356.

Chan JY-W, Siu KP-Y, and Fung K-P. (2006) Effect of arsenic trioxide on multidrug resistant hepatocellular carcinoma cells. *Cancer Lett*, **236**, 250-258.

Chan DC. (2012) Fusion and fission: interlinked processes critical for mitochondrial health. *Annu Rev Genet*, **46**, 265-287.

Chang CR and Blackstone C. (2007) Cyclic AMP-dependent protein kinase phosphorylation of Drp1 regulates its GTPase activity and mitochondrial morphology. *J Biol Chem*, **282**, 21583-21587.

Charmandari E, Tsigos C, and Chrousos G. (2005) Enocrinology of the stress response. *Annu Rev Physiol*, **67**, 259-284.

Chen H, Detmer SA, Ewald AJ, Griffin EE, Fraser SE, and Chan DC. (2003) Mitofusins Mfn1 and Mfn2 coordinately regulate mitochondrial fusion and are essential for embryonic development. *J Cell Biol*, **160**, 189-200.

Chen KH, Guo X, Ma D, Guo Y, Li Q, Yang D, Li P, Qiu X, Wen S, Xiao RP, and Tang J. (2004) Dysregulation of HSG triggers vascular proliferative disorders. *Nat Cell Biol*, **6**, 872-883.

Chen L, Kurokawa J, and Kass RS. (2005) Phosphorylation of the A-kinase-anchoring protein Yotiao contributes to protein kinase A regulation of a heart potassium channel. *J Biol Chem*, **280**, 31347-31352.

Chen L and Kass RS. (2006) Dual roles of the A kinase-anchoring protein Yotiao in the modulation of a cardiac potassium channel: a passive adaptor versus an active regulator. *Eur J Cell Biol*, **85**, 623-626.

Chen L, Marquardt ML, Tester DJ, Sampson KJ, Ackerman MJ, and Kass RS. (2007) Mutation of an A-kinase-anchoring protein causes long-QT syndrome. *Proc Natl Acad Sci USA*, **104**, 20990-20995.

Chen H and Chan CD. (2009) Mitochondrial dynamics – fusion, fission, movement, and mitophagy – in neurodegenerative diseases. *Hum Mol Genet*, **18**, R169-R176.

Cheng EP, Yuan C, Navedo MF, Dixon RE, Nieves-Cintrón M, Scott JD, and Santana LF. (2011) Restoration of normal L-type Ca2+ channel function during Timothy syndrome by ablation of an anchoring protein. *Circ Res*, **109**, 255-261.

Choi YH, Suzuki A, Hajarnis S, Ma Z, Chapin HC, Caplan MJ, Pontoglio M, Somlo S, and Igarashi P. (2011) Polycystin-2 and phosphodiesterase 4C are components of a ciliary A-kinase anchoring protein complex that is disrupted in cystic kidney diseases. *Proc Natl Acad Sci U S A*, **108**, 10679-10684.

Chou HY, Howng SL, Cheng TS, Hsiao YL, Lieu AS, Loh JK, Hwang SL, Lin CC, Hsu CM, Wang C, Lee CI, Lu PJ, Chou CK, Huang CY, and Hong YR. (2006) GSKIP is homologous to the Axin GSK3beta interaction domain and functions as a negative regulator of GSK3beta. *Biochemistry*, **45**, 11379-11389.

Ciampi R, Knauf JA, Kerler R, Gandhi M, Zhu Z, Nikiforova MN, Rabes HM, Fagin JA, and Nikiforov YE. (2005) Oncogenic AKAP9-BRAF fusion is a novel mechanism of MAPK pathway activation in thyroid cancer. *J Clin Invest*, **115**, 94-101.

Clark SLJ. (1957) Cellular diVerentiation in the kidneys of newborn mice studied with the electron microscope. *J Biophys Biochem Cytol*, **3**, 349-364.

Coba MP, Komiyama NH, Nithianantharajah J, Kopanitsa MV, Indersmitten T, Skene NG, Tuck EJ, Fricker DG, Elsegood KA, Stanford LE, Afinowi NO, Saksida LM, Bussey TJ, O'Dell TJ, and Grant SG. (2012) TNiK is required for postsynaptic and nuclear signaling pathways and cognitive function. *J Neurosci*, **32**, 13987-13999.

Cohen P. (2001) The role of protein phosphorylation in human health and disease. The Sir Hans Krebs Medal Lecture. *Eur J Biochem*, **268**, 5001-5010.

Cohen-Solal KA, Sood R, Marin Y, Crespo-Carbone SM, Sinsimer D, Martino JJ, Robbins C, Makalowska I, Trent J, and Chen S. (2003) Identification and characterization of mouse Rab32 by mRNA and protein expression analysis. *Biochim Biophys Acta*, **1651**, 68-75.

Collado-Hilly M and Coquil JF. (2009) Ins(1,4,5)P3 receptor type 1 associates with AKAP9 (AKAP450 variant) and protein kinase A type IIbeta in the Golgi apparatus in cerebellar granule cells. *Biol Cell*, **101**, 469-480.

Collas P, Le Guellec K, and Taskén K. (1999) The A-kinase-anchoring protein AKAP95 is a multivalent protein with a key role in chromatin condensation at mitosis. *J Cell Biol*, **147**, 1167-1180.

Cook SA, Sugden PH, and Clerk A. (1999) Regulation of bcl-2 family proteins during development and in response to oxidative stress in cardiac myocytes: association with changes in mitochondrial membrane potential. *Circ Res*, **85**, 940-949.

Costas J, Suárez-Rama JJ, Carrera N, Paz E, Páramo M, Agra S, Brenlla J, Ramos-Ríos R, and Arrojo M. (2013) Role of DISC1 Interacting Proteins in Schizophrenia Risk from Genome-Wide Analysis of Missense SNPs. *Ann Hum Genet*, ePub.

Davies SP, Reddy H, Caivano M, and Cohen P. (2000) Specificity and mechanism of action of some commonly used protein kinase inhibitors. *Biochem J*, **351**, 95-105.

Dhamodharan R and Wadsworth P. (1995) Modulation of microtubule dynamic instability in vivo by brain microtubule associated proteins. *J Cell Sci*, **108**, 1679-1689.

Diaz Z, Mann KK, Marcoux S, Kourelis M, Colombo M, Komarnitsky PB, and Miller WH Jr. (2008) A novel arsenical has antitumor activity toward As2O3-resistant and MRP1/ABCC1-overexpressing cell lines. *Leukemia*, **22**, 1853-1863.

Dictenberg JB, Zimmerman W, Sparks CA, Young A, Vidair C, Zheng Y, Carrington W, Fay FS, and Doxsey SJ. (1998) Pericentrin and gamma-tubulin form a protein complex and are organized into a novel lattice at the centrosome. *J Cell Biol*, **141**, 163-174.

Diviani D, Langeberg LK, Doxsey SJ, and Scott JD. (2000) Pericentrin anchors protein kinase A at the centrosome through a newly identified RII-binding domain. *Curr Biol*, **10**, 417-420.

Diviani D, Maric D, Pérez López I, Cavin S, and Del Vescovo CD. (2013) A-kinase anchoring proteins: molecular regulators of the cardiac stress response. *Biochim Biophys Acta*, **1833**, 901-908.

Dodson MW and Guo M. (2007) Pink1, parkin, DJ-1 and mitochondrial dysfunction in Parkinson's disease. *Curr Opin Neurobiol*, **17**, 331-337.

Dong F, Feldmesser M, Casadevall A, and Rubin CS. (1998) Molecular characterization of a cDNA that encodes six isoforms of a novel murine A kinase anchor protein. *J Biol Chem*, **273**, 6533-6541.

Dorn GW 2nd and Scorrano L. (2010) Two close, too close: sarcoplasmic reticulum-mitochondrial crosstalk and cardiomyocyte fate. *Circ Res*, **107**, 689-699.

Doxsey SJ, Stein P, Evans L, Calarco PD, and Kirschner M. (1994) Pericentrin, a highly conserved centrosome protein involved in microtubule organization. *Cell*, **76**, 639-650.

Duan XF, Wu YL, Xu HZ, Zhao M, Zhuang HY, Wang XD, Yan H, and Chen GQ. (2010) Synergistic mitosis-arresting effects of arsenic trioxide and paclitaxel on human malignant lymphocytes. *Chem Biol Interact*, **183**, 220-230.

Eggers CT, Schafer JC, Goldenring JR, and Taylor SS. (2009) D-AKAP2 interacts with Rab4 and Rab11 through its RGS domains and regulates transferrin receptor recycling. *J Biol Chem*, **284**, 32869-32880.

Ehtesham M, Sarangi A, Valadez JG, Chanthaphaychith S, Becher MW, Abel TW, Thompson RC, and Cooper MK. (2007) Ligand-dependent activation of the hedgehog pathway in glioma progenitor cells. *Oncogene*, **26**, 5752-5761.

Eiberg H, Kjer B, Kjer P, and Rosenberg T. (1994) Dominant optic atrophy (OPA1) mapped to chromosome 3q region. I. Linkage analysis. *Hum Mol Genet*, **3**, 977-980.

Eide T, Coghlan V, Orstavik S, Holsve C, Solberg R, Skâlhegg BS, Lamb NJ, Langeberg L, Fernandez A, Scott JD, Jahnsen T, and Taskén K. (1998) Molecular cloning, chromosomal localization, and cell cycle-dependent subcellular distribution of the A-kinase anchoring protein, AKAP95. *Exp Cell Res*, **238**, 305-316.

El Amraoui A, Schonn JS, Küssel-Andermann P, Blanchard S, Desnos C, Henry JP, Wolfrum U, Darchen F, and Petit C. (2002) MyRIP, a novel Rab effector, enables myosin VIIa recruitment to retinal melanosomes. *EMBO Rep*, **3**, 463-470.

El Din El Homasany BS, Volkov Y, Takahashi M, Ono Y, Keryer G, Delouvée A, Looby E, Long A, and Kelleher D. (2005) The scaffolding protein CG-NAP/AKAP450 is a critical integrating component of the LFA-1-induced signaling complex in migratory T cells. *J Immunol*, **175**, 7811-7818.

El Fatimy R, Tremblay S, Dury AY, Solomon S, De Koninck P, Schrader JW, and Khandjian EW. (2012) Fragile X mental retardation protein interacts with the RNA-binding protein Caprin1 in neuronal RiboNucleoProtein complexes [corrected]. *PLoS One*, **7**, e39338.

Ellison JW, Ramos C, Yen PH, and Shapiro LJ. (1992) Structure and expression of the human pseudoautosomal gene XE7. *Hum Mol Genet*, **1**, 691-696.

Elmore S. (2007) Apoptosis: a review of programmed cell death. *Toxicol Pathol*, **35**, 495–516.

Emery G and Ramel D. (2013) Cell coordination of collective migration by Rab11 and Moesin. *Commun Integr Biol*, **6**, e24587.

Faulkner G, Pallavicini A, Formentin E, Comelli A, Ievolella C, Trevisan S, Bortoletto G, Scannapieco P, Salamon M, Mouly V, Valle G, and Lanfranchi G. (1999) ZASP: a new Z-band alternatively spliced PDZ-motif protein. *J Cell Biol*, **146**, 465-475.

Feliciello A, Cardone L, Garbi C, Ginsberg MD, Varrone S, Rubin CS, Avvedimento EV, and Gottesman ME. (1999) Yotiao protein, a ligand for the NMDA receptor, binds and targets cAMP-dependent protein kinase II. *FEBS Lett*, **464**, 174-178.

Ferguson GT. (2006) Why does the lung hyperinflate? *Proc Am Thorac Soc*, **3**, 176-179.

Festjens N, Vanden Berghe T, and Vandenabeele P. (2006) Necrosis, a well-orchestrated form of cell demise: signalling cascades, important mediators and concomitant immune response. *Biochim Biophys Acta*, **1757**, 1371-1387.

Fiedler SE, Schillace RV, Daniels CJ, Andrews SF, and Carr DW. (2010) Myeloid translocation gene 16b is a dual A-kinase anchoring protein that interacts selectively with plexins in a phospho-regulated manner. *FEBS Lett*, **584**, 873-877.

Fink MA, Zakhary DR, Mackey JA, Desnoyer RW, Apperson-Hansen C, Damron DS, and Bond M. (2001) AKAP-mediated targeting of protein kinase a regulates contractility in cardiac myocytes. *Circ Res*, **88**, 291-297.

Flory MR, Moser MJ, Monnat RJ Jr, and Davis TN. (2000) Identification of a human centrosomal calmodulin-binding protein that shares homology with pericentrin. *Proc Natl Acad Sci U S A*, **97**, 5919-5923.

Frank B, Wiestler M, Kropp S, Hemminki K, Spurdle AB, Sutter C, Wappenschmidt B, Chen X, Beesley J, Hopper JL; Australian Breast Cancer Family Study Investigators,, Meindl A, Kiechle M, Slanger T, Bugert P, Schmutzler RK, Bartram CR, Flesch-Janys D, Mutschelknauss E, Ashton K, Salazar R, Webb E, Hamann U, Brauch H, Justenhoven C, Ko YD, Brüning T, Silva Idos S, Johnson N, Pharoah PP, Dunning AM, Pooley KA, Chang-Claude J, Easton DF, Peto J, Houlston R; Gene Environment Interaction and Breast Cancer in Germany Group, Kathleen Cuningham Foundation Consortium for Research into Familial Breast Cancer Investigators, Australian Ovarian Cancer Study Management Group, Chenevix-Trench G, Fletcher O, and Burwinkel B. (2008a) Association of a common AKAP9 variant with breast cancer risk: a collaborative analysis. *J Natl Cancer Inst*, **100**, 437-442.

Frank B, Burwinkel B, Bermejo JL, Försti A, Hemminki K, Houlston R, Mangold E, Rahner N, Friedl W, Friedrichs N, Buettner R, Engel C, Loeffler M, Holinski-Feder E, Morak M, Keller G, Schackert HK, Krüger S, Goecke T, Moeslein G, Kloor M, Gebert J, Kunstmann E, Schulmann K, Rüschoff J, Propping P and German HNPCC Consortium. (2008b) Ten recently identified associations between nsSNPs and colorectal cancer could not be replicated in German families. *Cancer Lett*, **271**, 153-157.

Fraser ID, Tavalin SJ, Lester LB, Langeberg LK, Westphal AM, Dean RA, Marrion NV, and Scott JD. (1998) A novel lipid-anchored A-kinase Anchoring Protein facilitates cAMP-responsive membrane events. *EMBO J*, **17**, 2261-2272.

Fukuda M and Kuroda TS. (2002) Slac2-c (synaptotagmin-like protein homologue lacking C2 domains-c), a novel linker protein that interacts with Rab27, myosin Va/VIIa, and actin. *J Biol Chem*, **277**, 43096-43103.

Fukuyama T, Sueoka E, Sugio Y, Otsuka T, Niho Y, Akagi K, and Kozu T. (2001) MTG8 proto-oncoprotein interacts with the regulatory subunit of type II cyclic AMP-dependent protein kinase in lymphocytes. *Oncogene*, **20**, 6225-6232.

Fulda S and Debatin K-M. (2004) Targeting apoptosis pathways in cancer therapy. *Curr Cancer Drug Targets*, **4**, 569-576.

Fulda S, Gorman AM, Hori O, and Samali A. (2010) Cellular stress responses: cell survival and cell death. *Int J Cell Biol*, **2010**, 214074.

Fusco A, Viglietto G, and Santoro M. (2005) A new mechanism of BRAF activation in human thyroid papillary carcinomas. *J Clin Invest*, **115**, 20-23.

Gama Sosa MA, De Gasperi R, and Elder GA. (2010) Animal transgenesis: an overview. *Brain Struct Funct*, **214**, 91-109.

Garnis C, Rosin MP, Zhang L, and Lam WL. (2005) Alteration of AKAP220, an upstream component of the Rb pathway, in oral carcinogenesis. *Int J Cancer*, **116**, 813-819.

Giamas G, Hirner H, Shoshiashvili L, Grothey A, Gessert S, Kühl M, Henne-Bruns D, Vorgias CE, and Knippschild U. (2007) Phosphorylation of CK1delta: identification of Ser370 as the major phosphorylation site targeted by PKA in vitro and in vivo. *Biochem J*, **406**, 389-398.

Gilbert DJ, Engel H, Wang X, Grzeschik KH, Copeland NG, Jenkins NA, and Kilimann MW. (1999) The neurobeachin gene (Nbea) identifies a new region of homology between mouse central chromosome 3 and human chromosome 13q13. *Mamm Genome*, **10**, 1030-1031.

Gillingham AK and Munro S. (2000) The PACT domain, a conserved centrosomal targeting motif in the coiled-coil proteins AKAP450 and pericentrin. *EMBO Rep*, **1**, 524-529.

Ginsberg MD, Feliciello A, Jones JK, Avvedimento EV, and Gottesman ME. (2003) PKA-dependent binding of mRNA to the mitochondrial AKAP121 protein. *J Mol Biol*, **327**, 885-897.

Goehring AS, Pedroja BS, Hinke SA, Langeberg LK, and Scott JD. (2007) MyRIP anchors protein kinase A to the exocyst complex. *J Biol Chem*, **282**, 33155-33167.

Gold MG. (2012) A frontier in the understanding of synaptic plasticity: solving the structure of the postsynaptic density. *Bioessays*, **34**, 599-608.

Gold MG, Reichow SL, O'Neill SE, Weisbrod CR, Langeberg LK, Bruce JE, Gonen T, and Scott JD. (2012) AKAP2 anchors PKA with aquaporin-0 to support ocular lens transparency. *EMBO Mol Med*, **4**, 15-26.

Gomes LC, Di Benedetto G, and Scorrano L. (2011) During autophagy mitochondria elongate, are spared from degradation and sustain cell viability. *Nat Cell Biol*, **13**, 589-598.

Gordon T, Grove B, Loftus JC, O'Toole T, McMillan R, Lindstrom J, and Ginsberg MH. (1992) Molecular cloning and preliminary characterization of a novel cytoplasmic antigen recognized by myasthenia gravis sera. *J Clin Invest*, **90**, 992-999.

Gorman AM. (2008) Neuronal cell death in neurodegenerative diseases: recurring themes around protein handling. *J Cell Mol Med*, **12**, 2263-2280.

Granger BL and Lazarides E. (1980) Synemin: a new high molecular weight protein associated with desmin and vimentin filaments in muscle. *Cell*, **22**, 727-738.

Gray PC, Johnson BD, Westenbroek RE, Hays LG, Yates JR 3rd, Scheuer T, Catterall WA, and Murphy BJ. (1998) Primary structure and function of an A kinase anchoring protein associated with calcium channels. *Neuron*, **20**, 1017-1026.

Greenwald EC and Saucerman JJ. (2011) Bigger, better, faster: principles and models of AKAP anchoring protein signaling. *J Cardiovasc Pharmacol*, **58**, 462-469.

Grill B, Wilson GM, Zhang KX, Wang B, Doyonnas R, Quadroni M, and Schrader JW. (2004) Activation/division of lymphocytes results in increased levels of cytoplasmic activation/proliferation-associated protein-1: prototype of a new family of proteins. *J Immunol*, **172**, 2389-2400.

Gulliver G. (1838) On Necrosis; being an experimental inquiry into the agency ascribed to the absorbents, in the removal of the sequestrum. *Med Chir Trans*, **21**, 1-19.

Gunter TE, Buntinas L, Sparagna G, Eliseev R, and Gunter K. (2000) Mitochondrial calcium transport: mechanisms and functions. *Cell Calcium*, **28**, 285-296.

Hanahan D and Weinberg RA. (2000) The hallmarks of cancer. *Cell*, **100**, 57-70.

Hart MP and Xu A. (2009) Mice Expressing Mutant Parkin Exhibit Hallmark Features of Parkinson's Disease. *J Neurosci*, **29**, 7392-7394.

Hasegawa K, Ono T, Matsushita H, Shimono M, Noguchi Y, Mizutani Y, Kodama J, Kudo T, and Nakayama E. (2004) A-kinase anchoring protein 3 messenger RNA expression in ovarian cancer and its implication on prognosis. *Int J Cancer*, **108**, 86-90.

Hauet T, Liu J, Li H, Gazouli M, Culty M, and Papadopoulos V. (2002) PBR, StAR, and PKA: partners in cholesterol transport in steroidogenic cells. *Endocr Res*, **28**, 395-401.

He C and Klionsky DJ. (2009) Regulation mechanisms and signaling pathways of autophagy. *Annu Rev Genet*, **43**, 67-93.

Henle, J. (1841) *Allgemeine Anatomie*. Leipzig.

Henn V, Edemir B, Stefan E, Wiesner B, Lorenz D, Theilig F, Schmitt R, Vossebein L, Tamma G, Beyermann M, Krause E, Herberg FW, Valenti G, Bachmann S, Rosenthal W, and Klussmann E. (2004) Identification of a novel A-kinase anchoring protein 18 isoform and evidence for its role in the vasopressin-induced aquaporin-2 shuttle in renal principal cells. *J Biol Chem*, **279**, 26654-26665.

Hofsli E, Wheeler TE, Langaas M, Laegreid A, and Thommesen L. (2008) Identification of novel neuroendocrine-specific tumour genes. *Br J Cancer*, **99**, 1330-1339.

Horbinski C and Chu CT. (2005) Kinase signaling cascades in the mitochondrion: a matter of life or death. *Free Radic Biol Med*, **38**, 2-11.

Huang LJ, Durick K, Weiner JA, Chun J, and Taylor SS. (1997a) D-AKAP2, a novel protein kinase A anchoring protein with a putative RGS domain. *Proc Natl Acad Sci U S A*, **94**, 11184-11189.

Huang LJ, Durick K, Weiner JA, Chun J, and Taylor SS. (1997b) Identification of a novel protein kinase A anchoring protein that binds both type I and type II regulatory subunits. *J Biol Chem*, **272**, 8057-8064.

Huang LJ, Wang L, Ma Y, Durick K, Perkins G, Deerinck TJ, Ellisman MH, and Taylor SS. (1999) NH2-Terminal targeting motifs direct dual specificity A-kinase-anchoring protein 1 (D-AKAP1) to either mitochondria or endoplasmic reticulum. *J Cell Biol*, **145**, 951-959.

Hundsrucker C, Skroblin P, Christian F, Zenn HM, Popara V, Joshi M, Eichhorst J, Wiesner B, Herberg FW, Reif B, Rosenthal W, and Klussmann E. (2010) Glycogen synthase kinase 3beta interaction protein functions as an A-kinase anchoring protein. *J Biol Chem*, **285**, 5507-5521.

Hur EM, Park YS, Huh YH, Yoo SH, Woo KC, Choi BH, and Kim KT. (2005) Junctional membrane inositol 1,4,5-trisphosphate receptor complex coordinates sensitization of the silent EGF-induced Ca2+ signaling. *J Cell Biol*, **169**, 657-667.

Hurtado L, Caballero C, Gavilan MP, Cardenas J, Bornens M, and Rios RM. (2011) Disconnecting the Golgi ribbon from the centrosome prevents directional cell migration and ciliogenesis. *J Cell Bio*, **193**, 917-933.

Jaggi AS, Bhatia N, Kumar N, Singh N, Anand P, and Dhawan R. (2011) A review on animal models for screening potential anti-stress agents. *Neurol Sci*, **32**, 993-1005.

Jarnaess E, Ruppelt A, Stokka AJ, Lygren B, Scott JD, and Taskén K. (2008) Dual specificity A-kinase anchoring proteins (AKAPs) contain an additional binding region that enhances targeting of protein kinase A type I. *J Biol Chem*, **283**, 33708-33718.

Jarnaess E, Stokka AJ, Kvissel AK, Skålhegg BS, Torgersen KM, Scott JD, Carlson CR, and Taskén K. (2009) Splicing factor arginine/serine-rich 17A (SFRS17A) is an A-kinase anchoring protein that targets protein kinase A to splicing factor compartments. *J Biol Chem*, **284**, 35154-35164.

Jin YN, Yu YV, Gundemir S, Jo C, Cui M, Tieu K, and Johnson GV. (2013) Impaired mitochondrial dynamics and Nrf2 signaling contribute to compromised responses to oxidative stress in striatal cells expressing full-length mutant huntingtin. *PLoS One*, **8**, e57932.

Jivan A, Earnest S, Juang YC, and Cobb MH. (2009) Radial spoke protein 3 is a mammalian protein kinase A-anchoring protein that binds ERK1/2. *J Biol Chem*, **284**, 29437-29445.

Johnstone RW, Ruefli AA, and Lowe SW. (2002) Apoptosis: a link between cancer genetics and chemotherapy. *Cell*, **108**, 153-164.

Jordan MA, Thrower D, and Wilson L. (1992) Effects of vinblastin, podophyllotoxin, and nocodazole on mitotic spindles. Implications for the role of microtubule dynamics in mitosis. *J Cell Sci*, **102**, 401-416.

Kabbarah O, Nogueira C, Feng B, Nazarian RM, Bosenberg M, Wu M, Scott KL, Kwong LN, Xiao Y, Cordon-Cardo C, Granter SR, Ramaswamy S, Golub T, Duncan LM, Wagner SN, Brennan C, and Chin L. (2010) Integrative genome comparison of primary and metastatic melanomas. *PLoS One*, **5**, e10770.

Kanamaru Y, Sekine S, Ichijo H, and Takeda K. (2012) The phosphorylation-dependent regulation of mitochondrial proteins in stress responses. *J Signal Transduct*, **2012**, 931215.

Karve TM and Cheema AK. (2011) Small Changes Huge Impact: The Role of Protein Posttranslational Modifications in Cellular Homeostasis and Disease. *J Amino Acids*, **2011**, 207691.

Kedersha NL, Gupta M, Li W, Miller I, and Anderson P. (1999) RNA-binding proteins TIA-1 and TIAR link the phosphorylation of eIF-2 alpha to the assembly of mammalian stress granules. *J Cell Biol*, **147**, 1431-1442.

Kedersha N, Stoecklin G, Ayodele M, Yacono P, Lykke-Andersen J, Fritzler MJ, Scheuner D, Kaufman RJ, Golan DE, and Anderson P. (2005) Stress granules and processing bodies are dynamically linked sites of mRNP remodeling. *J Cell Biol*, **169**, 871-884.

Kedersha N and Anderson P. (2007) Mammalian stress granules and processing bodies. *Methods Enzymol*, **431**, 61-81.

Keller DM, Zeng X, Wang Y, Zhang QH, Kapoor M, Shu H, Goodman R, Lozano G, Zhao Y, and Lu H. (2001) A DNA damage-induced p53 serine 392 kinase complex contains CK2, hSpt16, and SSRP1. *Mol Cell*, **7**, 283-292.

Kendler KS, Kalsi G, Holmans PA, Sanders AR, Aggen SH, Dick DM, Aliev F, Shi J, Levinson DF, and Gejman PV. (2011) Genomewide association analysis of symptoms of alcohol dependence in the molecular genetics of schizophrenia (MGS2) control sample. *Alcohol Clin Exp Res*, **35**, 963-975.

Kerr JF, Wyllie AH, and Currie AR. (1972) Apoptosis: a basic biological phenomenon with wide-ranging implications in tissue kinetics. *Br J Cancer*, **26**, 239–257.

Keryer G, Witczak O, Delouvée A, Kemmner WA, Rouillard D, Tasken K, and Bornens M. (2003a) Dissociating the centrosomal matrix protein AKAP450 from centrioles impairs centriole duplication and cell cycle progression. *Mol Biol Cell*, **14**, 2436-2446.

Keryer G, Di Fiore B, Celati C, Lechtreck KF, Mogensen M, Delouvee A, Lavia P, Bornens M, and Tassin AM. (2003b) Part of Ran is associated with AKAP450 at the centrosome: involvement in microtubule-organizing activity. *Mol Biol Cell*, **14**, 4260-4271.

Kim HS, Takahashi M, Matsuo K, and Ono Y. (2007) Recruitment of CG-NAP to the Golgi apparatus through interaction with dynein-dynactin complex. *Genes Cells*, **12**, 421-434.

Kim J, Lee JJ, Kim J, Gardner D, and Beachy PA. (2010) Arsenic antagonizes the Hedgehog pathway by preventing ciliary accumulation and reducing stability of the Gli2 transcriptional effector. *PNAS*, **107**, 13432-13437.

Kim H, Scimia MC, Wilkinson D, Trelles RD, Wood MR, Bowtell D, Dillin A, Mercola M, and Ronai ZA. (2011) Fine-tuning of Drp1/Fis1 availability by AKAP121/Siah2 regulates mitochondrial adaptation to hypoxia. *Mol Cell*, **44**, 532-544.

Kissová I, Deffieu M, Manon S, and Camougrand N. (2004) Uth1p is involved in the autophagic degradation of mitochondria. *J Biol Chem*, **279**, 39068-39074.

Kolobova E, Efimov A, Kaverina I, Rishi AK, Schrader JW, Ham AJ, Larocca MC, and Goldenring JR. (2009) Microtubule-dependent association of AKAP350A and CCAR1 with RNA stress granules. *Exp Cell Res*, **15**, 542-555.

Kouloumenta A, Mavroidis M, and Capetanaki Y. (2007) Proper perinuclear localization of the TRIM-like protein myospryn requires its binding partner desmin. *J Biol Chem*, **282**, 35211-35221.

Kraya T, Kress W, Stoevesant D, Deschauer M, and Zierz S. (2013) Myofibrillary myopathy due to the ZASP mutation Ala147Thr : two cases with exclusively distal leg involvement. *Nervenarzt*, **84**, 209-213.

Krebs E and Fischer E. (1956) The phosphorylase B to A converting enzyme of rabbit skeletal muscle. *Biochim Biophys Acta*, **1989**, 302-309.

Kultgen PL, Byrd SK, Ostrowski LE, and Milgram SL. (2002) Characterization of an A-kinase anchoring protein in human ciliary axonemes. *Mol Biol Cell*, **13**, 4156-4166.

Kültz D. (2005) Molecular and evolutionary basis of the cellular stress response. *Annu Rev Physiol*, **67**, 225-257.

Lacaná E, Maceyka M, Milstien S, and Spiegel S. (2002) Cloning and characterization of a protein kinase A anchoring protein (AKAP)-related protein that interacts with and regulates sphingosine kinase 1 activity. *J Biol Chem*, **277**, 32947-32953.

Lagouge M and Larsson NG. (2013) The role of mitochondrial DNA mutations and free radicals in disease and ageing. *J Intern Med*, **273**, 529-543.

Lankes WT and Furthmayr H. (1991) Moesin: a member of the protein 4.1-talin-ezrin family of proteins. *Proc Natl Acad Sci U S A*, **88**, 8297-8301.

Larocca MC, Shanks RA, Tian L, Nelson DL, Stewart DM, and Goldenring JR. (2004) AKAP350 interaction with cdc42 interacting protein 4 at the Golgi apparatus. *Mol Biol Cell*, **15**, 2771-2781.

Larocca MC, Jin M, and Goldenring JR. (2006) AKAP350 modulates microtubule dynamics. *Eur J Cell Biol*, **85**, 611-619.

Latonen L and Laiho M. (2005) Cellular UV damage responses--functions of tumor suppressor p53. *Biochim Biophys Acta*, **1755**, 71-89.

Lemasters JJ. (2005) Selective mitochondrial autophagy, or mitophagy, as a targeted defense against oxidative stress, mitochondrial dysfunction, and aging. *Rejuvenation Res*, **8**, 3-5.

Lemay J, Maidou-Peindara P, Cancio R, Ennifar E, Coadou G, Maga G, Rain JC, Benarous R, and Liu LX. (2008) AKAP149 binds to HIV-1 reverse transcriptase and is involved in the reverse transcription. *J Mol Biol*, **383**, 783-796.

Lester LB, Coghlan VM, Nauert B, and Scott JD. (1996) Cloning and characterization of a novel A-kinase anchoring protein. AKAP 220, association with testicular peroxisomes. *J Biol Chem*, **271**, 9460-9465.

Li H, Degenhardt B, Tobin D, Yao ZX, Tasken K, and Papadopoulos V. (2001) Identification, localization, and function in steroidogenesis of PAP7: a peripheral-type benzodiazepine receptor- and PKA (RIalpha)-associated protein. *Mol Endocrinol*, **15**, 2211-2228.

Li Y, Chen L, Kass RS, and Dessauer CW. (2012) The A-kinase anchoring protein Yotiao facilitates complex formation between adenylyl cyclase type 9 and the IKs potassium channel in heart. *J Biol Chem*, **287**, 29815-29824.

Li YR, King OD, Shorter J, and Gitler AD. (2013) Stress granules as crucibles of ALS pathogenesis. *J Cell Biol*, **201**, 361-372.

Liesa M, Palacín M, and Zorzano A. (2009) Mitochondrial dynamics in mammalian health and disease. *Physiol Rev*, **89**, 799-845.

Lin RY, Moss SB, and Rubin CS. (1995) Characterization of S-AKAP84, a novel developmentally regulated A kinase anchor protein of male germ cells. *J Biol Chem*, **270**, 27804-27811.

Lin JW, Wyszynski M, Madhavan R, Sealock R, Kim JU, and Sheng M. (1998) Yotiao, a novel protein of neuromuscular junction and brain that interacts with specific splice variants of NMDA receptor subunit NR1. *J Neurosci*, **18**, 2017-2027.

Lin C, Guo X, Lange S, Liu J, Ouyang K, Yin X, Jiang L, Cai Y, Mu Y, Sheikh F, Ye S, Chen J, Ke Y, and Cheng H. (2013) Cypher/ZASP is a novel A kinase anchoring protein. *J Biol Chem*, epub.

Ling Y-H, Jiang J-D, Holland JF, and Perez-Soler R. (2002) Arsenic trioxide produces polymerization of microtubules and mitotic arrest before apoptosis in human tumor cell lines. *Mol Pharmacol*, **62**, 529-538.

Lisse TS, Thiele F, Fuchs H, Hans W, Przemeck GK, Abe K, Rathkolb B, Quintanilla-Martinez L, Hoelzlwimmer G, Helfrich M, Wolf E, Ralston SH, and Hrabé de Angelis M. (2008) ER stress-mediated apoptosis in a new mouse model of osteogenesis imperfecta. *PLoS Genet*, **4**, e7.

Liu W, Guan M, Hu T, Gu X, and Lu Y. (2011) Re-expression of AKAP12 inhibits progression and metastasis potential of colorectal carcinoma in vivo and in vitro. *PLoS One*, **6**, e24015.

Livigni A, Scorziello A, Agnese S, Adornetto A, Carlucci A, Garbi C, Castaldo I, Annunziato L, Avvedimento EV, and Feliciello A. (2006) Mitochondrial AKAP121 links cAMP and src signaling to oxidative metabolism. *Mol Biol Cell*, **17**, 263-271.

Logue JS, Whiting JL, Tunquist B, Sacks DB, Langeberg LK, Wordeman L, and Scott JD. (2011) AKAP220 protein organizes signaling elements that impact cell migration. *J Biol Chem*, **286**, 39269-39281.

Lohmann SM, DeCamilli P, Einig E, and Walter U. (1984) High-affinity binding of regulatory subunit (RII) of cAMP-dependent protein kinase to microtubule-associated and other cellular proteins. *Proc Natl Acad Sci USA*, **81**, 6723-6727.

Long CS and Ordahl CP. (1998) Transcriptional repression of an embryo-specific muscle gene. *Dev Biol*, **127**, 228-234.

Low RB and White SL. (1998) Lung smooth muscle differentiation. *Int J Biochem Cell Biol*, **30**, 869-883.

Lowe SW and Lin AW. (2000) Apoptosis in cancer. *Carcinogenesis*, **21**, 485-495.

Lowe SW, Cepero E, and Evan G. (2004) Intrinsic tumour suppression. *Nature*, **432**, 307-315.

Lund LM, Kerr JP, Lupinetti J, Zhang Y, Russell MA, Bloch RJ, and Bond M. (2012) Synemin isoforms differentially organize cell junctions and desmin filaments in neonatal cardiomyocytes. *FASEB J*, **26**, 137-148.

Lutchman M and Rouleau GA. (1995) The neurofibromatosis type 2 gene product, schwannomin, suppresses growth of NIH 3T3 cells. *Cancer Res*, **55**, 2270-2274.

Lygren B, Carlson CR, Santamaria K, Lissandron V, McSorley T, Litzenberg J, Lorenz D, Wiesner B, Rosenthal W, Zaccolo M, Taskén K, and Klussmann E. (2007) AKAP complex regulates Ca2+ re-uptake into heart sarcoplasmic reticulum. *EMBO Rep*, **8**, 1061-1067.

Lygren B and Taskén K. (2008) The potential use of AKAP18delta as a drug target in heart failure patients. *Expert Opin Biol Ther*, **8**, 1099-1108.

Ma Y and Taylor S. (2002) A 15-residue bifunctional element in D-AKAP1 is required for both endoplasmic reticulum and mitochondrial targeting. *J Biol Chem*, **277**, 27328-27336.

Ma Y and Taylor SS. (2008) A molecular switch for targeting between endoplasmic reticulum (ER) and mitochondria. *J Biol Chem*, **283**, 11743-11751.

Makin G and Dive C. (2001) Apoptosis and cancer chemotherapy. *Trends Cell Biol*, **11**, S22-S26.

Mann KK, Wallner B, Lossos IS, and Miller Jr WH. (2009) Darinaparsin: a novel organic arsenical with promising anticancer activity. *Drug Evaluation*, **18**, 1727-1734.

Maron MB, Folkesson HG, Stader SM, and Walro JM. (2005) PKA delivery to the distal lung air spaces increases alveolar liquid clearance after isoproterenol-induced alveolar epithelial PKA desensitization. *Am J Physiol Lung Cell Mol Physiol*, **289**, L349-L354.

Marx SO, Kurokawa J, Reiken S, Motoike H, D'Armiento J, Marks AR, and Kass RS. (2002) Requirement of a macromolecular signaling complex for beta adrenergic receptor modulation of the KCNQ1-KCNE1 potassium channel. *Science*, **295**, 496-499.

Mason TA, Kolobova E, Liu J, Roland JT, Chiang C, and Goldenring JR. (2011) Darinaparsin is a multivalent chemotherapeutic which induces incomplete stress response with disruption of microtubules and Shh signaling. *PLoS One*, **6**, e27699.

Mattaloni SM, Kolobova E, Favre C, Marinelli RA, Goldenring JR, and Larocca MC. (2012) AKAP350 is involved in the development of apical "canalicular" structures in hepatic cells HepG2. *J Cell Physiol*, **227**, 160-171.

Matulis SM, Morales AA, Yehiayan L, Croutch C, Gutman D, Cai Y, Lee KP, and Boise LH. (2009) Darinaparsin induces a unique cellular response and is active in an arsenic-trioxide resistant myeloma cell line. *Mol Cancer Ther*, **8**, 1197-1206.

McCahill A, McSorley T, Huston E, Hill EV, Lynch MJ, Gall I, Keryer G, Lygren B, Tasken K, van Heeke G, and Houslay MD. (2005) In resting COS1 cells a dominant negative approach shows that specific, anchored PDE4 cAMP phosphodiesterase isoforms gate the activation, by basal cyclic AMP production, of AKAP-tethered protein kinase A type II located in the centrosomal region. *Cell Signal*, **17**, 1158-1173.

McCartney S, Little BM, Langeberg LK, and Scott JD. (1995) Cloning and characterization of A-kinase anchor protein 100 (AKAP100). A protein that targets A-kinase to the sarcoplasmic reticulum. *J Biol Chem*, **270**, 9327-9333.

Means CK, Lygren B, Langeberg LK, Jain A, Dixon RE, Vega AL, Gold MG, Petrosyan S, Taylor SS, Murphy AN, Ha T, Santana LF, Tasken K, and Scott JD. (2011) An entirely specific type I A-kinase anchoring protein that can sequester two molecules of protein kinase A at mitochondria. *Proc Natl Acad Sci U S A*, **108**, E1227-E1235.

Michel JJ and Scott JD. (2002) AKAP mediated signal transduction. *Annu Rev Pharmacol Toxicol*, **42**, 235-257.

Miki H, Suetsugu S, and Takenawa T. (1998) WAVE, a novel WASP-family protein involved in actin reorganization induced by Rac. *EMBO J*, **17**, 6932-6941.

Milne RL, Lorenzo-Bermejo J, Burwinkel B, Malats N, Arias JI, Zamora MP, Benítez J, Humphreys MK, García-Closas M, Chanock SJ, Lissowska J, Sherman ME, Mannermaa A, Kataja V, Kosma VM, Nevanlinna H, Heikkinen T, Aittomäki K, Blomqvist C, Anton-Culver H, Ziogas A, Devilee P, van Asperen CJ, Tollenaar RA, Seynaeve C, Hall P, Czene K, Liu J, Irwanto AK, Kang D, Yoo KY, Noh DY, Couch FJ, Olson JE, Wang X, Fredericksen Z, Nordestgaard BG, Bojesen SE, Flyger H, Margolin S, Lindblom A, Fasching PA, Schulz-Wendtland R, Ekici AB, Beckmann MW, Wang-Gohrke S, Shen CY, Yu JC, Hsu HM, Wu PE, Giles GG, Severi G, Baglietto L, English DR, Cox A, Brock I, Elliott G, Reed MW, Beesley J, Chen X, Investigators K; AOCS Group, Fletcher O, Gibson L, dos Santos Silva I, Peto J, Frank B, Heil J, Meindl A, Chang-Claude J, Hein R, Vrieling A, Flesch-Janys D, Southey MC, Smith L, Apicella C, Hopper JL, Dunning AM, Pooley KA, Pharoah PD, Hamann U, Pesch B, Ko YD; GENICA Network, Easton DF, and Chenevix-Trench G. (2011) 7q21-rs6964587 and breast cancer risk: an extended case-control study by the Breast Cancer Association Consortium. *J Med Genet*, **48**, 698-702.

Miyoshi H, Kozu T, Shimizu K, Enomoto K, Maseki N, Kaneko Y, Kamada N, and Ohki M. (1993) The t(8;21) translocation in acute myeloid leukemia results in production of an AML1-MTG8 fusion transcript. *EMBO J*, **12**, 2715-2721.

Moeller BJ, Cao Y, Li CY, and Dewhirst MW. (2004) Radiation activates HIF-1 to regulate vascular radiosensitivity in tumors: role of reoxygenation, free radicals, and stress granules. *Cancer Cell*, **5**, 429-441.

Moisoi N, Erent M, Whyte S, Martin S, and Bayley PM. (2002) Calmodulin-containing substructures of the centrosomal matrix released by microtubule perturbation. *J Cell Sci*, **115**, 2367-2379.

Moreno-Mateos MA, Espina ÁG, Torres B, Gámez del Estal MM, Romero-Franco A, Ríos RM, and Pintor-Toro JA. (2011) PTTG1/securin modulates microtubule nucleation and cell migration. *Mol Biol Cell*, **22**, 4302-4311.

Mori Y, Yin J, Sato F, Sterian A, Simms LA, Selaru FM, Schulmann K, Xu Y, Olaru A, Wang S, Deacu E, Abraham JM, Young J, Leggett BA, and Meltzer SJ. (2004) Identification of genes uniquely involved in frequent microsatellite instability colon carcinogenesis by expression profiling combined with epigenetic scanning. *Cancer Res*, **64**, 2434-2438.

Mostafa MR, Yahia RS, Abd El Messih HM, El-Sisy E, and El Ghannam DM. (2013) Gravin gene expression in acute myeloid leukemia. *Med Oncol*, **30**, 548.

Neben K, Tews B, Wrobel G, Hahn M, Kokocinski F, Giesecke C, Krause U, Ho AD, Krämer A, and Lichter P. (2004) Gene expression patterns in acute myeloid leukemia correlate with centrosome aberrations and numerical chromosome changes. *Oncogene*, **23**, 2379-2384.

Neuss M, Monticone R, Lundberg MS, Chesley AT, Fleck E, and Crow MT. (2001) The apoptotic regulatory protein ARC (apoptosis repressor with caspase recruitment domain) prevents oxidant stress-mediated cell death by preserving mitochondrial function. *J Biol Chem*, **276**, 33915-33922.

Newhall KJ, Criniti AR, Cheah CS, Smith KC, Kafer KE, Burkart AD, and McKnight GS. (2006) Dynamic anchoring of PKA is essential during oocyte maturation. *Curr Biol*, **16**, 321-327.

Nicolaou M, Andress EJ, Zolnerciks JK, Dixon PH, Williamson C, and Linton KJ. (2012) Canalicular ABC transporters and liver disease. *J Pathol*, **226**, 300-315.

Nishida H, Sato T, Ogura T, and Nakaya H. (2009) New aspects for the treatment of cardiac disease based on the diversity of functional controls on cardiac muscles: mitochondrial ion channels and cardioprotection. *J Pharmacol Sci*, **109**, 341-347.

Nishimura T, Takahashi M, Kim HS, Mukai H, and Ono Y. (2005) Centrosome-targeting region of CG-NAP causes centrosome amplification by recruiting cyclin E-cdk2 complex. *Genes Cells*, **10**, 75-86.

Nover L, Scharf KD, and Neumann D. (1989) Cytoplasmic heat shock granules are formed from precursor particles and are associated with a specific set of mRNAs. *Mol Cell Biol*, **9**, 1298-1308.

Numata S, Iga J, Nakataki M, Tayoshi S, Tanahashi T, Itakura M, Ueno S, and Ohmori T. (2009) Positive association of the pericentrin (PCNT) gene with major depressive disorder in the Japanese population. *J Psychiatry Neurosci*, **34**, 195-198.

Numata S, Nakataki M, Iga J, Tanahashi T, Nakadoi Y, Ohi K, Hashimoto R, Takeda M, Itakura M, Ueno S, and Ohmori T. (2010) Association study between the pericentrin (PCNT) gene and schizophrenia. *Neuromolecular Med*, **12**, 243-247.

Nunnari J and Suomalainen A. (2012) Mitochondria: In Sickness and in Health. *Cell*, **148**, 1145-1159.

Okunishi K, Sisson TH, Huang SK, Hogaboam CM, Simon RH, and Peters-Golden M. (2011) Plasmin overcomes resistance to prostaglandin E2 in fibrotic lung fibroblasts by reorganizing protein kinase A signaling. *J Biol Chem*, **286**, 32231-32243.

Orellana SA, Quinoñes AM, and Mandapat ML. (2003) Ezrin distribution is abnormal in principal cells from a murine model of autosomal recessive polycystic kidney disease. *Pediatr Res*, **54**, 406-412.

Oshimori N, Li X, Ohsugi M, and Yamamoto T. (2009) Cep72 regulates the localization of key centrosomal proteins and proper bipolar spindle formation. *EMBO J*, **28**, 2066-2076.

Otera H, Wang C, Cleland MM, Setoguchi K, Yokota S, Youle RJ, and Mihara K. (2010) Mff is an essential factor for mitochondrial recruitment of Drp1 during mitochondrial fission in mammalian cells. *J Cell Biol*, **191**, 1141-1158.

Otera H and Mihara K. (2011) Discovery of the membrane receptor for mitochondrial fission GTPase Drp1. *Small GTPases*, **2**, 167-172.

Ozaki Y, Matsui H, Asou H, Nagamachi A, Aki D, Honda H, Yasunaga S, Takihara Y, Yamamoto T, Izumi S, Ohsugi M, and Inaba T. (2012) Poly-ADP ribosylation of Miki by tankyrase-1 promotes centrosome maturation. *Mol Cell*, **47**, 694-706.

Palacino JJ, Sagi D, Goldberg MS, Krauss S, Motz C, Wacker M, Klose J, and Shen J. (2004) Mitochondrial dysfunction and oxidative damage in parkin-deficient mice. *J Biol Chem*, **279**, 18614-18622.

Pastori GM and Foyer CH. (2002) Common components, networks, and pathways of cross-tolerance to stress: the central role of "redox" and abscisic acid-mediated controls. *Plant Physiol*, **129**, 460-468.

Pećina-Šlaus N. (2013) Merlin, the NF2 gene product. *Pathol Oncol Res*, **19**, 365-373.

Perrino C, Feliciello A, Schiattarella GG, Esposito G, Guerriero R, Zaccaro L, Del Gatto A, Saviano M, Garbi C, Carangi R, Di Lorenzo E, Donato G, Indolfi C, Avvedimento VE, and Chiariello M. (2010) AKAP121 downregulation impairs protective cAMP signals, promotes mitochondrial dysfunction, and increases oxidative stress. *Cardiovasc Res*, **88**, 101-110.

Pich S, Bach D, Briones P, Liesa M, Camps M, Testar X, Palacín M, and Zorzano A. (2005) The Charcot-Marie-Tooth type 2A gene product, Mfn2, up-regulates fuel oxidation through expression of OXPHOS system. *Hum Mol Genet*, **14**, 1405-15.

Piggott LA, Bauman AL, Scott JD, and Dessauer CW. (2008)The A-kinase anchoring protein Yotiao binds and regulates adenylyl cyclase in brain. *Proc Natl Acad Sci USA*, **105**, 13835-13840.

Pihan GA, Purohit A, Wallace J, Knecht H, Woda B, Quesenberry P, and Doxsey SJ. (1998) Centrosome defects and genetic instability in malignant tumors. *Cancer Res*, **58**, 3974-3985.

Pitre A, Davis N, Paul M, Orr AW, and Skalli O. (2012) Synemin promotes AKT-dependent glioblastoma cell proliferation by antagonizing PP2A. *Mol Biol Cell*, **23**, 1243-1253.

Purohit A, Tynan SH, Vallee R, and Doxsey SJ. (1999) Direct interaction of pericentrin with cytoplasmic dynein light intermediate chain contributes to mitotic spindle organization. *J Cell Biol*, **147**, 481-492.

Quintás-Cardama A, Verstovsek S, Freireich E, Kantarjian H, Chen YW, and Zingaro R. (2008) Chemical and clinical development of darinaparsin, a novel organic arsenic derivative. *Anticancer Agents Med Chem*, **8**, 904-909.

Rall TW, Sutherland EW, and Berthet J. (1957) The relationship of epinephrine and glucagon to liver phosphorylase IV. Effect of epinephrine and glucagon on the reactivation of phosphorylase in liver homogenates. *J Biol Chem*, **224**, 463-475.

Rambold AS and Lippincott-Schwartz J. (2011) Mechanisms of mitochondria and autophagy crosstalk. *Cell Cycle*, **10**, 4032-4038.

Ranganathan G, Phan D, Pokrovskaya ID, McEwen JE, Li C, and Kern PA. (2002) The translational regulation of lipoprotein lipase by epinephrine involves an RNA binding

complex including the catalytic subunit of protein kinase A. *J Biol Chem*, **277**, 43281-43287.

Rauch A, Thiel CT, Schindler D, Wick U, Crow YJ, Ekici AB, van Essen AJ, Goecke TO, Al-Gazali L, Chrzanowska KH, Zweier C, Brunner HG, Becker K, Curry CJ, Dallapiccola B, Devriendt K, Dörfler A, Kinning E, Megarbane A, Meinecke P, Semple RK, Spranger S, Toutain A, Trembath RC, Voss E, Wilson L, Hennekam R, de Zegher F, Dörr HG, and Reis A. (2008) Mutations in the pericentrin (PCNT) gene cause primordial dwarfism. *Science*, **319**, 816-819.

Reinton N, Collas P, Haugen TB, Skâlhegg BS, Hansson V, Jahnsen T, and Taskén K. (2000) Localization of a novel human A-kinase-anchoring protein, hAKAP220, during spermatogenesis. *Dev Biol*, **223**, 194-204.

Reynolds JG, McCalmon SA, Donaghey JA, and Naya FJ. (2008) Deregulated protein kinase A signaling and myospryn expression in muscular dystrophy. *J Biol Chem*, **283**, 8070-8074.

Richards SA, Fu J, Romanelli A, Shimamura A, and Blenis J. (1999) Ribosomal S6 kinase 1 (RSK1) activation requires signals dependent on and independent of the MAP kinase ERK. *Curr Biol*, **9**, 810-820.

Rishi AK, Zhang L, Boyanapalli M, Wali A, Mohammad RM, Yu Y, Fontana JA, Hatfield JS, Dawson MI, Majumdar AP, and Reichert U. (2003) Identification and characterization of a cell cycle and apoptosis regulatory protein-1 as a novel mediator of apoptosis signaling by retinoid CD437. *J Biol Chem*, **278**, 33422-33435.

Rivero S, Cardenas J, Bornens M, and Rios RM. (2009) Microtubule nucleation at the cis-side of the Golgi apparatus requires AKAP450 and GM130. *EMBO J*, **28**, 1016-1028.

Rochford JJ, Semple RK, Laudes M, Boyle KB, Christodoulides C, Mulligan C, Lelliott CJ, Schinner S, Hadaschik D, Mahadevan M, Sethi JK, Vidal-Puig A, and O'Rahilly S. (2004) ETO/MTG8 is an inhibitor of C/EBPbeta activity and a regulator of early adipogenesis. *Mol Cell Biol*, **24**, 9863-9872.

Robles-Valero J, Martín-Cófreces NB, Lamana A, Macdonald S, Volkov Y, and Sánchez-Madrid F. (2010) Integrin and CD3/TCR activation are regulated by the scaffold protein AKAP450. *Blood*, **115**, 4174-4184.

Rogne M, Stokka AJ, Tasken K, Collas P, and Kuntziger T. (2009) Mutually exclusive binding of PP1 and RNA to AKAP149 affects the mitochondrial network. *Hum Mol Genet*, **18**, 978-987.

Romeo Y, Zhang X, and Roux PP. (2012) Regulation and function of the RSK family of protein kinases. *Biochem J*, **441**, 553-569.

Roubin R, Acquaviva C, Chevrier V, Sedjaï F, Zyss D, Birnbaum D, and Rosnet O. (2013) Myomegalin is necessary for the formation of centrosomal and Golgi-derived microtubules. *Biol Open*, **2**, 238-250.

Rouleau GA, Merel P, Lutchman M, Sanson M, Zucman J, Marineau C, Hoang-Xuan K, Demczuk S, Desmaze C, Plougastel B, Pulst SM, Lenoir G, Bijlsma E, Fashold R, Dumanski J, de Jong P, Parry D, Eldrige R, Aurias A, Delattre O, and Thomas G. (1993) Alteration in a new gene encoding a putative membrane-organizing protein causes neuro-fibromatosis type 2. *Nature*, **363**, 515-521.

Roussel BD, Kruppa AJ, Miranda E, Crowther DC, Lomas DA, and Marciniak SJ. (2013) Endoplasmic reticulum dysfunction in neurological disease. *Lancet Neurol*, **12**, 105-118.

Roy E, Bruyère J, Flamant P, Bigou S, Ausseil J, Vitry S, and Heard JM. (2012) GM130 gain-of-function induces cell pathology in a model of lysosomal storage disease. *Hum Mol Genet*, **21**, 1481-1495.

Rudd MF, Webb EL, Matakidou A, Sellick GS, Williams RD, Bridle H, Eisen T, Houlston RS, and GELCAPS Consortium. (2006) Variants in the GH-IGF axis confer susceptibility to lung cancer. *Genome Res*, **16**, 693-701.

Russell MA, Lund LM, Haber R, McKeegan K, Cianciola N, and Bond M. (2006) The intermediate filament protein, synemin, is an AKAP in the heart. *Arch Biochem Biophys*, **456**, 204-215.

Sacktor B. (1954) Investigations on the mitochondria of the housefly, Musca domestica L. III. Requirements for oxidative phosphorylation. *J Gen Physiol*, **37**, 343-359.

Saini S, Agarwal S, Sinha A, Verma A, Parashar D, Gupta N, Ansari AS, Lohiya NK, Jagadish N, and Suri A. (2013) Gene silencing of A-kinase anchor protein 4 inhibits cervical cancer growth in vitro and in vivo. *Cancer Gene Ther*, **20**, 413-420.

Sainz J, Huynh DP, Figueroa K, Ragge NK, Baser ME, and Pulst SM. (1994) Mutations of the neurofibromatosis type 2 gene and lack of the gene product in vestibular schwannomas. *Hum Mol Genet*, **3**, 885-891.

Salemi M, Barone C, Romano C, Salluzzo R, Caraci F, Cantarella RA, Salluzzo MG, Drago F, Romano C, and Bosco P. (2013) Pericentrin expression in Down's syndrome. *Neurol Sci*, ePub.

Samali A, Zhivotovsky B, Jones D, Nagata S, and Orrenius S. (1999) Apoptosis: cell death defined by caspase activation. *Cell Death Differ*, **6**, 495-496.

Santel A, Frank S, Gaume B, Herrler M, Youle RJ, and Fuller MT. (2003) Mitofusin-1 protein is a generally expressed mediator of mitochondrial fusion in mammalian cells. *J Cell Sci*, **116**, 2763-2774.

Sarkar D, Erlichman J, and Rubin CS. (1984) Identification of a calmodulin-binding protein that co-purifies with the regulatory subunit of brain protein kinase II. *J Biol Chem*, **259**, 9840-9846.

Sayner SL. (2011) Emerging themes of cAMP regulation of the pulmonary endothelial barrier. *Am J Physiol Lung Cell Mol Physiol*, **300**, L667-L678.

Schillace RV, Andrews SF, Liberty GA, Davey MP, and Carr DW. (2002) Identification and characterization of myeloid translocation gene 16b as a novel a kinase anchoring protein in T lymphocytes. *J Immunol*, **168**, 1590-1599.

Schimenti KJ, Feuer SK, Griffin LB, Graham NR, Bovet CA, Hartford S, Pendola J, Lessard C, Schimenti JC, and Ward JO. (2013) AKAP9 Is Essential for Spermatogenesis and Sertoli Cell Maturation in Mice. *Genetics*, **194**, 447-457.

Schmidt PH, Dransfield DT, Claudio JO, Hawley RG, Trotter KW, Milgram SL, and Goldenring JR. (1999) AKAP350, a multiply spliced protein kinase A-anchoring protein associated with centrosomes. *J Biol Chem*, **274**, 3055-3066.

Scott JD. (1997) Dissection of protein kinase and phosphatase targeting interactions. *Soc Gen Physiol Ser*, **52**, 227-239.

Sehrawat S, Ernandez T, Cullere X, Takahashi M, Ono Y, Komarova Y, and Mayadas TN. (2011) AKAP9 regulation of microtubule dynamics promotes Epac1-induced endothelial barrier properties. *Blood*, **117**, 708-718.

Shanks RA, Steadman BT, Schmidt PH, and Goldenring JR. (2002a) AKAP350 at the Golgi apparatus. I. Identification of a distinct Golgi apparatus targeting motif in AKAP350. *J Biol Chem*, **277**, 40967-40972.

Shanks RA, Larocca MC, Berryman M, Edwards JC, Urushidani T, Navarre J, and Goldenring JR. (2002b) AKAP350 at the Golgi apparatus. II. Association of AKAP350 with a novel chloride intracellular channel (CLIC) family member. *J Biol Chem*, **277**, 40973-40980.

Shibata D, Mori Y, Cai K, Zhang L, Yin J, Elahi A, Hamelin R, Wong YF, Lo WK, Chung TK, Sato F, Karpeh MS Jr, and Meltzer SJ. (2006) RAB32 hypermethylation and microsatellite instability in gastric and endometrial adenocarcinomas. *Int J Cancer*, **119**, 801-806.

Shimizu S, Kanaseki T, Mizushima N, Mizuta T, Arakawa-Kobayashi S, Thompson CB, and Tsujimoto Y. (2004) Role of Bcl-2 family proteins in a non-apoptotic programmed cell death dependent on autophagy genes. *Nat Cell Biol*, **6**, 1221-1228.

Shinotsuka C, Waguri S, Wakasugi M, Uchiyama Y, and Nakayama K. (2002) Dominant-negative mutant of BIG2, an ARF-guanine nucleotide exchange factor, specifically affects membrane trafficking from the trans-Golgi network through inhibiting membrane association of AP-1 and GGA coat proteins. *Biochem Biophys Res Commun*, **294**, 254-260.

Sillibourne JE, Milne DM, Takahashi M, Ono Y, and Meek DW. (2002) Centrosomal anchoring of the protein kinase CK1delta mediated by attachment to the large, coiled-coil scaffolding protein CG-NAP/AKAP450. *J Mol Biol*, **322**, 785-797.

Skroblin P, Grossmann S, Schäfer G, Rosenthal W, and Klussmann E. (2010) Mechanisms of protein kinase A anchoring. *Int Rev Cell Mol Biol*, **283**, 235-330.

Smith FD and Scott JD. (2013) A-kinase-anchoring protein-Lbc connects stress signaling to cardiac hypertrophy. *Mol Cell Biol*, **33**, 2-3.

Solomon S, Xu Y, Wang B, David MD, Schubert P, Kennedy D, and Schrader JW. (2007) Distinct structural features of caprin-1 mediate its interaction with G3BP-1 and its induction of phosphorylation of eukaryotic translation initiation factor 2alpha, entry to cytoplasmic stress granules, and selective interaction with a subset of mRNAs. *Mol Cell Biol*, **27**, 2324-2342.

Srivastava SP, Kumar KU, and Kaufman RJ. (1998) Phosphorylation of eukaryotic translation initiation factor 2 mediates apoptosis in response to activation of the double-stranded RNA-dependent protein kinase. *J Biol Chem*, **273**, 2416-2423.

Steadman BT, Schmidt PH, Shanks RA, Lapierre LA, and Goldenring JR. (2002) Transforming acidic coiled-coil-containing protein 4 interacts with centrosomal AKAP350 and the mitotic spindle apparatus. *J Biol Chem*, **277**, 30165-30176.

Steen RL, Martins SB, Taskén K, and Collas P. (2000) Recruitment of protein phosphatase 1 to the nuclear envelope by A-kinase anchoring protein AKAP149 is a prerequisite for nuclear lamina assembly. *J Cell Biol*, **150**, 1251-1262.

Steen RL, Beullens M, Landsverk HB, Bollen M, and Collas P. (2003) AKAP149 is a novel PP1 specifier required to maintain nuclear envelope integrity in G1 phase. *J Cell Sci*, **116**, 2237-2246.

Sterpetti P, Hack AA, Bashar MP, Park B, Cheng SD, Knoll JH, Urano T, Feig LA, and Toksoz D. (1999) Activation of the Lbc Rho exchange factor proto-oncogene by truncation of an extended C terminus that regulates transformation and targeting. *Mol Cell Biol*, **19**, 1334-1345.

Studier FW. (2005) Protein production by auto-induction in high-density shaking cultures. *Protein Expr Purif*, **41**, 207-234.

Subramaniam SR and Chesselet MF. (2013) Mitochondrial dysfunction and oxidative stress in Parkinson's disease. *Prog Neurobiol*, **S0301-0082**, 00040-00043.

Sumandea CA, Garcia-Cazarin ML, Bozio CH, Sievert GA, Balke CW, and Sumandea MP. (2011) Cardiac troponin T, a sarcomeric AKAP, tethers protein kinase A at the myofilaments. *J Biol Chem*, **286**, 530-541.

Sutherland EW and Rall TW. (1958) Fractionation and characterization of a cyclic adenine ribonucleotide formed by tissue particles. *J Biol Chem*, **232**, 1077-1091.

Takahashi M, Shibata H, Shimakawa M, Miyamoto M, Mukai H, and Ono Y. (1999) Characterization of a novel giant scaffolding protein, CG-NAP, that anchors multiple signaling enzymes to centrosome and the golgi apparatus. *J Biol Chem*, **274**, 17267-17274.

Takahashi M, Mukai H, Oishi K, Isagawa T, and Ono Y. (2000) Association of immature hypophosphorylated protein kinase cepsilon with an anchoring protein CG-NAP. *J Biol Chem*, **275**, 34592-34596.

Takahashi M, Yamagiwa A, Nishimura T, Mukai H, and Ono Y. (2002) Centrosomal proteins CG-NAP and kendrin provide microtubule nucleation sites by anchoring gamma-tubulin ring complex. *Mol Biol Cell*, **13**, 3235-3245.

Tanaka T, Yano H, Umezawa S, Shishiba Y, Okada K, Saito T, and Hibi I. (1989) Heterogeneity of big-big hPRL in hyperprolactinemia. *Horm Metab Res*, **21**, 84-88.

Tang TS and Bezprozvanny I. (2004) Dopamine receptor-mediated Ca(2+) signaling in striatal medium spiny neurons. *J Biol Chem*, **279**, 42082-42094.

Tardiff JC. (2005) Sarcomeric proteins and familial hypertrophic cardiomyopathy: linking mutations in structural proteins to complex cardiovascular phenotypes. *Heart Fail Rev*, **10**, 237-248.

Taskén KA, Collas P, Kemmner WA, Witczak O, Conti M, and Taskén K. (2001) Phosphodiesterase 4D and protein kinase a type II constitute a signaling unit in the centrosomal area. *J Biol Chem*, **276**, 21999-22002.

Terrin A, Monterisi S, Stangherlin A, Zoccarato A, Koschinski A, Surdo NC, Mongillo M, Sawa A, Jordanides NE, Mountford JC, and Zaccolo M. (2012) PKA and PDE4D3 anchoring to AKAP9 provides distinct regulation of cAMP signals at the centrosome. *J Cell Biol*, **198**, 607-621.

Tian J, Peehl D, and Knox SJ. (2010) Darinaparsin (ZIO-101) is a novel cytotoxic and radiosensitizing agent for prostate cancer. *Eur J Cancer Supplements*, **8**, 161.

Tingley WG, Pawlikowska L, Zaroff JG, Kim T, Nguyen T, Young SG, Vranizan K, Kwok PY, Whooley MA, and Conklin BR. (2007) Gene-trapped mouse embryonic stem cell-derived cardiac myocytes and human genetics implicate AKAP10 in heart rhythm regulation. *Proc Natl Acad Sci U S A*, **104**, 8461-8466.

Theurkauf WE and Vallee RB. (1982) Molecular characterization of the cAMP-dependent protein kinase bound to microtubule-associated protein 2. *J Biol Chem*, **257**, 3284-3290.

Thomas MG, Loschi M, Desbats MA, and Boccaccio GL. (2011) RNA granules: the good, the bad and the ugly. *Cell Signal*, **23**, 324-334.

Toksoz D and Williams DA. (1994) Novel human oncogene lbc detected by transfection with distinct homology regions to signal transduction products. *Oncogene*, **9**, 621-628.

Tourrière H, Chebli K, Zekri L, Courselaud B, Blanchard JM, Bertrand E, and Tazi J. (2003) The RasGAP-associated endoribonuclease G3BP assembles stress granules. *J Cell Biol*, **160**, 823-831.

Trendelenburg G, Hummel M, Riecken EO, and Hanski C. (1996) Molecular characterization of AKAP149, a novel A kinase anchor protein with a KH domain. *Biochem Biophys Res Commun*, **225**, 313-319.

Tröger J, Moutty MC, Skroblin P, and Klussmann E. (2012) A-kinase anchoring proteins as potential drug targets. *Br J Pharmacol*, **166**, 420-433.

Trotter KW, Fraser ID, Scott GK, Stutts MJ, Scott JD, and Milgram SL. (1999) Alternative splicing regulates the subcellular localization of A-kinase anchoring protein 18 isoforms. *J Cell Biol*, **147**, 1481-1492.

Truong T, Sauter W, McKay JD, Hosgood HD 3rd, Gallagher C, Amos CI, Spitz M, Muscat J, Lazarus P, Illig T, Wichmann HE, Bickeböller H, Risch A, Dienemann H, Zhang ZF, Naeim BP, Yang P, Zienolddiny S, Haugen A, Le Marchand L, Hong YC, Kim JH, Duell EJ, Andrew AS, Kiyohara C, Shen H, Matsuo K, Suzuki T, Seow A, Ng DP, Lan Q, Zaridze D, Szeszenia-Dabrowska N, Lissowska J, Rudnai P, Fabianova E, Constantinescu V, Bencko V, Foretova L, Janout V, Caporaso NE, Albanes D, Thun M, Landi MT, Trubicka J, Lener M, Lubinski J; EPIC-lung, Wang Y, Chabrier A, Boffetta P, Brennan P, and Hung RJ. (2010) International Lung Cancer Consortium: coordinated association study of 10 potential lung cancer susceptibility variants. *Carcinogenesis*, **31**, 625-633.

Tsimberidou AM, Camacho LH, Verstovsek S, Ng C, Hong DS, Uehara CK, Gutierrez C, Daring S. (2009) A phase I clinical trial of darinaparsin in patients with refractory solid tumors. *Clin Cancer Res*, **15**, 4769-4776.

Tu H, Tang TS, Wang Z, and Bezprozvanny I. (2004) Association of type 1 inositol 1,4,5-trisphosphate receptor with AKAP9 (Yotiao) and protein kinase A. *J Biol Chem*, **279**, 19375-19382.

Turner RM, Johnson LR, Haig-Ladewig L, Gerton GL, and Moss SB. (1998) An X-linked gene encodes a major human sperm fibrous sheath protein, hAKAP82. Genomic organization, protein kinase A-RII binding, and distribution of the precursor in the sperm tail. *J Biol Chem*, **273**, 32135-32141.

Ule J, Jensen K, Mele A, and Darnell RB. (2005) CLIP: a method for identifying protein-RNA interaction sites in living cells. *Methods*, **37**, 376-386.

Ullman E, Fan Y, Stawowczyk M, Chen HM, Yue Z, and Zong WX. (2008) Autophagy promotes necrosis in apoptosis-deficient cells in response to ER stress. *Cell Death Differ*, **15**, 422-425.

Uys GM, Ramburan A, Loos B, Kinnear CJ, Korkie LJ, Mouton J, Riedemann J, and Moolman-Smook JC. (2011) Myomegalin is a novel A-kinase anchoring protein involved in the phosphorylation of cardiac myosin binding protein C. *BMC Cell Biol*, **12**, 18.

Vandenabeele P, Galluzzi L, Vanden Berghe T, and Kroemer G. (2010) Molecular mechanisms of necroptosis: an ordered cellular explosion. *Nat Rev Mol Cell Biol*, **11**, 700-714.

Van Gele M, Dynoodt P, and Lambert J. (2009) Griscelli syndrome: a model system to study vesicular trafficking. *Pigment Cell Melanoma Res*, **22**, 268-282.

Varçin M, Bentea E, Michotte Y, and Sarre S. (2012) Oxidative Stress in Genetic Mouse Models of Parkinson's Disease. *Oxid Med Cell Longev*, **2012**, 624925.

Verde I, Pahlke G, Salanova M, Zhang G, Wang S, Coletti D, Onuffer J, Jin SL, and Conti M. (2001) Myomegalin is a novel protein of the golgi/centrosome that interacts with a cyclic nucleotide phosphodiesterase. *J Biol Chem*, **276**, 11189-11198.

Verstovsek S, Giles F, Quintás-Cardama A, Perez N, Ravandi-Kashani F, Beran M, Freireich E, Kantarjian H. (2006) Arsenic derivatives in hematologic malignancies: a role beyond acute promyelocytic leukemia? *Hematol Oncol*, **24**, 181-188.

Vijayaraghavan S, Liberty GA, Mohan J, Winfrey VP, Olson GE, and Carr DW. (1999) Isolation and molecular characterization of AKAP110, a novel, sperm-specific protein kinase A-anchoring protein. *Mol Endocrinol*, **13**, 705-717.

von Harsdorf R, Li PF, and Dietz R. (1999) Signaling pathways in reactive oxygen species-induced cardiomyocyte apoptosis. *Circulation*, **99**, 2934-2941.

Wang X, Herberg FW, Laue MM, Wullner C, Hu B, Petrasch-Parwez E, and Kilimann MW. (2000) Neurobeachin: A protein kinase A-anchoring, beige/Chediak-higashi protein homolog implicated in neuronal membrane traffic. *J Neurosci*, **20**, 8551-8565.

Wang L, Sunahara RK, Krumins A, Perkins G, Crochiere ML, Mackey M, Bell S, Ellisman MH, and Taylor SS. (2001) Cloning and mitochondrial localization of full-length D-AKAP2, a protein kinase A anchoring protein. *Proc Natl Acad Sci U S A*, **98**, 3220-3225.

Wang B, David MD, and Schrader JW. (2005) Absence of caprin-1 results in defects in cellular proliferation. *J Immunol*, **175**, 4274-4282.

Wang Z, Wu T, Shi L, Zhang L, Zheng W, Qu JY, Niu R, and Qi RZ. (2010) Conserved motif of CDK5RAP2 mediates its localization to centrosomes and the Golgi complex. *J Biol Chem*, **285**, 22658-22665.

Wasmeier C, Romao M, Plowright L, Bennett DC, Raposo G, and Seabra MC. (2006) Rab38 and Rab32 control post-Golgi trafficking of melanogenic enzymes. *J Cell Biol*, **175**, 271-281.

Webb EL, Rudd MF, Sellick GS, El Galta R, Bethke L, Wood W, Fletcher O, Penegar S, Withey L, Qureshi M, Johnson N, Tomlinson I, Gray R, Peto J, and Houlston RS. (2006) Search for low penetrance alleles for colorectal cancer through a scan of 1467 non-synonymous SNPs in 2575 cases and 2707 controls with validation by kin-cohort analysis of 14 704 first-degree relatives. *Hum Mol Genet*, **15**, 3263-3271.

Weil D, Blanchard S, Kaplan J, Guilford P, Gibson F, Walsh J, Mburu P, Varela A, Levilliers J, Weston MD, Kelley PM, Kimberling WJ, Wagenaar M, Levi-Acobas F, Larget-Piet D, Munnich A, Steel KP, Brown SDM, and Petit C. (1995) Defective myosin VIIA gene responsible for Usher syndrome type 1B. *Nature*, **374**, 60-61.

Welch EJ, Jones BW, and Scott JD. (2010) Networking with AKAPs: Context-dependent regulation of anchored enzymes. *Mol Interventions*, **10**, 86-97.

Westphal RS, Tavalin SJ, Lin JW, Alto NM, Fraser ID, Langeberg LK, Sheng M, and Scott JD. (1999) Regulation of NMDA receptors by an associated phosphatase-kinase signaling complex. *Science*, **285**, 93-96.

White JP and Lloyd RE. (2012) Regulation of stress granules in virus systems. *Trends Microbiol*, **20**, 175-183.

Wirtenberger M, Schmutzhard J, Hemminki K, Meindl A, Sutter C, Schmutzler RK, Wappenschmidt B, Kiechle M, Arnold N, Weber BH, Niederacher D, Bartram CR, and

Burwinkel B. (2007) The functional genetic variant Ile646Val located in the kinase binding domain of the A-kinase anchoring protein 10 is associated with familial breast cancer. *Carcinogenesis*, **28**, 423-426.

Witczak O, Skålhegg BS, Keryer G, Bornens M, Taskén K, Jahnsen T, and Orstavik S. (1999) Cloning and characterization of a cDNA encoding an A-kinase anchoring protein located in the centrosome, AKAP450. *EMBO J*, **18**, 1858-1868.

Wolozin B. (2012) Regulated protein aggregation: stress granules and neurodegeneration. *Mol Neurodegener*, **7**, 56.

Wosilait WD and Sutherland EW. (1957) The relationship of epinephrine and glucagon to liver phosphorylase. II. Enzymatic inactivation of liver phosphorylase. *J Biol Chem*, **218**, 469-481.

Wu J, Henderson C, Feun L, Van Veldhuizen P, Gold P, Zheng H, Ryan T, Blaszkowsky LS, Chen H, Costa M, Rosenzweig B, Nierodzik M, Hochster H, Muggia F, Abbadessa G, Lewis J, and Zhu AX. (2010) Phase II study of darinaparsin in patients with advanced hepatocellular carcinoma. *Invest New Drugs*, **28**, 670-676.

Wong W and Scott JD. (2004) AKAP signalling complexes: focal points in space and time. *Nat Rev Mol Cell Biol*, **5**, 959-970.

Xie G and Raufman JP. (2001) Association of protein kinase A with AKAP150 facilitates pepsinogen secretion from gastric chief cells. *Am J Physiol Gastrointest Liver Physiol*, **281**, G1051-G1058.

Xu K, Schwarz PM, and Ludueña RF. (2002) Interaction of nocodazole with tubulin isotypes. *Drug Dev Res*, **55**, 91-96.

Yang J, Drazba JA, Ferguson DG, and Bond M. (1998) A-kinase anchoring protein 100 (AKAP100) is localized in multiple subcellular compartments in the adult rat heart. *J Cell Biol*, **142**, 511-522.

Youle RJ and van der Bliek AM. (2012) Mitochondrial fission, fusion, and stress. *Science*, **337**, 1062-1065.

Young A, Dictenberg JB, Purohit A, Tuft R, and Doxsey SJ. (2000) Cytoplasmic dynein-mediated assembly of pericentrin and gamma tubulin onto centrosomes. *Mol Biol Cell*, **11**, 2047-2056.

Yu L, Alva A, Su H, Dutt P, Freundt E, Welsh S, Baehrecke EH, and Lenardo MJ. (2004) Regulation of an ATG7-beclin 1 program of autophagic cell death by caspase-8. *Science*, **304**, 1500-1502.

Zhang J and Dong XP. (2012) Dysfunction of microtubule-associated proteins of MAP2/tau family in Prion disease. *Prion*, **6**, 334-338.

Zhu X, Morales FC, Agarwal NK, Dogruluk T, Gagea M, and Georgescu MM. (2013) Moesin is a glioma progression marker that induces proliferation and Wnt/β-catenin pathway activation via interaction with CD44. *Cancer Res*, **73**, 1142-1155.

Züchner S, Mersiyanova IV, Muglia M, Bissar-Tadmouri N, Rochelle J, Dadali EL, Zappia M, Nelis E, Patitucci A, Senderek J, Parman Y, Evgrafov O, Jonghe PD, Takahashi Y, Tsuji S, Pericak-Vance MA, Quattrone A, Battaloglu E, Polyakov AV, Timmerman V, Schröder JM, and Vance JM. (2004) Mutations in the mitochondrial GTPase mitofusin 2 cause Charcot-Marie-Tooth neuropathy type 2A. *Nat Genet*, **36**, 449-451.